AD_____

Award Number: W81XWH-12-1-0319

TITLE: Novel Combinatory Approaches to Repair Visual System after Optic Nerve Damage

PRINCIPAL INVESTIGATOR: Kevin K. Park

CONTRACTING ORGANIZATION: University of Miami
 Miami, FL 33136

REPORT DATE: September 2013

TYPE OF REPORT: Annual Report

PREPARED FOR: U.S. Army Medical Research and Materiel Command
                Fort Detrick, Maryland 21702-5012

DISTRIBUTION STATEMENT: Approved for Public Release;
                Distribution Unlimited

The views, opinions and/or findings contained in this report are those of the author(s) and should not be construed as an official Department of the Army position, policy or decision unless so designated by other documentation.

REPORT DOCUMENTATION PAGE

Form Approved
OMB No. 0704-0188

1. REPORT DATE : September 2013	2. REPORT TYPE: Annual Report	3. DATES COVERED 30 August 2012-29 August 2013	
4. TITLE AND SUBTITLE Novel Combinatory Approaches to Repair Visual System After Optic Nerve Damage		**5a. CONTRACT NUMBER** W81XWH-12-1-0319	
		5b. GRANT NUMBER W81XWH-12-1-0319	
		5c. PROGRAM ELEMENT NUMBER	
6. AUTHOR(S) Kevin K. Park, PhD (PI) E-Mail: kpark@med.miami.edu		**5d. PROJECT NUMBER**	
		5e. TASK NUMBER	
		5f. WORK UNIT NUMBER	
7. PERFORMING ORGANIZATION NAME(S) AND ADDRESS(ES) University of Miami Miller School of Medicine \ Miami, FL 33136		**8. PERFORMING ORGANIZATION REPORT NUMBER**	
9. SPONSORING / MONITORING AGENCY NAME(S) AND ADDRESS(ES) USA MED RESEARCH ACQ ACTIVITY 820 CHANDLER ST FORT DETRICK MD 21702-5014		**10. SPONSOR/MONITOR'S ACRONYM(S)**	
		11. SPONSOR/MONITOR'S REPORT NUMBER(S)	

12. DISTRIBUTION / AVAILABILITY STATEMENT
Approved for Public Release; Distribution Unlimited

13. SUPPLEMENTARY NOTES N/A

14. ABSTRACT
Background: Death of retinal ganglion cells (RGCs) and poor regeneration are major obstacles for treating traumatic optic neuropathy after road accident, falls or combat blasts. Optic nerve regeneration from many long-term surviving RGCs, reconnecting the brain could potentially restore vision after injury. We previously determined that deletion of two genes, PTEN and SOCS3 induces optic nerve regeneration. On the other hand, genetic modification of CHOP and XBP1 in RGCs render them highly resistant to injury-induced death.

Objective/hypothesis: We will use knockout mice and therapeutically relevant short hairpin RNA (shRNA) approaches to determine the combined effects of targeting PTEN/SOCS3 and CHOP/XBP1 on RGC survival and regeneration after injury. In addition, we will examine the integrity of RGC functions after modification of these genes using pattern electroretinogram (PERG). We hypothesize that combined strategies to target PTEN/SOCS3 and CHOP/XBP1 will further enhance long-term RGC survival and regeneration, and RGCs in these animals exhibit normal physiological responses.

Specific Aims/Study Design:
Aim 1: Use knockout mice to examine the combined effects of targeting PTEN/SOCS3 and CHOP/XBP1 on RGC survival and regeneration. PTEN/SOCS3/CHOP knockout mice will receive AAV-assisted over-expression of XBP1, followed by nerve crush injury and assessment of RGC survival and regeneration.
Aim 2: Integrity of RGC functions after genetic modification of PTEN/SOCS3 or CHOP/XBP1 will be evaluated using PERG.
Aim 3: Optimize shRNA approach to promote RGC survival and regeneration. PTEN, SOCS3 and CHOP will be knocked down alone or in combination using shRNAs to improve RGC survival and regeneration.

Relevance: Military personnel run a high risk of incurring ocular nerve damage. This proposal will probe for genetic interventions to rescue dying neurons and promote regeneration, and restore vision, with the potential to be administered to the clinic and battlefield.

15. SUBJECT TERMS: PTEN, SOCS3, CHOP, XBP1, Regeneration, Neurons, Axons

16. SECURITY CLASSIFICATION OF: U			17. LIMITATION OF ABSTRACT	18. NUMBER OF PAGES	19a. NAME OF RESPONSIBLE PERSON USAMRMC
a. REPORT U	**b. ABSTRACT** U	**c. THIS PAGE** U	UU	62	**19b. TELEPHONE NUMBER** *(include area code)*

Table of Contents

INTRODUCTION:

Death of retinal ganglion cells (RGCs) and poor regeneration are major obstacles for treating traumatic optic neuropathy after road accident, falls or combat blasts. Optic nerve regeneration from many long-term surviving RGCs, reconnecting the brain could potentially restore vision after injury. We previously determined that deletion of two genes, PTEN and SOCS3 induces optic nerve regeneration (Park *et al.*, 2008; Smith *et al.*, 2009; Sun *et al.*, 2011). On the other hand, genetic modification of CHOP and XBP1 in RGCs render them highly resistant to injury-induced death (Hu *et al.*, 2012). We hypothesize that combined strategies to target PTEN/SOCS3 and CHOP/XBP1 will further enhance long-term RGC survival and regeneration, and RGCs in these animals exhibit normal physiological responses. In this proposal, we have used knockout mice and therapeutically relevant short hairpin RNA (shRNA) approaches to determine the combined effects of targeting PTEN/SOCS3 and CHOP/XBP1 on RGC survival and regeneration after injury. Further, we examined the integrity of RGC functions after modification of these genes using pattern electroretinogram (PERG). In addition, we have developed new imaging techniques to assess optic nerve regeneration in whole animal tissues without histological sectioning. Overall, this proposal investigates genetic interventions to rescue dying neurons and promote regeneration, and restore vision, with the potential to be administered to the clinic and battlefield.

BODY:

Aim 1: Use knockout mice to examine the combined effects of targeting PTEN/SOCS3 and CHOP/XBP1 on RGC survival and regeneration. PTEN/SOCS3/CHOP knockout mice will receive AAV-assisted over-expression of XBP1, followed by nerve crush injury and assessment of RGC survival and regeneration.

In this Aim, we have mated PTEN/SOCS3$^{f/f}$ mice with CHOP KO mice to generate triple mutant mice, PTEN/SOCS3$^{f/f}$/CHOP KO mice. Adult mice received various AAV treatments as outlined in Table 1 below.

Groups (n=8-10/group)	Intravitreal Viral Treatment	Outcome Measures
PTEN/SOCS3$^{f/f}$	AAV-GFP (Control)	RGC staining and axon tracing
PTEN/SOCS3$^{f/f}$	AAV-Cre	" "
CHOP$^{-/-}$	AAV-XBP1	" "
CHOP$^{-/-}$/PTEN/SOCS3$^{f/f}$	AAV-Cre/AAV-XBP1	" "

At different time points after intraorbital optic nerve crush, animals were analyzed for RGC survival and axon regeneration using immunohistochemistry and axon tracing methods used in our previous studies. At 4 and 8 weeks after injury, retinas were immunostained with an antibody against beta III tubulin (TUJ1) to estimate RGC survival. The degree of axon regeneration, assessed by dye-labeled fibers was quantified and compared among the control animal groups. Using histology, axon regeneration into various visual targets including the lateral geniculate nucleus, superior colliculus, olivary pretectal nucleus and suprachiasmatic nucleus was assessed. As shown in Fig. 1, we have found that while manipulation of two genes (i.e. PTEN/SOCS3 or CHOP/XBP1) in combination resulted in some degree of neuroprotection after optic nerve injury, the ultimate combination targeting all four genes (PTEN/SOCS3/CHOP/XBP1) led to marked improvement in the rate of RGC survival at 4 and 8 weeks after injury. These results represent one of the most powerful genetic strategies that protect injured RGCs reported to date. Importantly, our unique approaches use gene therapy strategy which raises hope for treating damaged optic nerve.

In addition to RGC survival, we examined the rate of axon regeneration in the combinatorial treatment groups. Successful re-innervation of regenerated axons to their targets is of paramount interest. Thus, the next important question is whether the number of axons that regenerate long distances into the visual targets is also increased in these animals. In order to determine this, we are currently analyzing the sectioned brain tissues to identify and quantify the number of regenerated axons in various visual targets.

As shown in Fig. 2, we observed that combinatorial treatments result in enhanced axon regeneration along the damaged optic nerve.
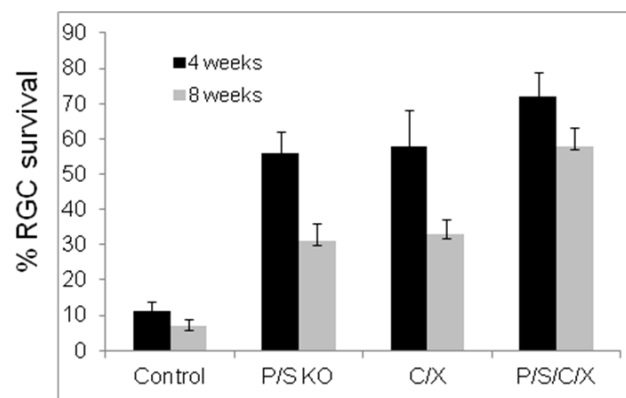
2

Figure 1. Combined modulation of PTEN/SOCS3/CHOP and XBP1 further enhances RGC survival after injury. Data are presented as mean % of RGC number compared to the uninjured contralateral eye at 4 and 8 weeks after injury. P/S KO, PTEN/SOCS3 KO; C/X, CHOP KO/XBP1 mice; P/S/C/X, PTEN/SOCS3/CHOP KO/XBP1 mice.
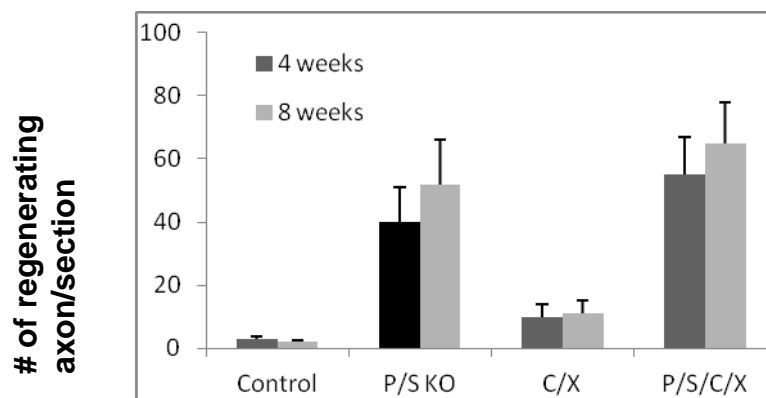

Figure 2. Combined modulation of PTEN/SOCS3/CHOP and XBP1 further enhances RGC axon regeneration. Data are presented as mean number of axons counted/ optic nerve section at 3 mm distal to the lesion site at 4 and 8 weeks after injury. Consistent with previous findings, control and C/X animals did not have regenerated axons. P/S KO, PTEN/SOCS3 KO; C/X, CHOP KO/XBP1 mice; P/S/C/X, PTEN/SOCS3/CHOP KO/XBP1 mice.

Aim 2: Integrity of RGC functions after genetic modification of PTEN/SOCS3 or CHOP/XBP1 will be evaluated using PERG.

In this Aim, we have used PERG to investigate whether RGCs subjected to different genetic manipulations exhibit normal physiological functions.

Groups (n=7-14/group)	Outcome Measures
PTEN/SOCS3 modified	PERG
WT control	" "

At different time points (0, 7, 40 and 60 days) after intraorbital optic nerve crush, PTEN/SOCS3-modified or control animals were analyzed for PERG measurement. The PERG amplitude in PTEN/SOCS3-modified animals decreased 7 days after injury but in 4 eyes out of 7, the PERG signal then progressively tended to a recovery. In control animals PERG did not show any obvious recovery (data not shown).
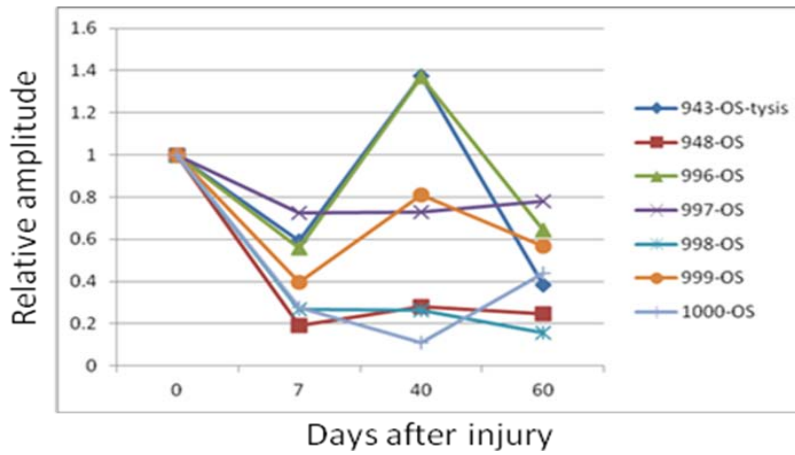

Figure 3. Mean PERG amplitude in Pten/Socs3-modified mice before and at different times after injury. All data were normalized to mean baseline values.

In addition, we have recently developed new methods to analyze optic axon regeneration in animal tissues without physical sectioning.

Traditional methods of assessing RGC axon regeneration rely on histological sectioning. However, tissue sections provide fragmentary information about axonal trajectory and termination. To unequivocally evaluate regenerating RGC axons, we apply tissue clearance and light sheet fluorescence microscopy (LSFM) to image axons in whole optic nerve and brain without histological sectioning. In this way, we demonstrate the strength of LSFM for comprehensive assessment of RGC axon regeneration, and unequivocally reveal significant axon misguidance after injury. This work (Luo *et al.*, 2013) has been published in **Experimental Neurology (2013 September Cover Issue)** titled, *Three-dimensional evaluation of retinal ganglion cell axon regeneration and pathfinding in unsectioned tissue after optic nerve injury.*

Aim 3: Optimize shRNA approach to promote RGC survival and regeneration. PTEN, SOCS3 and CHOP will be knocked down alone or in combination using shRNAs to improve RGC survival and regeneration.

In this Aim, we harness shRNA approach to knockdown CHOP, PTEN or SOCS3 in RGCS to promote RGC survival and axon regeneration.

4

Using concatenated shRNA construct methods (Chung et al., Nucleic Acids Res. 2006; 34(7): e53), we generated shRNA plasmid targeting CHOP. This shRNA method allows insertion of multiple sets of shRNA sequences into one vector, thus providing high degree of knockdown efficacy. After confirming plasmid knockdown efficacy in HEK 293 cells subjected to ER stress (treatment with ER stress inducer thapsigargin), we generated AAV2-shRNA CHOP to test CHOP knockdown effects on RGC survival in optic nerve crush injury model. Our AAV2 at certain titer allows infection of RGC specifically, with minimum infection of non-RGC cells. RGCs infected with AAV2-shRNA CHOP show reduction CHOP expression using immunohistochemistry (unpublished data).

Adult mice received AAV-shRNA CHOP injection intravitreously. At 14 days after injection, animals received intraorbital optic nerve crush injury. At 14 days after crush, CHOP knockdown (Kd) animals were analyzed for RGC survival and axon regeneration. Immunostaining using RGC-specific marker was used to examine RGC survival. Our preliminary results show that there is approximately two fold increase in RGC survival (42% RGC survival in shRNA CHOP treated animals, compared to 18% in control animals).
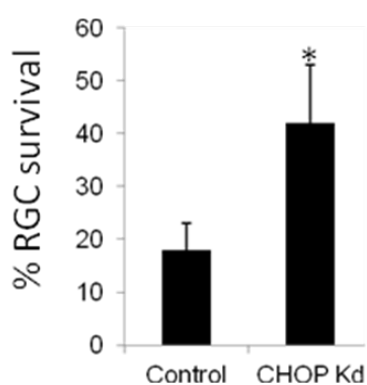
CHOP knockdown promotes RGC survival following axotomy. Data are presented as mean % of RGC number compared to the uninjured contralateral eye at 2 weeks after injury. CHOP Kd, adult mice subjected to AAV-shRNA CHOP injection two weeks prior to crush injury. Control, Adult mice subjected to AAV-shRNA targeting luciferase (control AAV). N=3/group. $*<0.05$, Student t test.

Thus, our data demonstrate enhanced RGC survival following optic nerve damage by targeting ER stress using a shRNA viral approach. We are in the process of examining whether AAV administered days after optic nerve injury will also result in enhanced RGC survival.

In addition to CHOP shRNA, we have used the same shRNA strategy to knockdown PTEN (Fig, 4). Using in vivo model of optic nerve crush injury, we show, for the first time, extensive RGC axon regeneration using AAV-shRNA approach (Fig. 5). **This portion of work involving shRNA has been submitted to a high impact journal and is currently under a review.**
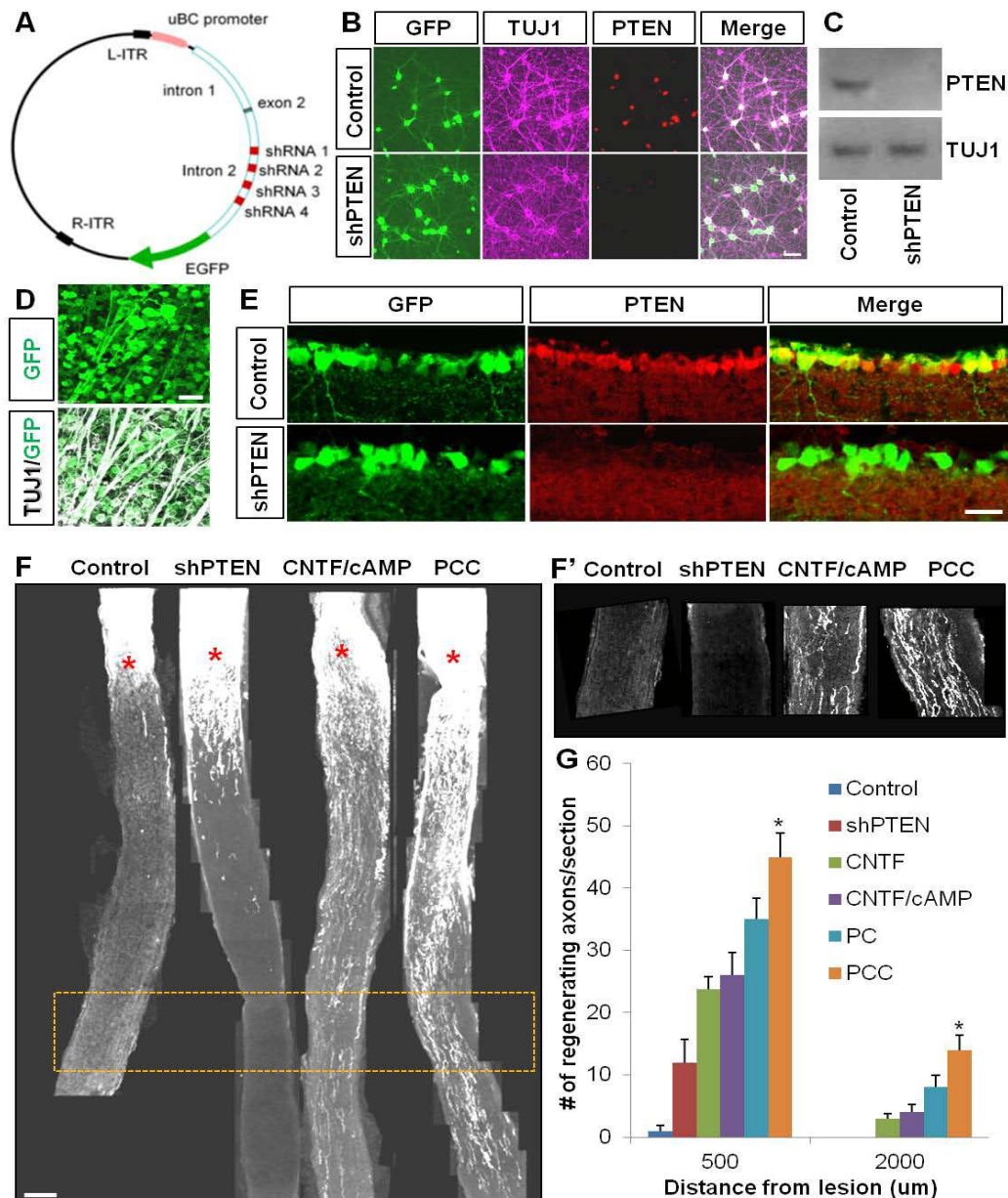
Figure 5. AAV modulation of PTEN combined with other growth inducing factors improve axon regeneration. (**A**) AAV2-shPTEN construct map. Control and shPTEN constructs contain EGFP reporter (**B**) PTEN knockdown shown by immunocytochemistry in cultured cortical neurons. (**C**) Western blot of protein lysates from treated cortical neurons. (**D**) Flat-mounted retina 2 weeks following intravitreal injection of AAV2-shPTEN, and staining with antibodies against GFP and TUJ1 (i.e. RGC-marker) shows >90% transduction efficacy in RGCs. (**E**) Retina sections following control AAV or AAV2-shPTEN injection show PTEN knockdown in ganglion cell layer. (**F**) Representative sectioned optic nerves of mice receiving various AAV treatments. Control, AAV-anti-Luc/EGFP; shPTEN, AAV2-PTEN; CNTF/cAMP, AAV2-CNTF/cpt-cAMP; PC, AAV2-shPTEN/AAV2-CNTF; PCC, AAV2-shPTEN/AAV2-CNTF/cpt-cAMP. Asterisk: lesion site. (**F'**) Higher-magnification images of the boxed area in (**F**). (**G**) Quantification of regenerating axon (n=6-8/group). *: $p<0.05$, Bonferroni test (PCC significantly different to all treatment groups except to PC). Error bars, SEM. Scale bars: B-E, 20 µm; F, 100 µm.

6

KEY RESEARCH ACCOMPLISHMENTS: Bulleted list of key research accomplishments emanating from this research.

- Successful generation of triple knockout mice (i.e. PTEN/SOCS3/CHOP knockout mice) required for Aim 1 of the proposal.
- Successful assessment of retinal ganglion cell survival and axon regeneration in different animal groups subjected to combinatory PTEN/SOCS3/CHOP and XBP1 manipulation.
- Successful assessment of retinal ganglion cell survival and axon regeneration in different animal groups subjected to combinatory PTEN/SOCS3/CHOP and XBP1 manipulation.
- Successful assessment of pattern electroretinograph (PERG) on animals subjected to PTEN/SOCS3 pathway manipulation.
- Establishment of novel methods (tissue clearance and light sheet fluorescent microscopy) to assess optic axon regeneration in whole mouse tissues.
- Successful generation of shRNA plasmid against CHOP.
- Successful generation of adeno-associated virus (AAV)-shRNA against CHOP.
- Initiation of assessment of gene therapy (AAV) approach to target CHOP to promote RGC survival.
- Successful generation of adeno-associated virus (AAV)-shRNA against PTEN.
- Paper presentation at the 2013 ARVO meeting on our data pertaining to axon regeneration and new imaging techniques.

REPORTABLE OUTCOMES: Provide a list of reportable outcomes that have resulted from this research to include:

Publications:

Luo, X., Salgueiro, Y., Beckerman, S.R., Lemmon, V.P., Tsoulfas, P., Park, K.K., Three-dimensional evaluation of retinal ganglion cell axon regeneration and path-finding in whole mouse tissue after injury. *Experimental Neurology,* 247:653-62, 2013 *(Issue Cover).*

Chou, T.H., Park, K.K., Luo, X., Porciatti, V., Retrograde signaling in the optic nerve is necessary for electrical responsiveness of retinal ganglion cells. *Invest. Ophthalmol. Vis. Sci.,* 54:1236-43, 2013.

Luo, X., Park, K.K., Neuron-intrinsic inhibitors of axon regeneration: PTEN and SOCS3. *Int. Rev. Neurobiol.,* 105:141-73, 2012.

Luo, X., Yungher, B., Park, K.K., Application of tissue clearance and light sheet fluorescent microscopy to assess optic nerve regeneration in whole mouse tissue. *Methods in Molecular Biology*, Invited Review (in press).

7

Award: 2013 FASEB BioArt (Video winner) Competition. One of the two winners of the Federation of American Societies for Experimental Biology's (FASEB) BioArt competition. The winning images will be used in FASEB's efforts to engage Members of Congress and educate the general public in dialogue regarding the immense value of the biomedical and biological research. (http://www.faseb.org/About-FASEB/Scientific-Contests/BioArt/Winners/2013-BioArt-Winners.aspx)

CONCLUSION: In summary, we have had a very successful and fruitful year undertaking the proposed studies. Mostly importantly, we have performed large parts of the Proposed Aims from which we have obtained extremely interesting and promising results. We have discovered that combining genetic modulations to target multiple genes, namely PTEN, SOCS3, CHOP and XBP1 promotes striking neuronal survival and axon regeneration. Further, we observed that genetically modified RGCs exhibit relatively normal physiology, a critical aspect in our quest to achieve functional restoration after optic nerve damage. In addition, we have successfully developed and optimized AAV and shRNA approaches to target multiple genes, and promote RGC survival and axon regeneration. This is extremely exciting because we now show for the first that a non-transgenic approach can induce extensive optic nerve regeneration in post-injury treatment paradigm. This part of work has been submitted for publication, and is currently being reviewed. We also established new imaging methodologies using tissue clearing and light sheet fluorescent microscope to evaluate optic nerve regeneration without histological sectioning. This technique will change the way researchers assess optic nerve regeneration in animal models. We anticipate that next year will be even more fruitful and exciting given the accumulation of intriguing data which we expect to submit for additional publications in the months to come.

REFERENCES:

Hu Y, Park KK, Yang L, Wei X, Yang Q, Cho KS, Thielen P, Lee AH, Cartoni R, Glimcher LH, Chen DF, He Z (2012) Differential effects of unfolded protein response pathways on axon injury-induced death of retinal ganglion cells. Neuron 73:445-452.

Luo X, Salgueiro Y, Beckerman SR, Lemmon VP, Tsoulfas P, Park KK (2013) Three-dimensional evaluation of retinal ganglion cell axon regeneration and pathfinding in whole mouse tissue after injury. Exp Neurol 247:653-662.

Park KK, Liu K, Hu Y, Smith PD, Wang C, Cai B, Xu B, Connolly L, Kramvis I, Sahin M, He Z (2008) Promoting axon regeneration in the adult CNS by modulation of the PTEN/mTOR pathway. Science 322:963-966.

Smith PD, Sun F, Park KK, Cai B, Wang C, Kuwako K, Martinez-Carrasco I, Connolly L, He Z (2009) SOCS3 deletion promotes optic nerve regeneration in vivo. Neuron 64:617-623.

Sun F, Park KK, Belin S, Wang D, Lu T, Chen G, Zhang K, Yeung C, Feng G, Yankner BA, He Z (2011) Sustained axon regeneration induced by co-deletion of PTEN and SOCS3. Nature 480:372-375.

APPENDICES: Attach all appendices that contain information that supplements, clarifies or supports the text. Examples include original copies of journal articles, reprints of manuscripts and abstracts, a curriculum vitae, study questionnaires, and surveys, etc.

SUPPORTING DATA: All figures and/or tables shall include legends and be clearly marked with figure/table numbers
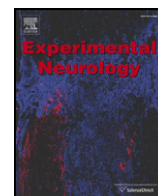
Three-dimensional evaluation of retinal ganglion cell axon regeneration and pathfinding in whole mouse tissue after injury

Xueting Luo, Yadira Salgueiro, Samuel R. Beckerman, Vance P. Lemmon, Pantelis Tsoulfas, Kevin K. Park *

Miami Project to Cure Paralysis, University of Miami, Miller School of Medicine, Miami, FL, 33136, USA
Department of Neurosurgery, University of Miami, Miller School of Medicine, Miami, FL, 33136, USA

ARTICLE INFO

ABSTRACT

Injured retinal ganglion cell (RGC) axons do not regenerate spontaneously, causing loss of vision in glaucoma and after trauma. Recent studies have identified several strategies that induce long distance regeneration in the optic nerve. Thus, a pressing question now is whether regenerating RGC axons can find their appropriate targets. Traditional methods of assessing RGC axon regeneration use histological sectioning. However, tissue sections provide fragmentary information about axonal trajectory and termination. To unequivocally evaluate regenerating RGC axons, here we apply tissue clearance and light sheet fluorescence microscopy (LSFM) to image whole optic nerve and brain without physical sectioning. In mice with PTEN/SOCS3 deletion, a condition known to promote robust regeneration, axon growth followed tortuous paths through the optic nerve, with many axons reversing course and extending towards the eye. Such aberrant growth was prevalent in the proximal region of the optic nerve where strong astroglial activation is present. In the optic chiasms of PTEN/SOCS3 deletion mice and PTEN deletion/Zymosan/cAMP mice, many axons project to the opposite optic nerve or to the ipsilateral optic tract. Following bilateral optic nerve crush, similar divergent trajectory is seen at the optic chiasm compared to unilateral crush. Centrally, axonal projection is limited predominantly to the hypothalamus. Together, we demonstrate the applicability of LSFM for comprehensive assessment of optic nerve regeneration, providing in-depth analysis of the axonal trajectory and pathfinding. Our study indicates significant axon misguidance in the optic nerve and brain, and underscores the need for investigation of axon guidance mechanisms during optic nerve regeneration in adults.

© 2013 Elsevier Inc. All rights reserved.

Introduction

Retinal ganglion cells (RGCs) do not regenerate their axons, leading to loss of visual functions in glaucoma and after trauma or stroke. Studies on the limited regenerative capacity of RGCs have identified several strategies that stimulate axon regeneration. These include enhancing the intrinsic growth capacity as well as neutralizing repulsive cues in the environment (Cho et al., 2005; Duffy et al., 2012; Leaver et al., 2006; Lingor et al., 2008; Liu et al., 2006; Muller et al., 2007; Qiu et al., 2002; Su et al., 2008; Winzeler et al., 2011; Wong et al., 2003). We and others have used knockout (KO) mice to demonstrate that RGC-specific deletion of PTEN (phosphatase and tensin homolog), SOCS3 (suppressor of cytokine signaling 3) or KLF4 (Krüppel like factor 4) induces RGC axon regeneration (Moore et al., 2009; Park et al., 2008; Smith et al., 2009). More recent studies have shown that

combining PTEN KO mice with either SOCS3 deletion, or Zymosan and a cAMP analogue leads to substantially more regeneration than targeting them individually (de Lima et al., 2012; Kurimoto et al., 2010; Sun et al., 2011), pointing to the importance of targeting multiple factors to induce extensive regeneration.

With the recent progress made in promoting RGC axon regeneration, it is becoming increasingly important to investigate whether regenerating RGC axons can find their targets in the brain. While appropriate pathfinding of RGC axons has been documented comprehensively in regeneration-competent species including fish and amphibians (Beazley et al., 1997; Becker and Becker, 2007; Stelzner et al., 1986), the degree to which RGC axons in adult mammals correctly reinnervate their targets is unclear.

A common method for assessing optic nerve regeneration is histological sectioning. However, tissue sections provide incomplete spatial information. For instance, it is difficult to determine the precise trajectory of axons or their final destinations. In this study, we applied a tetrahydrofuran (THF) based-clearing method that renders tissues relatively transparent (Becker et al., 2012; Erturk et al., 2012), and combined it with LSFM, allowing deep tissue fluorescence imaging in unsectioned optic nerve and brain. Using these methods, we found in PTEN/SOCS3 KO mice that regenerating axons follow circuitous paths, with many axons

---

* Corresponding author at: Miami Project to Cure Paralysis, University of Miami, Miller School of Medicine, Miami, FL, 33136, USA.
E-mail addresses: Xluo@med.miami.edu (X. Luo), Ysalgueiro@med.miami.edu (Y. Salgueiro), Sbeckerman@med.miami.edu (S.R. Beckerman), Vlemmon@med.miami.edu (V.P. Lemmon), Ptsoulfa@med.miami.edu (P. Tsoulfas), Kpark@med.miami.edu (K.K. Park).

making multiple turns and extending back to the eye. Axon turning was prevalent in nerve regions with strong astroglial activation. Many RGC axons generated branches in the optic nerve and brain as they re-grow. In the optic chiasm, a major decision point en route to visual targets, high numbers of regenerating axons in PTEN/SOCS3 KO mice or PTEN KO/Zymosan/cAMP analogue-treated mice diverge into the ipsilateral optic tract or to the opposite optic nerve. Following bilateral optic nerve crush, a similar growth pattern is seen at the optic chiasm compared to unilateral crush. Centrally, axonal projection is limited primarily to the hypothalamus. In summary, we demonstrated the combined application of tissue clearance and LSFM for comprehensive analysis of optic nerve regeneration, providing in-depth assessment of the axonal trajectory. Our study shows substantial misdirection of RGC axon growth in adult mice, and underscores the need for investigation into the mechanisms that underlie misguidance during regeneration in adults.

Materials and methods

All experimental procedures were performed in compliance with animal protocols approved by the IACUC at the University of Miami Miller School of Medicine. For all surgical procedures, mice were anaesthetized with ketamine and xylazine. Eye ointment containing atropine sulfate was applied preoperatively to protect the cornea during surgery, and Buprenorphine (0.05 mg/kg, Bedford Lab) was administrated as post-operative analgesic.

Mice, optic nerve crush injury and intravitreal injection

SOCS3$^{f/f}$/PTEN$^{f/f}$ (Sun et al., 2011) mice (female; 4–6 week old) were intravitreally injected with 1–2 μl volume of AAV2-Cre in the left eyes at 2 weeks prior to crush injury. 1 μl (1 μg/μl) ciliary neurotrophic factor (CNTF; Pepro Tech) was intravitreally injected immediately after injury and at 3 days post-injury, and bi-weekly thereafter. PTEN KO/ZYM/cAMP mice, PTEN$^{f/f}$ (Groszer et al., 2001) (female; 8 week old) received intravitreal AAV2-Cre injection followed by optic nerve crush 2 weeks later. Zymosan (Sigma-Aldrich; 12.5 μg/μL) along with the cAMP analogue CPT-cAMP (Sigma; 50 μM, 3 μL) was injected as described (de Lima et al., 2012). Zymosan and CPT-cAMP were injected intravitreally immediately after crush injury, and additional Zymosan at half the original dose plus CPT-cAMP at the original dose again 3 and 6 week later. For each intravitreal injection, a glass micropipette was inserted into the peripheral retina, just behind the ora serrata, and was deliberately angled to avoid damage to the lens. For optic nerve crush injury, the optic nerve was exposed intraorbitally and crushed with jeweler's forceps (Dumont #5; tip dimension, 0.1 × 0.06 mm) for 5 s approximately 1 mm behind the optic disc. Using retrograde and anterograde experiments, completeness of axotomy has been confirmed in our previous study (Park et al., 2008). Two to 7 days before sacrifice, l–2 μl of cholera toxin β subunit (CTB)-Alexa 555 (2 μg/μl, Invitrogen) was injected into the vitreous with a Hamilton syringe (Hamilton) to anterogradely label regenerating RGC axons. ALDH1L1-EGFP (Doyle et al., 2008; Yang et al., 2011), PLP-EGFP (Mallon et al., 2002) and CX3CR1-EGFP mice (Jung et al., 2000) received unilateral optic nerve crush. At 14–17 days later, optic nerves from these transgenic mice were treated for tissue clearance and analyzed for the distribution of glial cells in the injured optic nerve. Uninjured mice (C57BL/6 at 5 week old) with bilateral CTB tracing received intravitreal CTB-555 injection in the right eye and CTB-488 injection in the left eye.

AAVs

cDNA of Cre was inserted downstream of the CMV promoter/β-globin intron enhancer in the plasmid pAAV-MCS (Stratagene), containing the AAV2 inverted terminal repeats and a human growth hormone polyA signal. pAAV-RC (Stratagene) that encodes the AAV2 genes (rep and cap) and the helper plasmid (Stratagene) that encodes

E2A, E4 and VA were used for co-transfection of 293T cells to generate recombinant AAV. AAV2 viral particles were prepared by the University of Miami Viral Vector Core using an FPLC method to produce titers of approximately 4×10^{13} particles/mL.

Tissue preparation and clearing

Mice were perfused transcardially with PBS followed by 4% paraformaldehyde (PFA) in phosphate buffered saline (PBS) at 5 ml/min. The optic nerve and the brain were dissected and post-fixed with 4% PFA in PBS overnight. For histological sectioning, samples were cryoprotected by incubating in 30% sucrose overnight. For tissue clearing, samples were rinsed with PBS and stored at 4 °C until needed. Tissue clearing was performed as described (Becker et al., 2012; Erturk et al., 2012), with minor modifications. Samples underwent dehydration by incubation in increasing concentration of THF (Sigma-Aldrich) solutions under constant rocking. Optic nerves were incubated in 50% THF (diluted in water v/v), 80% THF (v/v) and 100% THF for 15 min each. Dehydrated optic nerve was rendered clear by incubating in BABB (a mixture of benzyl alcohol and benzyl benzoate (Sigma-Aldrich) at a ratio of 1:2) for 20 min. Adult mouse brain was incubated in 50% THF for 12 h, 80% THF for 12 h, 100% THF for 3 × 12 h, and BABB for 12 h before imaging.

LSFM (ultramicroscopy)

Ultramicroscope illuminates specimen with a thin sheet of light formed by two lenses, allowing imaging of large tissues, yet with cellular resolution (Fig. 1C). Ultramicroscopy was performed as previously described (Erturk et al., 2012). Between 100 and 500 optical slices were imaged. The scan speed was 0.5–1.5 s per section, which was about 2–3 min for the optic nerve and 5–10 min for the brain for a complete scan of the tissue. Images were collected at 2 to 5 μm increment in Z axis.

Image processing, neurite tracing and statistical analysis

Images, videos and 3D volume rendering were prepared using Imaris software v7.6.1 (Bitplane). CTB-labeled RGC axons in the optic nerve and brain were traced using Imaris Filament Tracer Module. To quantify the number of axons that regenerated long distances in the optic nerve, we counted the CTB-labeled fibers that crossed different distances from the lesion site after scanning through 100 to 200 individual horizontal optical slices. To quantify the number of axons that extended into different regions beyond the optic chiasm, we counted the CTB-labeled fibers that were found in the optic tracts, opposite optic nerve and hypothalamus after scanning through 100 to 300 individual horizontal optical slices. We used Student's t test for two group comparisons using SPSS statistics software.

Results

3D visualization of RGC axonal projections in uninjured mouse

In this study, we set out to apply tissue clearance and LSFM to evaluate regeneration of RGC axons without histological sectioning. Initially we visualized RGC axonal projections in the whole brain of uninjured animal. Adult mice received intravitreal injection of fluorophore-conjugated CTB, a lipophilic tracer used routinely to label CNS axons in regeneration studies. Seven days later, samples were processed for tissue clearance. THF-based clearing methods rendered mouse optic nerve and brain transparent to a large extent (Figs. 1A and B). A total of 1 h incubation in THF/BABB solutions was sufficient to clear the optic nerve, while it took approximately 3 days for the brain. Normally, RGCs send axons to central targets including the lateral geniculate nucleus (LGN) and superior colliculus (SC), which are
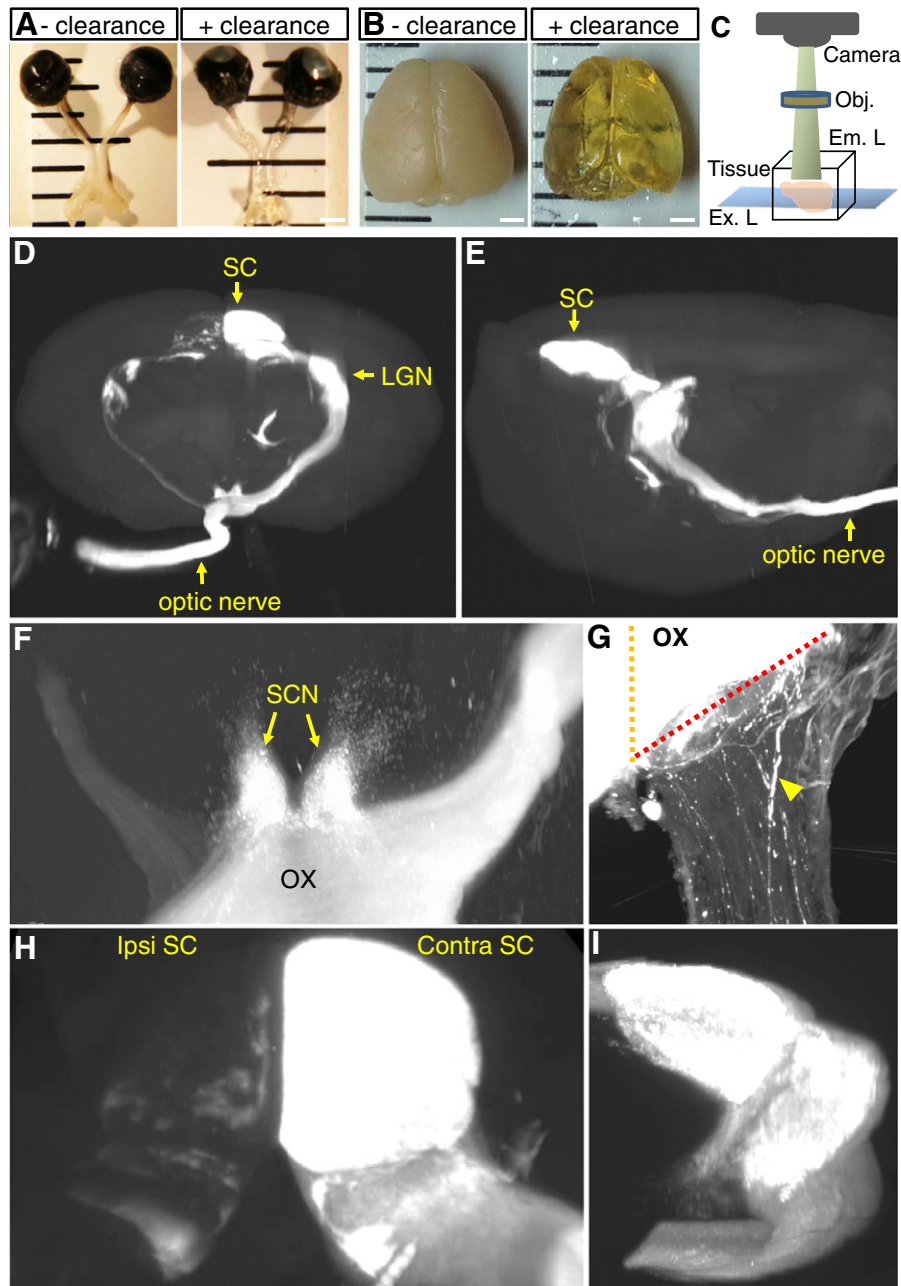
Fig. 1. Tetrahydrofuran (THF)-based tissue clearing and LSFM methods allow 3D visualization of RGC axonal projections in whole tissue. A, adult mouse optic nerve and chiasm, and B, whole brain before and after clearance with THF and BABB. C, principle of LSFM. Optic nerves and brains were cleared, and then imaged under an Ultramicroscope (LaVision Biotec). Horizontal optical slices were compiled using Imaris software for 3D reconstruction. D–I, snapshot images from 3D reconstruction video. Anterior, D and lateral, E views of a cleared brain displaying the trajectory of CTB-labeled RGC axons from the eye, through the chiasm and into the brain. All visual targets including the suprachiasmatic nucleus, lateral geniculate nucleus and superior colliculus both in the ipsilateral and contralateral sides of the brain can be clearly visualized. F–I, higher magnification images taken from 3D reconstruction showing axonal projections to the chiasm and SCN, and diverging into the ipsilateral and contralateral optic tracts in F, to the opposite optic nerve in G (arrowhead indicates CTB-labeled axons), ipsilateral and contralateral superior colliculus in H, and contralateral lateral geniculate nucleus in I. In G, yellow and red dotted lines represent the chiasm midline and the optic nerve-chiasm transition zone, respectively. Ex. L, excitation light; Em. L, emission light; Obj, objective; SC, superior colliculus; SCN, suprachiasmatic nucleus; LGN, lateral geniculate nucleus; ipsi, ipsilateral; contra, contralateral; OX, optic chiasm. Scale bars, 1 mm in A and B.

involved in image-forming visual functions. RGC axons also innervate the suprachiasmatic nucleus (SCN) and olivary pretectal nucleus (OPT) that are involved in non-image forming visual functions. After imaging the entire depth of the brain, approximately 500 optical slices (Movie 1) were compiled using Imaris software for 3D reconstruction. RGC axons can be visualized in 3D with remarkable detail along the entire visual pathway through the optic nerve, chiasm and optic tracts to the SCN, OPT, LGN, and SC (Figs. 1D–I, Movies 1 and 2). In mice, a small proportion of RGCs located in the ventro-temporal retina send

their axons to the ipsilateral brain. The ipsilateral projection stemming from the optic chiasm to the various brain regions is clearly visible (Movie 2), with axons terminating in the dorsal and ventral LGN (Figs. 1D–I), and in the different layers of the SC (Fig. 1H). We also detected several RGC axons (10–30 axons; n = 4) that turn at the optic chiasm and project to the opposite optic nerve (Fig. 1G), confirming that some axons are misrouted at the chiasm during development (Bunt et al., 1983). Together, we show that tissue clearance combined with LSFM allows 3D visualization of the entire optic pathway as well as

single axons that leave the main bundle, providing excellent details regarding the paths taken by RGC axons.

3D assessment of regenerating axons shows high degree of axon turning

Next, we assessed regenerating RGC axons following injury. To this end, we analyzed animals with genetic deletion of PTEN/SOCS3 in adult RGCs, together with intravitreal injection of CNTF, a condition known to promote long distance regeneration of many RGC axons after an optic nerve crush (Sun et al., 2011). Adult PTEN/SOCS3$^{f/f}$ mice received intravitreal injection of AAV2-Cre to induce PTEN/SOCS3 deletion in adult RGCs, followed by an intraorbital crush injury

2 weeks later (Sun et al., 2011). Animals received CNTF injection on the day of injury, at 3 day post-injury, and bi-weekly thereafter. Previously, we have demonstrated that AAV2-Cre at appropriate viral titers infects the majority of RGCs in adult mice (Park et al., 2008; Sun et al., 2011). Control animals received AAV-GFP injection. Two days prior to sacrifice, animals received CTB injection to label regenerating RGC axons. In control animals, a few axons sprouted short distances at the lesion site, but no axons were found beyond 1 mm from the lesion site at 17 day post-injury (n = 5; Fig. 2A, Movie 3). On the other hand, many axons extended into and beyond the lesion in PTEN/SOCS3 KO mice (Figs. 2A and E, Movie 4). The use of LSFM allowed comprehensive evaluation of three different aspects
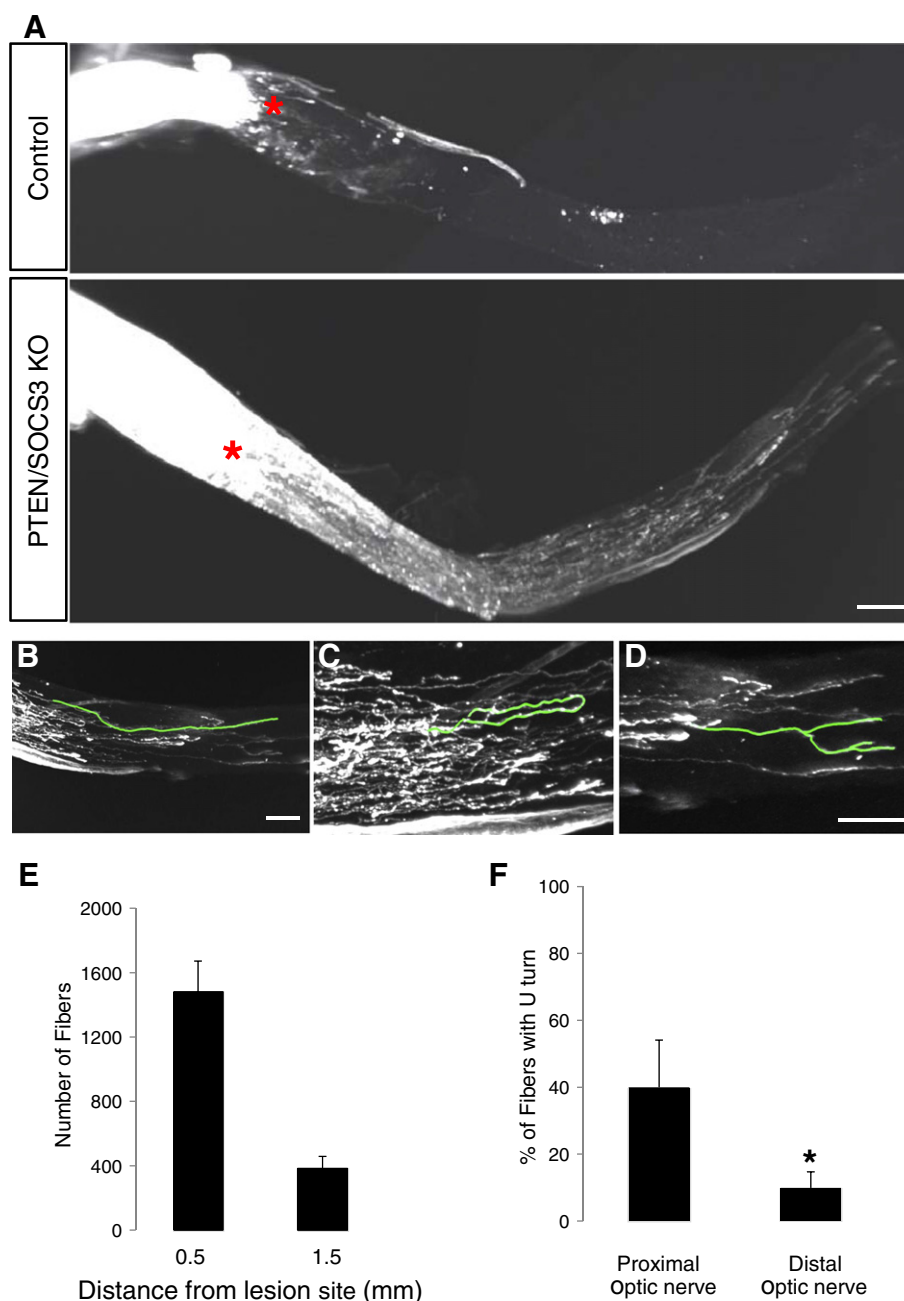
Fig. 2. 3D assessment of regenerated RGC axons in the cleared optic nerve. A, 3D reconstructed optic nerves of control AAV-GFP treated mice and PTEN/SOCS3 KO mice at 17 day post-injury. B–D, neurite tracing of single fiber showing different growth patterns. Some axons travel in a relatively straight along the optic nerve towards the chiasm (to the right side of the image) as shown in B, or loop back towards the eye (to the left side of the image) as shown in C. Some axons generate branches as they extend within the optic nerve as shown in D. E, quantification of the number of CTB-labeled axons found at different distances away from the lesion site (n = 5). Red asterisk, lesion site. *p < 0.01, Student's *t* test. Scale bars, 200 μm.

of axon growth that are difficult to obtain in histological sections. First, LSFM allowed direct counting of almost all fibers that have regenerated long distances through the optic nerve. By scanning through individual optical slices (i.e. z-stack images taken at 2–5 μm increments; a total of 150–200 optical slices/optic nerve), we could count individual CTB labeled fibers crossing different distances distal to the lesion site in PTEN/SOCS3 KO mice (n = 5; Fig. 2E). Second, it allowed unequivocal examination of the axonal trajectories along their regenerative paths, and where the regenerated axons terminate. Notably, we found that while a few RGC axons project relatively straight towards the brain (Fig. 2B), most axons have a meandering path. Many axons made sharp turns (often multiple occasions) with some axons reversing course and projecting towards the eye (Fig. 2C & Movie 4). These results are consistent with a recent study by Pernet et al., in which many axons that were induced to regenerate were shown to take circuitous paths in the optic nerve following elevation of CNTF (Pernet et al., 2012). We noticed in our study that these "turning events" seemed highly prevalent in the proximal nerve regions close to the lesion site. We traced the paths of axons (a total of 80 axons) within this proximal nerve region (i.e. a region covering 0.2–0.4 mm distal to the optic nerve head) and found that about 40% of axons made at least one U-turn (Fig. 2F). On the other hand, only about 10% of regenerating axons made U-turn in the more distal nerve region (i.e. 1–1.2 mm distal to the optic nerve head; Fig. 2F). We performed optic nerve crush in transgenic mice in which astrocytes, oligodendrocytes or microglial cells are labeled with EGFP to examine the correlation between the presence of glial cells and axon turning (Supplementary Fig. 1). After LSFM, we observed high astrocyte density in the proximal region of the optic nerve close to the lesion site in ALDH1L1-EGFP mice (n = 3; Supplementary Fig. 1). These results suggest that the nerve region with a high degree of axon turning may correspond to the areas with strong astroglial activation. Third, 3D visualization provided detailed examination of the axonal morphologies. For instance, it is clear that some RGC axons generate branches as they re-grow along the optic nerve (Fig. 2D & Movie 4), a morphogenetic process normally found in growing axons during nervous system development. Approximately 10–20% of axons traced in PTEN/SOCS3 KO showed at least one axonal branch. Together, we demonstrate that at present, tissue clearance combined with LSFM represents the most precise method to assess RGC axon regeneration, allowing unequivocal assessment of axonal trajectories and growth patterns in the optic nerve.

3D assessment of axonal projections to the brain

Recent studies from us and others demonstrated that PTEN KO alone or in combination with other strategies, such as SOCS3 deletion, promote long distance axon regeneration, with RGC axons projecting to the brain (de Lima et al., 2012; Kurimoto et al., 2010; Sun et al., 2011). Because histological sections provide incomplete spatial information about axonal trajectory and where RGC axons terminate in the brain, we applied LSFM to examine axonal projections in the brain. After imaging the entire brain, approximately 500 optical slices were compiled using Imaris software for 3D reconstruction. At 10 week post-injury, RGC axons were not detected in the optic chiasm or brain of AAV-GFP control animals (data not shown). In PTEN/SOCS3 KO animals however, many CTB-labeled regenerating axons reached the optic nerve/chiasm transition zone (OCTZ) (a mean of 119 fibers/animal; n = 8; SEM = 16.5). To evaluate the axonal projections through the optic chiasm and to the brain, we measured the number of axons projecting to different brain regions. In all animals examined (n = 8), similar or higher numbers of axons were found in the ipsilateral optic tract than in the contralateral optic tract (Figs. 3E and G, Movie 5). In all animals, we observed that a small percentage of RGC axons also extend into the opposite uninjured optic nerve (Figs. 3E and G, Movie 5). Some axons appeared to be inhibited from entering the OCTZ, or turn sharply at the OCTZ before continuing to project into the optic tracts

(Fig. 3B). In the brain, a few axons extended medial-dorsally into the hypothalamic brain regions including the SCN and medial pre-optic area, while some axons exited the optic tracts to reach the lateral hypothalamus (Figs. 3C and D, Supplementary Fig. 2). In some animals, we found regenerating axons in abnormal regions that are not typically associated with the optic pathway including the fornix and extended amygdala (unpublished data). RGC axons were not detected in the more distant visual targets including LGN or SC (Fig. 3, Supplementary Fig. 2, Movie 5). We also examined axon regeneration in animals subjected to shorter and longer survival times (i.e. 8 and 16 weeks after injury; unpublished data). However, among these time points, we observed the greatest degree of axon regeneration (i.e. axon number and length in the brain) in the brain at 10 week post-injury time point.

To ensure that the axonal projections observed using LSFM are not under-represented by potential loss of CTB signal during the clearing procedure, LSFM results were corroborated by examining fibers in coronal brain sections from a separate set of animals (n = 8). In coronal sections, CTB-labeled RGC axons were found mainly in the hypothalamus region including the SCN, anterior hypothalamic area and ventromedial hypothalamus (Supplementary Fig. 2). Laterally, some axons travelled short distances within the degenerated optic tracts. RGC axons were not found in the more distant targets, LGN and SC (Supplementary Fig. 2). Immunohistochemical staining of the brain sections using CTB antibody to amplify the signal did not detect regenerated axons in midbrain targets, LGN and SC.

3D assessment of axonal projection in PTEN KO/Zymosan/cAMP analogue-treated mice

It was recently reported that PTEN KO combined with Zymosan and the cAMP analogue (PTEN KO/ZYM/cAMP) promotes extensive long distance regeneration of RGC axons. Strikingly, regenerating RGC axons in these mice were reported to re-innervate all the major visual targets including the OPT, LGN and SC (de Lima et al., 2012). Thus, we applied LSFM to examine axon regeneration to the brain in PTEN KO/ZYM/cAMP mice. Adult PTEN$^{f/f}$ mice received an intravitreal AAV-Cre injection 2 weeks prior to a crush injury, and Zymosan and the cAMP analogue were administered during the survival time as previously described (de Lima et al., 2012). At 10 to 12 weeks after injury, the optic nerves and brains were cleared using THF and imaged with the LSFM. Five to 7 days prior to sacrifice, CTB was injected to label the regenerating axons. As expected, many axons regenerated long distances in the optic nerve of the PTEN KO/ZYM/cAMP mice (Fig. 4B). Similar to the axon number reported previously (de Lima et al., 2012), many RGC axons (a mean of 112 fibers/animal; n = 9; SEM = 19.5) elongated long distances (4–5 mm distal to the lesion site) to reach the optic chiasm (Fig. 4B). In the brain, the axonal projection was similar to that of PTEN/SOCS3 KO mice. In general, similar or higher numbers of axons were found in the ipsilateral optic tract than in the contralateral optic tract (Figs. 4E and G). A few RGC axons extended into the opposite uninjured optic nerve (Figs. 4E and G), while others projected dorsally to the SCN (Supplementary Fig. 3). Some axons also exited the optic tracts and extended into the lateroanterior hypothalamic nucleus or supraoptic nucleus. RGC axons were not detected in the OPT, LGN and SC (Supplementary Fig. 3).

3D assessment of axonal projections following bilateral optic nerve crush

The optic chiasm is a region where RGC axons from each eye meet (Movie 6). As previously mentioned, some regenerating axons made sharp turns upon reaching the optic chiasm, suggesting that intact axons from the contralateral eye may affect the trajectory of regenerating axons in this region. To examine this possibility, we carried out a bilateral crush experiment. AAV-Cre/rCNTF was injected into the left eye of PTEN/SOCS3 floxed mice, followed by crush on both optic nerves 2 weeks later. At 10 weeks after bilateral crush
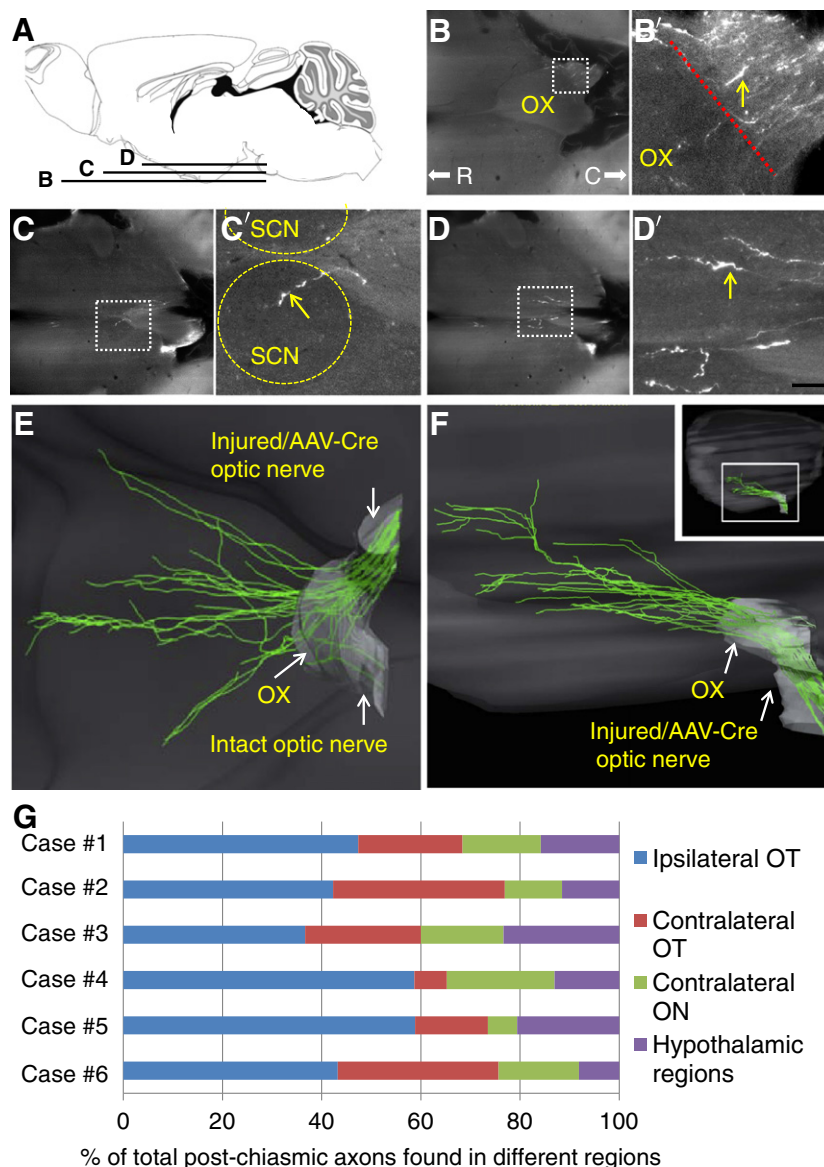
Fig. 3. 3D visualization of axonal projections in the brain. A, schematic diagram of mouse brain showing horizontal planes at which individual optical slices in B–D are derived from. B–D, several representative horizontal optical slices collected from an unsectioned brain of PTEN/SOCS3 KO animal following LSFM. B′–D′, higher magnification of the respective white boxed area in B–D. Yellow arrows indicate CTB-labeled axons. CTB-labeled axons are found immediately before the optic chiasm as shown in B. Some axons extended medial-dorsally into the hypothalamic brain regions including the SCN as shown in C, and medial pre-optic area as shown in D. E, ventral view of the 3D reconstruction of traced fibers near the optic chiasm. Neurite tracing and 3D volume rendering were done using Imaris software. F, lateral view of the 3D reconstruction of axonal projections into the brain. Inset shows low magnification of the whole brain following 3D reconstruction. G, quantification of axonal trajectory into different regions (i.e. ipsi/contralateral optic tracts, opposite optic nerve or hypothalamic regions). Values are presented as percentages of total axons that have exited the optic chiasm in 6 individual animals (case #1–6). C, caudal; ON, optic nerve; OT, optic tract; OX, optic chiasm; R, rostral; SCN, suprachiasmatic nucleus. Scale bar, 100 μm in D.

injury, we observed that while similar numbers of axons regenerated up to the optic chiasm compared to the animals receiving a unilateral crush, higher numbers of axons regenerated into and beyond the optic chiasm. However, the overall trajectory pattern at the optic chiasm was similar compared to unilateral crush. Similar or higher numbers of axons extended into the ipsilateral optic tract than to the contralateral optic tract, with a few axons extending also into the opposite optic nerve. Some axons projected dorsally to reach the SCN, or medial pre-optic area (Fig. 5).

Discussion

We have applied tissue clearance and LSFM to obtain a comprehensive assessment of RGC axon regeneration after injury. Using these methods, we were able to image the entire mouse optic nerve

and brain, providing 3D visualization of the optic pathways from the eye through the brain. This approach allowed not only visualization of the main axon bundles that make up the visual pathway in normal animals, but it also enabled detection of single axons that leave the main pathway to stream into aberrant regions. For instance, in all uninjured control mice examined, between 10 and 30 axons were found to turn at the optic chiasm and project long distances into the contralateral optic nerve, confirming that some RGC axons are misrouted at the chiasm during development and persist in the adult (Bunt et al., 1983). Thus, these results highlight the strength of 3D imaging to detect small numbers of axons that would have been difficult to identify in histological sections. In addition to observing axonal trajectories, we also found that some RGC axons generate branches as they regenerate. During development, RGC axons generate branches to connect with multiple synaptic targets, a process
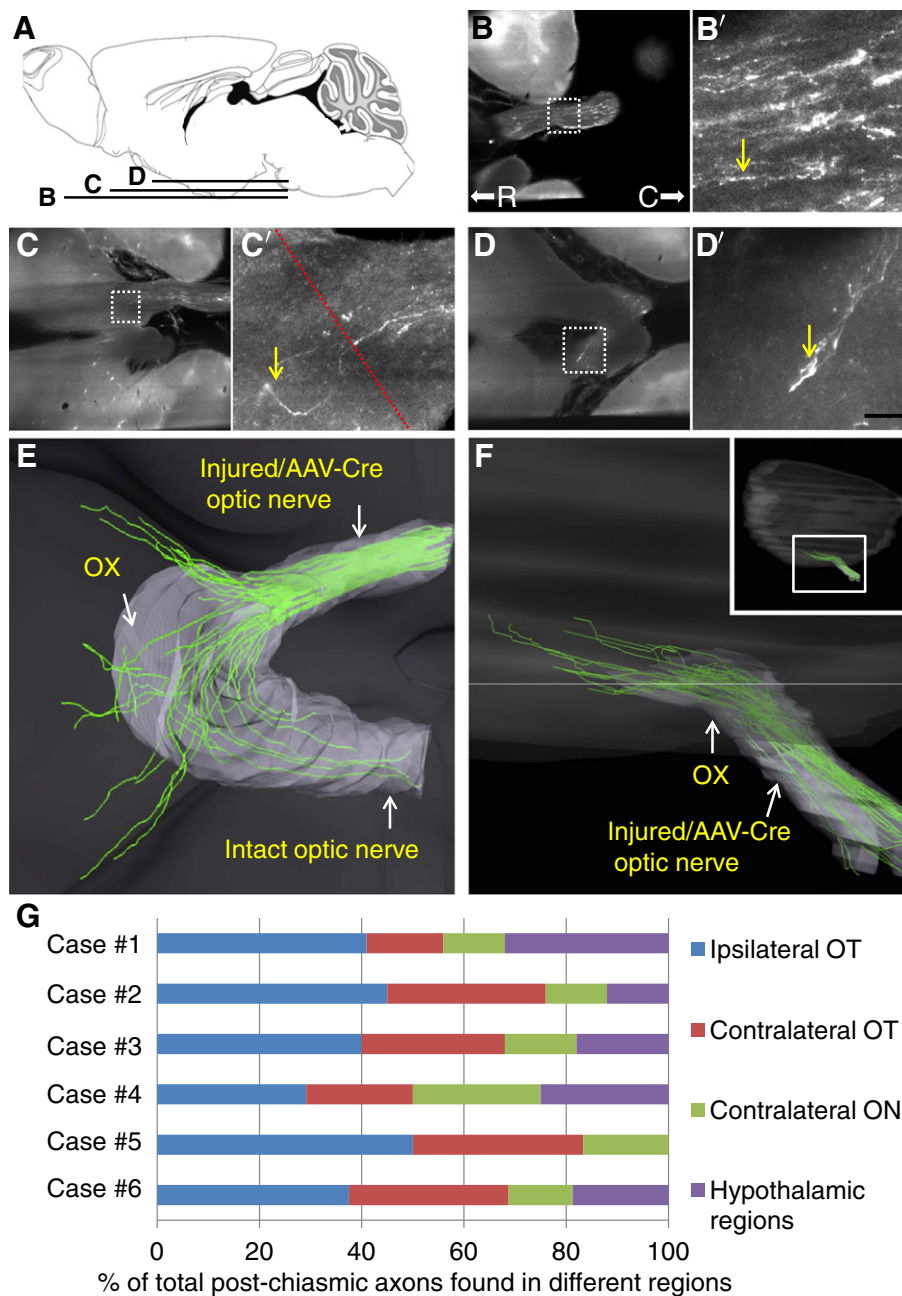
Fig. 4. 3D visualization of axonal projections in the brain of PTEN KO/ZYM/cAMP mice. A, schematic diagram of mouse brain showing horizontal planes at which the images in B–D are derived from. B–D, several representative horizontal optical slices collected from an unsectioned brain of PTEN KO/ZYM/cAMP animal following LSFM. B′–D′, higher magnification of the respective white boxed area in B–D. Yellow arrows indicate CTB-labeled axons. CTB-labeled axons are found in the distal optic nerve near the optic chiasm as shown in B, in the SCN as shown in C and in the optic tract as shown in D. E, ventral view of the 3D reconstruction of traced fibers near the optic chiasm. F, lateral view of the 3D reconstruction of axonal projections into the brain. Inset shows low magnification of the whole brain following 3D reconstruction. G, quantification of axonal trajectory into different regions (i.e. ipsi/contralateral optic tracts, opposite optic nerve or hypothalamic regions). Values are presented as percentages of total axons that have exited the optic chiasm in 6 individual animals (case #1–6). Red dotted line in C′ represents optic nerve-optic chiasm transition zone. C, caudal; ON, optic nerve; OT, optic tract; OX, optic chiasm; R, rostral; SCN, suprachiasmatic nucleus. Scale bar, 100 μm in D.

known to be regulated in part by target-derived trophic factors such as nerve growth factor and brain derived neurotrophic factor (Gibson and Ma, 2011). Although some regenerated axons in our study generated branches prematurely within optic nerve, other axons generated branches in the hypothalamus, raising the possibility that the regenerated axons could, in principle, re-establish connections with multiple synaptic targets in the adults. LSFM also allowed more accurate determination of regenerating fiber numbers. While it was challenging to directly count the axons close to the lesion because of the dense axonal projection, we were able to directly count virtually all axons that regenerated long distances.

To innervate the visual targets in the brain, regenerating RGC axons must travel long distance along the optic nerve and then correctly pathfind through various regions in the brain. While it has been a major challenge to develop strategies that stimulate RGC axons to regenerate long distances in the first place, studies over the past several years have shown that this is feasible, at least for some RGCs. For example, in adult Bcl-2tg mice, virally-induced over-expression of CNTF promotes long distance regeneration to the optic chiasm (Leaver et al., 2006). Very recently, Pernet et al., demonstrated that the expression of CNTF using AAV2 alone induces long distance regeneration of RGC axons in wild type mice (Pernet et al.,
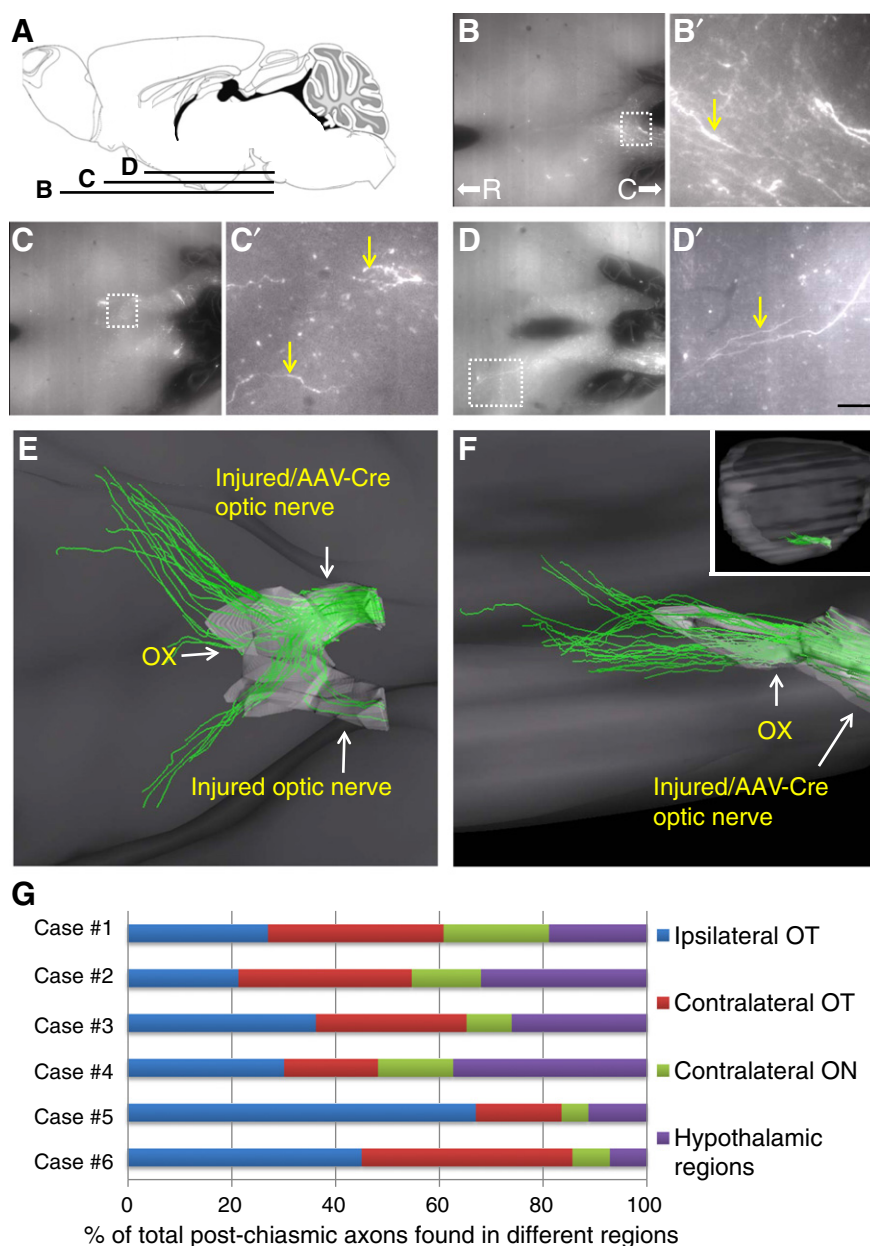
Fig. 5. 3D visualization of axonal projections in the brain following bilateral optic nerve crush. A, schematic diagram of mouse brain showing horizontal planes at which the images in B–D are derived from. B–F, several representative horizontal optical slices collected from an unsectioned brain of PTEN/SOCS3 KO animal following LSFM. B′–D′, higher magnification of the respective white boxed area in B–F. Yellow arrows indicate CTB-labeled axons. CTB-labeled axons extend through the optic chiasm and into the optic tracts and hypothalamus. E, ventral view of the 3D reconstruction of traced fibers near the optic chiasm. F, lateral view of the 3D reconstruction of axonal projections into the brain. Inset shows low magnification of the whole brain following 3D reconstruction. G, quantification of axonal trajectory into different regions (i.e. ipsi/contralateral optic tracts, opposite optic nerve or hypothalamic regions). Values are presented as percentages of total axons that have exited the optic chiasm in 6 individual animals (case #1–6). C, caudal; ON, optic nerve; OT, optic tract; OX, optic chiasm; R, rostral; SCN, suprachiasmatic nucleus. Scale bar, 100 μm in D.

2012). In addition, PTEN deletion in RGCs, combined with SOCS3 deletion/CNTF injection (Sun et al., 2011), or with Zymosan and cAMP analogue (de Lima et al., 2012; Kurimoto et al., 2010) promoted extensive long distance regeneration in the optic nerve, allowing some RGC axons to reach into the brain. Using LSFM, we observed that many axons grew in tortuous paths in the optic nerve, making multiple turns, and often projecting back to the eye. Thus, our data are in agreement with the recent study from Pernet et al., in which extensive axon turning was evident in optic nerves of animals treated with AAV-CNTF (Pernet et al., 2012). Collectively, these studies indicate that there is considerable axon misguidance within the injured

optic nerve during regeneration, which may limit some RGC axons extending into the brain and ultimately to their targets.

During development, de novo RGC axons enter the optic nerve and travel in a fasciculated manner towards the brain. This process is tightly regulated by signaling molecules expressed and released by neuronal and non-neuronal cells in the interstitial spaces and the extracellular matrix. For example, Sema5A which is found on neuroepithelial cells surrounding the retinal axons along the optic nerve, was shown to induce growth cone collapse, and antibodies against SemaA5 cause retinal axons to escape from the optic nerve bundle (Oster et al., 2003). Other axon repulsive cues such as myelin associated glycoproteins, semaphorins,

ephrins, chondroitin sulfate proteoglycans (CSPGs) and their respective receptors have also been shown to be expressed in the injured retina and optic nerve (Cai et al., 2012; Du et al., 2007; Goldberg et al., 2004; Hunt et al., 2003; Liu et al., 2006; Park et al., 2008; Selles-Navarro et al., 2001; Shirvan et al., 2002), and could, in principle, contribute to the heterogeneous axon growth patterns seen in the optic nerves. In ALDH1L1-EGFP tg mice in which astrocytes are labeled with EGFP, strong astroglial activation is seen in the nerve regions close to the lesion site. Given that axon turning in PTEN/SOCS3 KO mice was especially prevalent in these regions, it is plausible that high concentration of CSPGs and other repulsive factors (or growth factors) released by reactive astrocytes may contribute to the extensive axon turning. It is currently unclear to what extent these and other growth inhibitory (or attractive) cues present in the injured optic nerve contribute to the aberrant axon trajectories observed in the adult optic nerve.

One major decision point for growing RGC axons en route to their central targets is the optic chiasm where axons must decide whether or not to cross. The majority of animals in our study had similar or higher numbers of axons extending to the ipsilateral side of the brain than the contralateral side. This observation is consistent with the previous report demonstrating large ipsilateral projections of regenerating RGC axons in perinatal Bcl-2 transgenic mice (Cho et al., 2005). Potentially, intact RGC axons from the opposite eye could affect the course of growing axons at the optic chiasm. For instance, previous studies in frogs have demonstrated that the number of axons that regenerate to the opposite nerve is less in animals subjected to a bilateral optic nerve lesion compared to unilaterally lesioned animals (Bohn and Stelzner, 1981). On the other hand, studies using a prechiasmic lesion in adult rats showed no obvious difference in the divergence patterns of regenerating axons at the optic chiasm between animals subjected to bilateral and unilateral crush (Berry et al., 1999). Consistent with this latter study, the overall divergence pattern at the optic chiasm was similar in both of our injury models in mice, supporting the idea that interactions between regenerating axons and the intact axons from the uninjured eye may not be responsible for establishing the aberrant trajectories.

Axonal pathfinding at the optic chiasm during development is regulated by EphB1/ephrinB2 signaling: the Ephb1 receptor is expressed in a small population of RGCs, and axons extending from these RGCs are repelled by ephrinB2 ligand expressed in the chiasm midline, thus giving rise to the ipsilateral projection (Williams et al., 2003). Other guidance cues and receptors involved in pathfinding through the chiasm during nervous system development include Zic2, NrCAM, Islet-1, Plexin-A1 and semaphorin6D (Herrera et al., 2003; Kuwajima et al., 2012; Pak et al., 2004; Petros et al., 2008; Williams et al., 2006). The expression levels of Eph1B and ephrinB2 in the adult mouse retina and optic chiasm, and whether the higher percentage of ipsilaterally projecting axons seen in these studies are due to EphB1/ephrinB2 signaling or other aforementioned guidance factors is not yet known. Nonetheless, our results indicate that the molecular and cellular mechanisms that once guided axons through the optic chiasm during development are not preserved in adult mice.

With the recent progress made in promoting long distance regeneration in the optic nerve, a pressing question is to what extent do these axons navigate correctly to re-innervate their central targets? In both PTEN/SOCS3 KO and PTEN KO/ZYM/cAMP mice, RGC axons projected dorsally into the hypothalamus or short distances laterally to the optic tracts or projected to the uninjured contralateral optic nerve. Centrally, axonal projections were limited primarily to the hypothalamus. Thus, our findings are in contrast to the previous study using PTEN KO/ZYM/cAMP mice in which many regenerating axons were reported to elongate long distances within the brain, correctly navigating and re-innervating all the major visual targets including the SCN, OPT, MTN, LGN and SC (de Lima et al., 2012). The reasons behind these differing results are not clear. Of note, in this present study, similar number of axons regenerated long distances up to the

optic chiasm in the PTEN KO/ZYM/cAMP treated mice as reported previously (de Lima et al., 2012), confirming the effectiveness of this combinatorial approach in promoting RGC axon regeneration.

In nearly all animals, regenerating axons were found in the SCN, the master pacemaker of circadian rhythm. In normal mammals, the SCN receives axons predominantly from melanopsin expressing-intrinsically photosensitive RGCs (ipRGCs). These RGCs directly send photic information to the SCN which in turn regulates daily rhythmicity such as sleep, body temperature and food intake (Do and Yau, 2010; Schmidt et al., 2011). This raises questions as to whether or to what extent the regenerated RGC axons found in the SCN originate from the ipRGCs, and whether they form functional synaptic connections with the SCN neurons. In addition, our results demonstrated that some axons generated branches, raising a question as to whether axonal branching during regeneration is a feature unique to a specific RGC subset, or occurs at random in any regenerating RGC axon. The combined use of tissue clearance and 3D visualization together with transgenic mice in which axons from known subtypes of RGCs are GFP-labeled may facilitate addressing these questions. In summary, we demonstrated, for the first time, integration of tissue clearance and LSFM for comprehensive analysis of RGC axon regeneration in mouse models. Our study shows misdirected growth in the optic nerve and brain, indicating that the adult mammalian CNS lacks the signals necessary for proper pathfinding of regenerating RGC axons.

Supplementary data to this article can be found online at http://dx.doi.org/10.1016/j.expneurol.2013.03.001.

Acknowledgments

References

Beazley, L.D., Sheard, P.W., Tennant, M., Starac, D., Dunlop, S.A., 1997. Optic nerve regenerates but does not restore topographic projections in the lizard *Ctenophorus ornatus*. J. Comp. Neurol. 377, 105–120.

Becker, C.G., Becker, T., 2007. Growth and pathfinding of regenerating axons in the optic projection of adult fish. J. Neurosci. Res. 85, 2793–2799.

Becker, K., Jahrling, N., Saghafi, S., Weiler, R., Dodt, H.U., 2012. Chemical clearing and dehydration of GFP expressing mouse brains. PLoS One 7, e33916.

Berry, M., Carlile, J., Hunter, A., Tsang, W., Rosenstiel, P., Sievers, J., 1999. Optic nerve regeneration after intravitreal peripheral nerve implants: trajectories of axons regrowing through the optic chiasm into the optic tracts. J. Neurocytol. 28, 721–741.

Bohn, R.C., Stelzner, D.J., 1981. The aberrant retinol–retinal projection during optic nerve regeneration in the frog. III. Effects of crushing both nerves. J. Comp. Neurol. 196, 633–643.

Bunt, S.M., Lund, R.D., Land, P.W., 1983. Prenatal development of the optic projection in albino and hooded rats. Brain Res. 282, 149–168.

Cai, X., Yuan, R., Hu, Z., Chen, C., Yu, J., Zheng, Z., Ye, J., 2012. Expression of PirB protein in intact and injured optic nerve and retina of mice. Neurochem. Res. 37, 647–654.

Cho, K.S., Yang, L., Lu, B., Feng Ma, H., Huang, X., Pekny, M., Chen, D.F., 2005. Re-establishing the regenerative potential of central nervous system axons in postnatal mice. J. Cell Sci. 118, 863–872.

de Lima, S., Koriyama, Y., Kurimoto, T., Oliveira, J.T., Yin, Y., Li, Y., Gilbert, H.Y., Fagiolini, M., Martinez, A.M., Benowitz, L., 2012. Full-length axon regeneration in the adult mouse optic nerve and partial recovery of simple visual behaviors. Proc. Natl. Acad. Sci. U. S. A. 109, 9149–9154.

Do, M.T., Yau, K.W., 2010. Intrinsically photosensitive retinal ganglion cells. Physiol. Rev. 90, 1547–1581.

Doyle, J.P., Dougherty, J.D., Heiman, M., Schmidt, E.F., Stevens, T.R., Ma, G., Bupp, S., Shrestha, P., Shah, R.D., Doughty, M.L., Gong, S., Greengard, P., Heintz, N., 2008. Application of a translational profiling approach for the comparative analysis of CNS cell types. Cell 135, 749–762.

Du, J., Tran, T., Fu, C., Sretavan, D.W., 2007. Upregulation of EphB2 and ephrin-B2 at the optic nerve head of DBA/2J glaucomatous mice coincides with axon loss. Invest. Ophthalmol. Vis. Sci. 48, 5567–5581.

Duffy, P., Wang, X., Seigel, C.S., Tu, N., Henkemeyer, M., Cafferty, W.B., Strittmatter, S.M., 2012. Myelin-derived ephrinB3 restricts axonal regeneration and recovery after adult CNS injury. Proc. Natl. Acad. Sci. U. S. A. 109, 5063–5068.

Erturk, A., Mauch, C.P., Hellal, F., Forstner, F., Keck, T., Becker, K., Jahrling, N., Steffens, H., Richter, M., Hubener, M., Kramer, E., Kirchhoff, F., Dodt, H.U., Bradke, F., 2012. Three-dimensional imaging of the unsectioned adult spinal cord to assess axon regeneration and glial responses after injury. Nat. Med. 18, 166–171.

Gibson, D.A., Ma, L., 2011. Developmental regulation of axon branching in the vertebrate nervous system. Development 138, 183–195.

Goldberg, J.L., Vargas, M.E., Wang, J.T., Mandemakers, W., Oster, S.F., Sretavan, D.W., Barres, B.A., 2004. An oligodendrocyte lineage-specific semaphorin, Sema5A, inhibits axon growth by retinal ganglion cells. J. Neurosci. 24, 4989–4999.

Groszer, M., Erickson, R., Scripture-Adams, D.D., Lesche, R., Trumpp, A., Zack, J.A., Kornblum, H.I., Liu, X., Wu, H., 2001. Negative regulation of neural stem/progenitor cell proliferation by the PTEN tumor suppressor gene in vivo. Science 294, 2186–2189.

Herrera, E., Brown, L., Aruga, J., Rachel, R.A., Dolen, G., Mikoshiba, K., Brown, S., Mason, C.A., 2003. Zic2 patterns binocular vision by specifying the uncrossed retinal projection. Cell 114, 545–557.

Hunt, D., Coffin, R.S., Prinjha, R.K., Campbell, G., Anderson, P.N., 2003. Nogo-A expression in the intact and injured nervous system. Mol. Cell. Neurosci. 24, 1083–1102.

Jung, S., Aliberti, J., Graemmel, P., Sunshine, M.J., Kreutzberg, G.W., Sher, A., Littman, D.R., 2000. Analysis of fractalkine receptor CX(3)CR1 function by targeted deletion and green fluorescent protein reporter gene insertion. Mol. Cell. Biol. 20, 4106–4114.

Kurimoto, T., Yin, Y., Omura, K., Gilbert, H.Y., Kim, D., Cen, L.P., Moko, L., Kugler, S., Benowitz, L.I., 2010. Long-distance axon regeneration in the mature optic nerve: contributions of oncomodulin, cAMP, and PTEN gene deletion. J. Neurosci. 30, 15654–15663.

Kuwajima, T., Yoshida, Y., Takegahara, N., Petros, T.J., Kumanogoh, A., Jessell, T.M., Sakurai, T., Mason, C., 2012. Optic chiasm presentation of Semaphorin6D in the context of Plexin-A1 and Nr-CAM promotes retinal axon midline crossing. Neuron 74, 676–690.

Leaver, S.G., Cui, Q., Plant, G.W., Arulpragasam, A., Hisheh, S., Verhaagen, J., Harvey, A.R., 2006. AAV-mediated expression of CNTF promotes long-term survival and regeneration of adult rat retinal ganglion cells. Gene Ther. 13, 1328–1341.

Lingor, P., Tonges, L., Pieper, N., Bermel, C., Barski, E., Planchamp, V., Bahr, M., 2008. ROCK inhibition and CNTF interact on intrinsic signalling pathways and differentially regulate survival and regeneration in retinal ganglion cells. Brain 131, 250–263.

Liu, X., Hawkes, E., Ishimaru, T., Tran, T., Sretavan, D.W., 2006. EphB3: an endogenous mediator of adult axonal plasticity and regrowth after CNS injury. J. Neurosci. 26, 3087–3101.

Mallon, B.S., Shick, H.E., Kidd, G.J., Macklin, W.B., 2002. Proteolipid promoter activity distinguishes two populations of NG2-positive cells throughout neonatal cortical development. J. Neurosci. 22, 876–885.

Moore, D.L., Blackmore, M.G., Hu, Y., Kaestner, K.H., Bixby, J.L., Lemmon, V.P., Goldberg, J.L., 2009. KLF family members regulate intrinsic axon regeneration ability. Science 326, 298–301.

Muller, A., Hauk, T.G., Fischer, D., 2007. Astrocyte-derived CNTF switches mature RGCs to a regenerative state following inflammatory stimulation. Brain 130, 3308–3320.

Oster, S.F., Bodeker, M.O., He, F., Sretavan, D.W., 2003. Invariant Sema5A inhibition serves an ensheathing function during optic nerve development. Development 130, 775–784.

Pak, W., Hindges, R., Lim, Y.S., Pfaff, S.L., O'Leary, D.D., 2004. Magnitude of binocular vision controlled by islet-2 repression of a genetic program that specifies laterality of retinal axon pathfinding. Cell 119, 567–578.

Park, K.K., Liu, K., Hu, Y., Smith, P.D., Wang, C., Cai, B., Xu, B., Connolly, L., Kramvis, I., Sahin, M., He, Z., 2008. Promoting axon regeneration in the adult CNS by modulation of the PTEN/mTOR pathway. Science 322, 963–966.

Paxinos, G., Franklin, K.B.J., 2004. The Mouse Brain in Stereotaxic Coordinates, Compact2nd edn. Elsevier Academic Press, Amsterdam; Boston.

Pernet, V., Joly, S., Dalkara, D., Jordi, N., Schwarz, O., Christ, F., Schaffer, D.V., Flannery, J.G., Schwab, M.E., 2012. Long-distance axonal regeneration induced by CNTF gene transfer is impaired by axonal misguidance in the injured adult optic nerve. Neurobiol. Dis. 51, 202–213.

Petros, T.J., Rebsam, A., Mason, C.A., 2008. Retinal axon growth at the optic chiasm: to cross or not to cross. Annu. Rev. Neurosci. 31, 295–315.

Qiu, J., Cai, D., Filbin, M.T., 2002. A role for cAMP in regeneration during development and after injury. Prog. Brain Res. 137, 381–387.

Schmidt, T.M., Chen, S.K., Hattar, S., 2011. Intrinsically photosensitive retinal ganglion cells: many subtypes, diverse functions. Trends Neurosci. 34, 572–580.

Selles-Navarro, I., Ellezam, B., Fajardo, R., Latour, M., McKerracher, L., 2001. Retinal ganglion cell and nonneuronal cell responses to a microcrush lesion of adult rat optic nerve. Exp. Neurol. 167, 282–289.

Shirvan, A., Kimron, M., Holdengreber, V., Ziv, I., Ben-Shaul, Y., Melamed, S., Melamed, E., Barzilai, A., Solomon, A.S., 2002. Anti-semaphorin 3A antibodies rescue retinal ganglion cells from cell death following optic nerve axotomy. J. Biol. Chem. 277, 49799–49807.

Smith, P.D., Sun, F., Park, K.K., Cai, B., Wang, C., Kuwako, K., Martinez-Carrasco, I., Connolly, L., He, Z., 2009. SOCS3 deletion promotes optic nerve regeneration in vivo. Neuron 64, 617–623.

Stelzner, D.J., Bohn, R.C., Strauss, J.A., 1986. Regeneration of the frog optic nerve. Comparisons with development. Neurochem. Pathol. 5, 255–288.

Su, Y., Wang, F., Zhao, S.G., Pan, S.H., Liu, P., Teng, Y., Cui, H., 2008. Axonal regeneration after optic nerve crush in Nogo-A/B/C knockout mice. Mol. Vis. 14, 268–273.

Sun, F., Park, K.K., Belin, S., Wang, D., Lu, T., Chen, G., Zhang, K., Yeung, C., Feng, G., Yankner, B.A., He, Z., 2011. Sustained axon regeneration induced by co-deletion of PTEN and SOCS3. Nature 480, 372–375.

Williams, S.E., Grumet, M., Colman, D.R., Henkemeyer, M., Mason, C.A., Sakurai, T., 2006. A role for Nr-CAM in the patterning of binocular visual pathways. Neuron 50, 535–547.

Williams, S.E., Mann, F., Erskine, L., Sakurai, T., Wei, S., Rossi, D.J., Gale, N.W., Holt, C.E., Mason, C.A., Henkemeyer, M., 2003. Ephrin-B2 and EphB1 mediate retinal axon divergence at the optic chiasm. Neuron 39, 919–935.

Winzeler, A.M., Mandemakers, W.J., Sun, M.Z., Stafford, M., Phillips, C.T., Barres, B.A., 2011. The lipid sulfatide is a novel myelin-associated inhibitor of CNS axon outgrowth. J. Neurosci. 31, 6481–6492.

Wong, E.V., David, S., Jacob, M.H., Jay, D.G., 2003. Inactivation of myelin-associated glycoprotein enhances optic nerve regeneration. J. Neurosci. 23, 3112–3117.

Yang, Y., Vidensky, S., Jin, L., Jie, C., Lorenzini, I., Frankl, M., Rothstein, J.D., 2011. Molecular comparison of GLT1 + and ALDH1L1 + astrocytes in vivo in astroglial reporter mice. Glia 59, 200–207.

CHAPTER SEVEN

Neuron-Intrinsic Inhibitors of Axon Regeneration: PTEN and SOCS3

Xueting Luo, Kevin K. Park[1]
Miami Project to Cure Paralysis, Department of Neurological Surgery, University of Miami Miller School of Medicine, Miami, Florida, USA
[1]Corresponding author: e-mail address: kpark@med.miami.edu

Contents

Abstract

Our understanding of how axon regeneration is controlled in both the peripheral and central nervous systems remains fragmentary. Research into the regenerative capacity of adult neurons has elucidated PTEN and SOCS3 as distinctive but complementary arms of the regenerative program. These molecules act as negative regulators of major signaling pathways and impact the processes occurring in the cell body, such as protein translation and transcription, and in the axons, such as cytoskeleton assembly. In this review, we summarize the role of PTEN and SOCS3 in limiting axon regeneration and discuss the molecular and cellular mechanisms underlying their growth-inhibitory effects.

141

1. INTRODUCTION

Neurons of the mammalian central nervous system (CNS) generally do not regenerate axons after injury, whereas those of the peripheral nervous system (PNS) do. What accounts for such a disparity in the regenerative ability between these two systems? This question has been a subject of intense investigation in neuroscientific research. The past decade has seen much progress toward understanding why injured CNS axons fail to regenerate. One contributing factor is the growth-inhibitory environment of the CNS, with several constituents of the CNS myelin and glial scar at the lesion site identified as barriers of axon regeneration (Filbin, 2003; Fitch & Silver, 2008; Yiu & He, 2006). Accordingly, pharmacological and genetic strategies that neutralize these extrinsic inhibitors yielded some degree of axon regeneration. However, while some injured axons are able to regrow into the permissive grafts, the majority of adult neurons fail to regenerate axons even when provided with permissive substrates (Aguayo, David, & Bray, 1981; Aguayo et al., 1990; Richardson, McGuinness, & Aguayo, 1980). Thus, the prevailing view is that, in addition to the environmental impediments, axon regeneration failure is due also to a limited growth capacity of adult CNS neurons. What neuron-intrinsic factors could limit axon regeneration in the mammalian CNS? Advances in our ability to modulate gene expression in cell-specific and time-specific manners using genetically modified animals, as well as the emergence of high-throughput screening techniques have transformed our ways of investigating this question. Researches utilizing these and other analytical models have elucidated several genetic and molecular signatures within neurons that influence intrinsic regenerative capacity. They indicate that the sequential steps of axon regeneration from growth cone generation and axon extension require modulation of gene transcription and protein translation at the cell body and axonal level. Recently, considerable attention has been paid to two intracellular signaling components that mediate these processes to influence intrinsic axon regrowth capacity in both the PNS and CNS: PTEN (phosphatase and tensin homologue) and SOCS3 (suppressor of cytokine signaling 3). In this review, we describe and summarize the participation of the PTEN and SOCS3 pathways in the regulation of the process of axon growth and regeneration. We also discuss the potential molecular and cellular mechanisms by which these signaling pathways regulate such processes.

2. PTEN: A NEGATIVE REGULATOR OF CELL AND AXON GROWTH

Activation of phosphoinositide 3-kinase (PI3K) in response to a variety of extracelluar stimuli including growth factors, mitogens, and hormones regulates key biological processes including cell growth, proliferation, survival, and motility. This lipid kinase phosphorylates converts the lipid second messenger phosphatidylinositol (4,5) bisphosphate (PIP_2) into phosphatidylinositol (3,4,5) trisphosphate (PIP_3), which in turn recruits and activates phosphatidylinositol–dependent kinase 1/2 (PDK1/2), resulting in the activation of AKT (Song, Ouyang, & Bao, 2005; Vogt, Gymnopoulos, & Hart, 2009) (Fig. 7.1). On the other side, PTEN functions both as a dual specificity protein phosphatase and lipid phosphatase. Although it can dephosphorylate protein substrates such as FAK (focal adhesion kinase), PTEN's predominant enzymatic activity seems to be the dephosphorylation of the $3'$ phosphate of the inositol ring in PIP_3, resulting in the biphosphate product PIP_2 (PtdIns $(4,5)P_2$) (Di Cristofano & Pandolfi, 2000; Leslie & Downes, 2004; Tamguney & Stokoe, 2007) (Fig. 7.1). Thus, inactivation of PTEN results in the accumulation of PIP_3 and hyperactivation of AKT. As PI3K/AKT signals control the cell metabolism, growth, proliferation, and survival, deregulation PTEN has been closely associated with development of certain tumor cells (Carracedo, Alimonti, & Pandolfi, 2011; Di Cristofano & Pandolfi, 2000). In the nervous system, neuron-specific loss of PTEN during mouse development causes high levels of phosphorylated AKT and a gradual increase in soma size without causing abnormal proliferation (Kwon, Zhu, Zhang, & Baker, 2003; Kwon et al., 2001). In the mature CNS, PTEN depletion in neurons has been shown to prevent apoptotic cell death in acute and degenerative injury models (Kirby et al., 2011; Li et al., 2009; Park et al., 2008; Shi et al., 2011). In addition to its role in cell growth and survival, recent studies point to the importance of PTEN in regulating axon growth/regeneration. Because multiple downstream effectors of PTEN operate in both neuronal soma and axon terminal, PTEN is ideally positioned to coordinate different steps of axon growth during development and injury-induced axon regeneration.

2.1. PTEN is an intrinsic blocker of axon regrowth

Several studies have indicated PTEN as a factor within neurons that impede axon regeneration. These studies have shown that pharmacological or genetic inactivation of PTEN in neurons enhances axon regeneration both
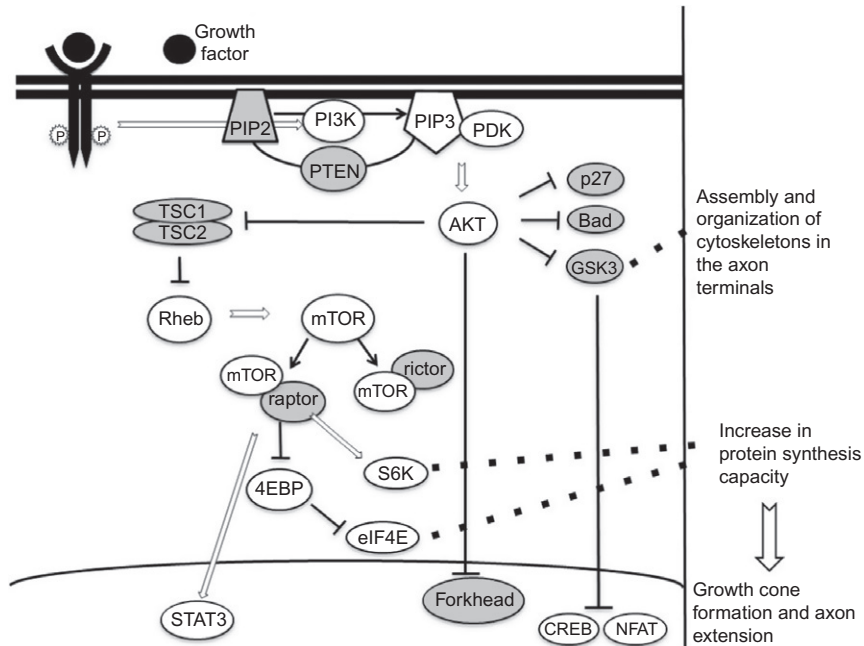
Figure 7.1 PTEN pathway and axon growth inhibition. Activated PI3K catalyzes conversion of membrane-bound lipid secondary messenger phosphatidylinositol (4,5) bisphosphate (PIP2) into phosphatidylinositol (3,4,5) trisphosphate (PIP3). This reaction is antagonized by PTEN, which maintains a low level of PIP3 in the membrane. Upon activation of receptor tyrosine kinase (i.e., by growth factors), PI3K is activated and PIP3 accumulates. Cytoplasmic PDK is subsequently recruited and activated, which in turn activates AKT. Activated AKT inhibits the TSC1/2 complex, thereby releases Rheb from inhibition and activates mTOR. Activated mTOR exists in two forms. The rapamycin-sensitive mTOR/raptor complex regulates global translation by activation of S6K, the kinase that phosphorylates ribosomal protein S6 in the 40S subunit, and eIF4E, the general initiation factor for 5′cap-dependent translation. Activated mTOR/raptor complex is also implicated in upregulation of STAT3 transcriptional activity. Activated AKT regulates activation and deactivation of many downstream targets including Forkhead, p27 and Bad to affect cell cycle and apoptosis. Also regulated by PTEN/AKT pathways is the GSK3 which regulates cytoskeletal dynamic and microtubule assembly, and transcription factors including NFAT and CREB to facilitate axon growth

in the CNS and PNS. One of the early evidence supporting the inhibitory role of PTEN involved an *in vivo* screen to identify factors that block axon regeneration of retinal ganglion cells (RGCs; whose axons form the optic nerve). Cre recombinase–mediated PTEN deletion in murine RGCs promoted considerable axon regeneration after optic nerve injury (Park et al., 2008). Further characterization of axon growth revealed that the axons

of PTEN–deleted RGCs overcome the growth–inhibitory environment (i.e., chondroitin sulfate proteoglycan (CSPG)–rich region) in the lesion site, regenerating over long distances in the degenerated optic nerve (Park et al., 2008). The corticospinal tract (CST) that controls voluntary movements is particularly important for functional recovery after spinal cord injury. Injured CST axons are particularly refractory to regeneration, and efforts to promote regenerative growth of CST axons in animal injury models have yielded only limited success (Lee et al., 2010; Zheng et al., 2005). Liu et al. (2010) demonstrated using adeno–associated virus (AAV) expressing Cre recombinase that deletion of PTEN in corticospinal neurons promotes substantial axon regrowth following spinal cord injury. In this study, several injury models including pyramidotomy, dorsal hemisection, and complete crush were utilized to demonstrate that PTEN deletion in CST neurons enhance axon sprouting/plasticity (axon growth from uninjured, spared neurons) and regeneration (axon growth from axotomized neurons). Further, immunohistochemical and electron microscopic analysis showed that regenerated axons in the spinal cord of PTEN–deleted animals reformed synapse–like structures distal to the injury site (Liu et al., 2010). The inhibitory role of PTEN on axon growth was also shown in cortical neurons using *in vitro* assays. Cultured cortical neurons exhibit limited neurite outgrowth when plated on myelin–associated glycoprotein (MAG)–expressing substrate cells (Perdigoto, Chaudhry, Barnes, Filbin, & Carter, 2011). Deletion or knockdown of PTEN in cortical neurons using knockout mice or short hairpin RNAs (shRNAs) resulted in enhanced neurite outgrowth when the neurons are plated on MAG–substrate cells. On the other hand, PTEN inactivation did not affect neurite outgrowth when the cortical neurons were plated on non–MAG expressing control cells (Perdigoto et al., 2011), suggesting that PTEN contributes to the growth–inhibitory signal resulting from MAG.

Outside of the CNS, PTEN was also shown to affect axon regeneration in the PNS. Dorsal root ganglia (DRG) neurons are able to regenerate peripheral, but not central branches in the adult spinal cord. However, a preconditioning lesion to the peripheral branches allows the subsequently injured central branches to grow into and beyond a lesion site (Bisby & Pollock, 1983; Hoffman, 2010; McQuarrie, Grafstein, & Gershon, 1977; Neumann & Woolf, 1999; Richardson & Issa, 1984). This preconditioning model has been an invaluable tool to study the intrinsic mechanisms that allow enhanced regenerative ability in neurons. Inhibition of PTEN activity led to significant increase in neurite outgrowth for both un–preconditioned and

preconditioned neurons (Christie, Webber, Martinez, Singh, & Zochodne, 2010). Further, *in vivo* regeneration following severe sciatic nerve injuries was accelerated after local inhibition of PTEN at the injury site. Thus, while previous studies showed enhanced axon regeneration after neuron–specific suppression of PTEN (Liu et al., 2010; Park et al., 2008; Sun et al., 2011), axon regeneration seen after local inhibition of PTEN at the lesion site (Christie et al., 2010) raises the possibility that inactivation of PTEN in neighboring cells (including PTEN-expressing Schwann cells) may have contributed to the enhanced axon regrowth in the PNS. Overall, these findings clearly demonstrated that PTEN has a role in limiting axon regeneration, and relieving its actions on neurons permit enhanced axon growth. One important question remains: how does inactivation of PTEN increases axon growth potential?

2.2. Downstream effectors of PTEN

2.2.1 PI3K/AKT

There has been a surge of new information in the past several years concerning how the PI3K/AKT signal might be conveyed to its downstream targets to regulate different steps of axon growth from initial axon formation to axon extension. This pathway has been shown to influence many features of axon growth including axon elongation, branching, caliber, growth cone assembly and polarity. Such different functions are likely to be mediated by different downstream effectors of this pathway. Given the negative role of PTEN on activation of PI3K/AKT, axon regeneration induced after PTEN inactivation could be explained partially by downstream activation of PI3K/ AKT signaling. In support of this, PTEN inactivation leading to increased AKT activity or direct overexpression of activated AKT is sufficient to increase neurite outgrowth *in vitro* (Perdigoto et al., 2011). However, whether or not overexpression of active AKT in different neuronal cell types could enhance *in vivo* axon regeneration is less clear. Also, direct evidence of the involvement of AKT activation on axon regeneration in the background of PTEN deletion is lacking. Recently, AAV–expressing constitutively active AKT induced robust regrowth of axons from dopaminergic neurons after axon lesion induced by a neurotoxin. Moreover, this treatment led to target reinnervation and partial behavioral recovery (Kim, Chen, et al., 2011). Of note, axon damage resulting from a neurotoxin is progressive and does not produce disruption of brain parenchyma (i.e., absence of glial scar and myelin disruption). Nonetheless, it seems that at least for certain CNS neurons, forced AKT activation is sufficient to

enhance an axon regeneration response. Activation of AKT influences activation of numerous downstream molecules including mTOR, FAK, GSK–3β (glucose synthase kinase–3β), GS (glucose synthase), PRAS40, Bad, FoxO1, and Myt1 to control key biological functions such as metabolism, growth, cell cycle, and survival (Cardone et al., 1998; Diehl, Cheng, Roussel, & Sherr, 1998; Hers, Vincent, & Tavare, 2011; Okumura et al., 2002; Sarbassov, Guertin, Ali, & Sabatini, 2005; Wang et al., 2012). Among these downstream targets, mTOR and GSKβ have attracted considerable attention recently for their abilities to regulate axon growth.

2.2.2 mTOR and axon regeneration

mTOR, also known as FK506 binding protein 12-rapamycin–associated protein 1 (FRAP1), is an intracellular sensor that integrates signals regarding cellular nutrient/energy/redox states to control protein synthesis and cell growth. At the molecular level, activated mTOR exists in two structurally and functionally distinct complexes in the cytoplasm. One such complex contains raptor (regulatory–associated protein of TOR), a protein partner for mTOR. This complex, known as mTORC1, is rapamycin-sensitive and able to phosphorylate S6 kinase and 4EBP1 (Fig. 7.1). The other type contains rictor (rapamycin–insensitive companion of TOR) and is associated with cytoskeleton regulation (mTORC2) (Oh & Jacinto, 2011). Because of its relevance to axon regeneration, only mTORC1 will be discussed in this review (hereafter referred to simply as mTOR). The activity of this complex is stimulated by insulin, mitogens, growth factors, and serum, and inhibited by low nutrient levels, growth factor deprivation, and reductive stress (Hay & Sonenberg, 2004; Kim & Sabatini, 2004; Kim et al., 2002; Laplante & Sabatini, 2012). The regulation of mTOR activity in response to growth factors is mediated mainly by the PI3K/AKT signaling pathway. AKT activation leads to phosphorylation and inhibition of tuberous sclerosis protein complex (TSC) which in turn results in subsequent engagement of Ras homolog enriched in brain (Rheb) to activate mTOR (Fig. 7.1). mTOR regulates global protein translation and ribosome biogenesis through phosphorylation of different substrates, which are involved in the initiation of cap–dependent protein translation, a rate-limiting step of protein synthesis (Ma & Blenis, 2009). Deletion or functional mutation of PTEN results in hyperactivation of AKT/mTOR, and subsequently leads to an increase in cell growth capacity (Kwon et al., 2003; Liu, Zhou, Reske, & Shen, 2008). In mouse retinae, mTOR

activity in RGCs declines progressively during development (Park et al., 2008); however, by adulthood, only a small population of total RGCs (5–10%) retains mTOR activity (Leibinger, Andreadaki, & Fischer, 2012; Park et al., 2008), which correlates with the loss of regenerative capacity of mature RGCs. Axon injury to adult RGCs, however, triggers further decline of mTOR activity (Leibinger et al., 2012; Park et al., 2008), whereas PTEN deletion in RGCs prevents this axotomy-induced mTOR suppression (Park et al., 2008). It is unclear why and how the mTOR activity is retained in only a small subset of adult RGCs, and what signal causes its suppression in the injured neurons. Systemic application of rapamycin, a potent mTOR inhibitor in PTEN-deleted animals resulted in significant reduction in optic axon regeneration (Park et al., 2008), pointing to a pivotal role for mTOR activation on axon regeneration in the background PTEN deletion. Similarly, PTEN depletion in purified motor neurons using siRNAs promoted significant axon growth, an effect that was inhibited by rapamycin treatment (Ning et al., 2010). On the contrary, in the PNS, increased neurite outgrowth from DRG neurons after PTEN inactivation was not affected by pharmacological inhibition of mTOR. More direct approaches to activate mTOR were also shown to promote axon regeneration: RGC-specific deletion of TSC1, a direct negative regulator of mTOR (Fig. 7.1) also prevented axotomy-induced suppression of mTOR activity and promoted regeneration of injured RGC axons (Park et al., 2008). Similarly, viral-mediated overexpression of Rheb, a direct activator of mTOR (Fig. 7.1), promoted extensive axon regeneration of dopaminergic neurons (Kim, Chen, et al., 2011). In the PNS, forced mTOR activation in DRG neurons by Advilin-Cre mediated deletion of TSC2 was sufficient to enhance axon/neurite growth both *in vivo* and *in vitro* in the absence of preconditioning injury. Collectively, these studies indicate that forcing mTOR activation facilitates the regenerative response in several types of CNS and PNS neurons. Others have suggested the potential role of mTOR in facilitating different features of axon growth: axon initiation and axon elongation.

In the visual system, inflammatory stimulation (i.e., penetrating lens injury) in the eye stimulates axon regeneration in the injured optic nerve. Inactivation of mTOR decreased the number of axons regenerating over long distances, without inhibiting the initial switch of RGCs into the regenerative state (i.e., did not decrease the number of axons regenerating short

distances) (Leibinger et al., 2012), suggesting that activation of mTOR has a more prominent role in supporting the elongation of regenerating axons than triggering the initial growth.

How could mTOR facilitate axon regeneration? The two best characterized downstream targets of mTOR are S6K1 (p70–S6 Kinase 1) and 4E–BP1 (the eukaryotic initiation factor 4E (eIF4E) binding protein 1). Phosphorylation of S6K1 by mTOR leads to activation and consequent phosphorylation of rS6 (ribosomal S6). This causes increased translation of mRNAs containing a $5'$ tract of oligopyrimidine that encode components of the translation apparatus including ribosomal proteins and elongation factors (Dobashi, Watanabe, Miwa, Suzuki, & Koyama, 2011; Huang & Manning, 2009; Proud, 2007, 2009). Nonphosphorylated 4E–BP1 binds to the translation initiation factor eIF4E, preventing it from binding to $5'$-capped mRNAs and recruiting them to the ribosomal initiation complex (Fig. 7.1). mTOR phosphorylation of 4E–BP1 releases eIF4E, allowing it to initiate cap-dependent translation (Proud, 2007, 2009). Overall, activation of mTOR by various external stimuli (i.e., growth factors, nutrients, and hormones) positively controls protein synthesis and cell growth by enhancing the cellular capacity for ribosome biogenesis, translation initiation, and elongation. Injury to the axons of central neurons (e.g., RGCs and CST neurons) was shown to suppress protein synthesis and mTOR activity at the cell body level (Leibinger et al., 2012; Liu et al., 2010; Park et al., 2008). In contrast, axon injury to the peripheral neurons (e.g., DRG neurons) triggers increase in the level of neuronal mTOR activation (Abe, Borson, Gambello, Wang, & Cavalli, 2010). What accounts for this profound disparity in injury response between these neurons is unknown, but it may reflect differential regulation of cytokine, hormone, and growth factor receptor expression in these neurons after injury. Enhanced axon regeneration seen after mTOR activation in injured neurons could be ascribed partially to increased capacity of neurons to synthesize *de novo* proteins required for the building blocks of newly extending axons. Several studies have indicated that local protein synthesis at the axon level is critical for the formation of growth cones in response to axotomy. Using *in vitro* outgrowth assays, Verma et al. (2005) demonstrated that protein synthesis inhibitors (e.g., cyclohexamide) or rapamycin impairs formation of the growth cone in embryonic sensory axons. As formation of a growth cone is a prerequisite for axon regeneration (Bradke, Fawcett, & Spira, 2012), protein synthesis in a cut axon that facilitates growth cone formation is likely an integral component of axon regeneration for sensory axons.

To what extent this applies to CNS axons is less clear. In the cell soma, sustained synthesis of cellular building blocks (e.g., microtubules and integrated proteins) is also indispensable for sustained growth of injured axons. Therefore, maintenance of mTOR and the protein translation activity in the soma and axon, to a large extent, retains the normal cellular activity that could support axon regrowth. mTOR may also influence axon regeneration by mechanisms other than translational control. The activity of several transcription factors, particularly those involved in growth, metabolic, and biosynthetic pathways, including STAT1 and STAT3 (Kristof, Marks-Konczalik, Billings, & Moss, 2003), and the nuclear receptor peroxisome proliferator-activated receptor-γ (Kim & Chen, 2004) are regulated by mTOR in a rapamycin-sensitive manner. mTOR has also been shown to be critical for the optimal activation of STAT3 by CNTF (ciliary neurotrophic factor; Yokogami, Wakisaka, Avruch, & Reeves, 2000), all of which suggest that the function of mTOR is not limited to translational control, but may extend to include transcriptional regulation.

2.2.3 Local PTEN/GSK3 signaling

In addition to mTOR, other downstream targets of the PTEN pathway may well be involved in promoting axon regrowth. This is evident by the lesser extent of axon regeneration in the optic nerve after TSC1 deletion compared to PTEN deletion (Park et al., 2008). While PTEN deletion induces AKT activation and many downstream targets associated with it, TSC1 lies downstream of PTEN, and deletion of TSC1 leads predominantly to mTOR activation (Fig. 7.1). GSK3, a major substrate of AKT has been implicated in regulation of neurogenesis, polarization, and axon growth (Kim, Hur, Snider, & Zhou, 2011; Liu, Hur, & Zhou, 2012). GSK3 is constitutively active in resting cells, which acts to inhibit cell signaling. Activation of AKT in response to extracellular stimuli leads to GSK3 phosphorylation and subsequent inactivation, thereby allowing the propagation of GSK3 signaling cascades (Kim, Hur, et al., 2011; Liu et al., 2012). To date, there is no evidence of GSK3 playing a direct role in PTEN deletion-mediated axon regeneration; however, the existence of multiple downstream targets of GSK3, each with potent roles in axon growth/plasticity, makes it a strong candidate to mediate PTEN's effects on axon growth. Studies have indicated that PTEN expressed at the axon tip has a potent role in regulating the PI3K/AKT/GSK3 signaling pathway as well as growth cone collapse. Growth cones *in vitro* collapse in the presence of semaphorin 3A (Sema3A) (Fan & Raper, 1995; Jackson & Eickholt, 2009). Chadborn et al.

reported the presence of PTEN in the axon compartment of DRG growth cones during axon growth, and following exposure to Sema3A, PTEN accumulates rapidly at the growth cone membrane. Further, Sema3A suppresses PI3K signaling and leads to activation of GSK3, a sequence of event dependent on the phosphatase activity of PTEN. These findings demonstrate the role of axonal PTEN in regulating GSK3 signaling in response to growth-inhibitory cues and highlighted the importance of subcellular localization of PTEN to regulate growth cone dynamic (Chadborn et al., 2006). Continuous addition of microtubules at the growth cone is a key for successful axon regeneration, a process that is tightly controlled by coordinated regulation of microtubule dynamics and actin rearrangement in the growth cone. Many microtubule binding proteins (MBPs) including collapsin response mediator protein 2 (CRMP2), adenomatous polyposis coli (APC), Tau, and MAP 1b are known to regulate this process in response to various extracellular stimuli. GSK3 is regarded as a key mediator that integrates extracellular signals and MBP to control axon growth by modulating microtubule dynamics and stability (Hur & Zhou, 2010). Phosphorylation of these MBPs by GSK3 eliminates their ability to associate with microtubules. Conversely, inhibition of GSK3 facilitates the binding of CRMP2 to tubulin dimers and promotes axon growth by enhancing microtubule assembly in the growth cone (Fukata et al., 2002; Yoshimura et al., 2005). Several studies have reported that inactivation of GSK3 promotes axon growth, suggesting that the level of GSK3 activity and subcellular localization of inactivated GSK3 may influence the overall growth cone behavior. Hur et al. (2011) recently reported the role of cytoplasmic linker-associated protein (CLASP, a microtubule stabilizing protein) in transducing GSK3 activity levels to differentially regulate axon growth (i.e., either inhibit or promote growth) by coordinating the stability and arrangement of growth cone microtubules. In addition to its action on microtubule polymerization and assembly, GSK3 is known to regulate the activity (or degradation) of several transcription factors known to affect axon regeneration. These include AP1, p53, SMAD, NFAT (nuclear factor activated T-cells), and NFκB. Several reviews have recently described in greater detail the potential mechanisms and downstream targets of GSK3 in regulating the process of growth cone formation and axon growth (Kim, Hur, et al., 2011; Liu et al., 2012). Overall, considering its potent roles in growth cone formation and axon extension, GSK3 may contribute to downstream PTEN effects on axon regeneration.

2.2.4 Modulation of PTEN/mTOR and desensitization to MAG/CSPGs

Axon regeneration failure in the CNS can be partly explained by numerous inhibitory environmental cues present at the lesion site that chemically impede axon growth. Of these, the myelin-associated inhibitors (MAI; e.g., nogo, MAG and OMgp) and CSPGs have been studied most extensively. It is known that CNS neurons express various MAG receptors including the Nogo receptors (NgR1 and NgR2) (Domeniconi et al., 2002; Liu, Fournier, GrandPre, & Strittmatter, 2002; Venkatesh et al., 2005), gangliosides GD1a, GT1b (Yang et al., 1996) (Vinson et al., 2001; Vyas et al., 2002), and paired immunoglobulin-like receptor B (PirB) (Atwal et al., 2008). CSPG receptors expressed by CNS neurons identified so far are protein tyrosine phosphatase σ, NgR1 and NgR3 (Dickendesher et al., 2012; Shen et al., 2009). Binding of these receptors to MAIs or CSPGs triggers intracellular signaling leading to RhoA/ROCK activation and growth cone collapse (Hall & Lalli, 2010; Monnier, Sierra, Schwab, Henke-Fahle, & Mueller, 2003; Niederost, Oertle, Fritsche, McKinney, & Bandtlow, 2002). Studies have demonstrated that depletion of PTEN in neurons confers axons with the ability to overcome these growth-inhibitory factors. In the optic nerve, CSPGs accumulate at the lesion site within 1 day after crush injury, and persist for several days (Park et al., 2008; Selles-Navarro, Ellezam, Fajardo, Latour, & McKerracher, 2001). While RGC axons in wild-type animals are mostly unable to grow into the lesion site in the optic nerve, axons of PTEN-deleted RGCs show enhanced growth into the CSPG-rich lesion site shortly after injury. *In vitro* inactivation of PTEN in dissociated cortical neurons increased neurite outgrowth over MAG (Perdigoto et al., 2011) whereas inhibition of mTOR activity reduced neurite outgrowth of cultured RGCs on myelin or CSPGs (Leibinger et al., 2012). Thus, these studies indicate that PTEN has a role in the growth cone collapse in response to MAG, whereas mTOR activity is important to overcome the inhibitory effects of myelin and CSPGs. What are the intracellular mechanisms by which inactivation of PTEN desensitizes axons to these inhibitory substrate components? Similar to the effects seen after PTEN inactivation, expression of constitutively active AKT in cortical neurons is sufficient to reverse the inhibition of neurite outgrowth by MAG, suggesting that AKT may act downstream to PTEN in overcoming MAG inhibition. Further, it was shown that MAG reduces AKT phosphorylation in cortical neurons *in vitro* (Perdigoto et al., 2011). Suppression of AKT activity would increase the activation of GSK3 and impair growth cone formation (as described in Section 2.2.3). PTEN has

been shown to be a target of Sema3A in triggering growth cone collapse of sensory neurons (Chadborn et al., 2006). Sema3A induces a rapid local accumulation of PTEN at the growth cone, possibly leading to a depletion of PIP3 and AKT (Chadborn et al., 2006). Thus, in addition to the Rho/ROCK cascade, PTEN seems to be another signal transduction pathway that is activated by inhibitors of axon growth.
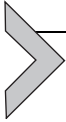
3. SOCS3: AN INHIBITOR OF CYTOKINE-INDUCED AXON REGENERATION

Several recent studies have indicated that SOCS3 is another neuron-intrinsic blocker of axon regeneration. It is one of the most highly upregulated genes in neurons following axonal injury (Fischer, Petkova, Thanos, & Benowitz, 2004; Veldman, Bemben, Thompson, & Goldman, 2007). Over 30 cytokines, including CNTF, leukemia inhibitory factor (LIF), interleukin-6 (IL6), IL10, and interferon (IFN)-gamma are known inducers of SOCS expression (Croker, Kiu, & Nicholson, 2008; Lehmann et al., 2003; Park et al., 2009; Strebovsky, Walker, & Dalpke, 2012). Cytokine binding to a cognate receptor leads to activation of the JAK (Janus kinase)/STAT pathway and induction of *Socs* gene transcription in a STAT-dependent manner (Cooney, 2002; Croker et al., 2008). The SOCS proteins then inhibit cytokine signaling either by direct binding to JAKs and inhibiting their catalytic activity or by binding to the receptor site and preventing recruitment of STAT. Alternatively, SOCS proteins interact with the cellular ubiquitination machinery and direct JAKs or receptors for ubiquitin-mediated proteasomal degradation (Fig. 7.2) (Alexander & Hilton, 2004; Cooney, 2002). Through this negative feedback system, the SOCS family is able to tightly regulate the intensity and duration of cytokine signaling, which is critical to prevent aberrant cellular responses in the event of sudden increases in cytokine concentration. Of the different SOCS members, SOCS3, which has been shown to be expressed in immune cells and play prominent roles in modulating immune reactions (Baker, Akhtar, & Benveniste, 2009; Li, de Haar, Peppelenbosch, & van der Woude, 2012; Tamiya, Kashiwagi, Takahashi, Yasukawa, & Yoshimura, 2011) has attracted considerable attention recently for its prominent role in limiting cytokine-mediated axon regeneration. One of the early evidence indicating a direct role for SOCS3 in limiting axon regeneration showed that overexpression of SOCS3 blocks nuclear translocation of STAT3
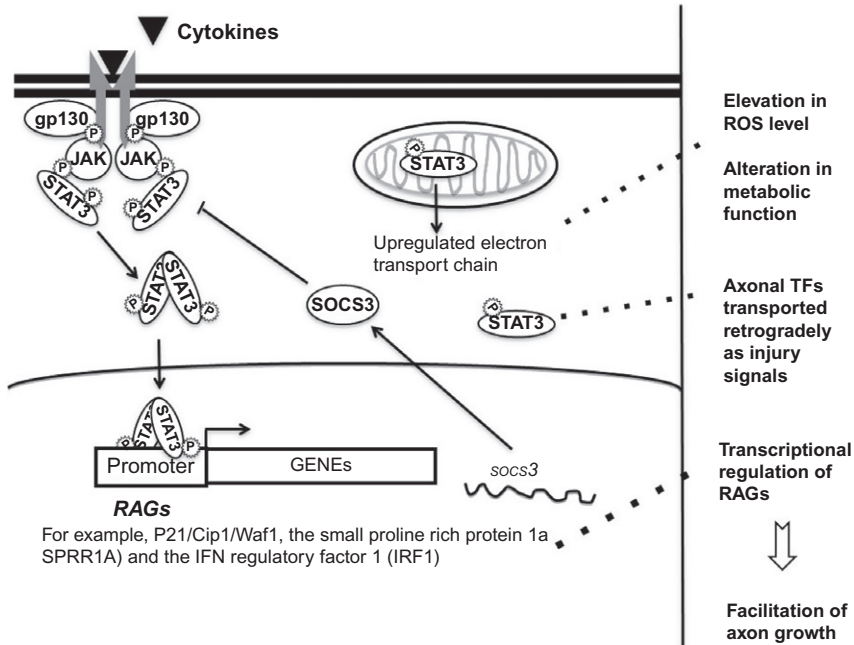
Figure 7.2 SOCS3 pathway and axon growth inhibition. Cytokines of gp130 family, including IL6, LIF, and CNTF, are upregulated after injury. Cytokine binding leading to activation of gp130 and coreceptors results in transphosphorylation at receptor intracellular domains, which leads to JAK recruitment and JAK phosphorylation. STAT3 is subsequently recruited to the activated peripheral complexes by phosphorylated-JAK. Upon JAK phosphorylation, STAT3 is phophorylated (activated), dimmerizes, translocates into the nuclei, and recruited to DNA binding sites of many genes including regeneration-associated genes (RAG) including the cell cycle inhibitor P21/Cip1/Waf1, the small proline rich protein 1a (SPRR1A), and the IFN regulatory factor 1 (IRF1). SOCS3 is a direct target of STAT3, acts as a feedback mechanism, and inhibits JAK-STAT signaling in the cytoplasm. Activated STAT3 is also found in mitochondria, which were shown to contribute to neurite outgrowth in response to nerve growth factor. STAT3 is also retrogradely transported from the lesioned axon to the cell body, possibly acting as a signal to initiate neuronal injury responses.

and neurite outgrowth of DRG neurons. Further, inhibition of endogenous SOCS3 through overexpression of a dominant negative (DN) mutant SOCS3 stimulates neurite outgrowth (Miao et al., 2006).

3.1. Glycoprotein 130 family of cytokines triggers axon regeneration

Axon injury in the PNS and CNS is followed by upregulation of cytokines at the lesion site and around the cell body. Both neurons and glial cells are responsible for increasing the production and release of cytokines, thereby

affecting neuronal responses to injury in autocrine and paracrine manners (Hans et al., 1999; Kirsch, Schneider, Lee, & Hofmann, 1998; Leibinger et al., 2009; Schwartz et al., 1994; Subang & Richardson, 2001). Cytokines are also retrogradely transported by axons to their cell bodies after injury (Abe & Cavalli, 2008; Curtis et al., 1994; Kirsch, Terheggen, & Hofmann, 2003; Thompson, Vernallis, Heath, & Priestley, 1997; Zigmond & Sun, 1997). In the PNS, such injury responses seem to alter neuronal gene expression and facilitate initiation of axon regrowth following axotomy. The most extensively studied cytokines in the context of axon regeneration are those that belong to the IL6 family or the glycoprotein 130 (gp130) family. This family includes, among other cytokines, IL-6, IL-11, oncostatin M, and cardiotrophin-1 along with LIF and CNTF (Taga & Kishimoto, 1997). Cytokine binding leads to dimerization of gp130 (Taga et al., 1989) and phosphorylation of receptor-associated JAK. This, in turn, phosphorylates causes the dimerization of STAT3, allowing nuclear translocation and the transcription of target genes (Fig. 7.2). STAT3 is the major signaling pathway in this context, but gp130 also activates other signaling pathways including extracellular-regulated kinase (ERK) and PI3K (Heinrich et al., 2003). Several studies have demonstrated that neuropoietic cytokine activation of gp130 facilitates axon regeneration in the PNS neurons. This effect seems to be mediated primarily via downstream activation of the JAK/STAT signaling pathway (discussed further in Section 3.3). IL6 levels increase in DRGs after nerve injury (Murphy, Grondin, Altares, & Richardson, 1995), and regeneration is impaired in knockout mice with deletion of LIF (Cafferty et al., 2001) or IL6 (Cafferty et al., 2004; Galiano et al., 2001). Genetic deletion of gp130 in sympathetic neurons inhibits the enhancement of axon growth occurring after conditioning lesion (Hyatt Sachs, Rohrer, & Zigmond, 2010). Overall, these studies indicate that injury-induced upregulation of cytokines may act as an injury signal in the activation of the regenerative program in peripheral neurons.

3.2. SOCS3 inhibits CNTF effects

One of the gp130 family of cytokines most extensively studied for axon regeneration is CNTF, a polypeptide hormone originally characterized as a potent survival factor for chick ciliary neurons (Adler, Landa, Manthorpe, & Varon, 1979; Barbin, Manthorpe, & Varon, 1984; Lin et al., 1989). CNTF uses a multimeric receptor composed of the gp130 signal-transducing protein associated with LIF receptor and the CNTF binding

receptor α component (Davis et al., 1993; Stahl & Yancopoulos, 1994). Besides, its neuroprotective role, several studies have reported the axon regenerative effects of CNTF. Early evidence supporting a positive role demonstrated that administering recombinant CNTF enhances the number of regenerating axons after sciatic nerve transection (Sahenk, Seharaseyon, & Mendell, 1994). CNTF at a high concentration was shown to enhance neurite outgrowth from purified RGCs *in vitro*, and repeated intravitreous delivery of recombinant CNTF enhances axon regeneration after optic nerve injury (Lingor et al., 2008; Muller, Hauk, Leibinger, Marienfeld, & Fischer, 2009; Smith et al., 2009). Further, recombinant CNTF protects RGCs from death after axotomy and promotes axon regeneration into a transplanted peripheral nerve graft (Cui & Harvey, 2000; Mey & Thanos, 1993; Park, Luo, Hisheh, Harvey, & Cui, 2004). However, the extent of axon growth in RGCs induced after bolus injection of CNTF has been quite modest (i.e., only small numbers of neurons extending lengthy axons). The low efficacy could result from the relatively short half-life of CNTF or from the inner retinal membrane acting as a physical barrier (van Adel, Arnold, Phipps, Doering, & Ball, 2005). In support of this idea, viral delivery of CNTF into the vitreous body, which allows integrated expression and sustained supply of CNTF from the inner retinal cells, promotes considerable axon regrowth (Leaver et al., 2006). In contrast, other studies, in fact, have reported a minimum role of CNTF in promoting axon regeneration. CNTF elevation failed to stimulate optic nerve regeneration *in vivo*, and it failed to enhance neurite outgrowth in retinal explants *ex vivo* (Cen et al., 2007; Jo, Wang, & Benowitz, 1999; Yin et al., 2003, 2006, 2009). These data challenged the role of CNTF as a direct stimulator of axon regrowth. A recent study provided hints on why some injured neurons respond so poorly to CNTF. Following an axon injury, SOCS3 is upregulated rapidly in injured neurons (Fischer et al., 2004; Park et al., 2009), an event which likely restricts the actions of CNTF on neurons. Smith et al. (2009) reported that conditional deletion of SOCS3 in RGCs was sufficient to enhance axon regeneration after optic nerve injury. This effect can be abolished with concomitant deletion of gp130, indicating that gp130 mediates the SOCS3 knockout effect on axon regeneration (Smith et al., 2009). Further, while injection of CNTF alone yielded only limited extent of axon regeneration, CNTF treatment in SOCS3-deleted mice led to robust axon regeneration (Smith et al., 2009). More recently, viral-mediated overexpression of DN SOCS3 in adult RGCs diminished CNTF-induced axon regeneration into a

peripheral nerve graft (Hellstrom et al., 2011). Together, these data support a model in which SOCS3 suppresses axon regeneration by antagonizing the cytokine regulated gp130 signaling pathway, and that relieving SOCS3 activity further potentiates cytokine (e.g., CNTF) effects on regeneration. The gp130 pathway may be triggered by inflammatory cytokines after injury but would remain unproductive owing to subsequent induction of and suppression by the SOCS proteins.

What are the downstream intracellular mechanisms underlying the enhanced axon regeneration induced by CNTF elevation or SOCS3 deletion? STAT3 is activated in RGCs after CNTF treatment, and JAK/STAT inhibitors attenuate CNTF-stimulated neurite outgrowth from purified RGCs (Leibinger et al., 2009; Lingor et al., 2008; Muller et al., 2009). These data indicate that CNTF exerts its effect at least in part through the JAK/STAT pathway. CNTF has also been shown to activate several other intracellular signaling pathways including MAPK/ERK and PI3K/AKT pathways (Alonzi et al., 2001; Leibinger et al., 2009; Muller et al., 2009; Park et al., 2004). Inhibition of MAPK and PI3K reduces CNTF's effect on axon growth in peripheral neurons and RGCs (Alonzi et al., 2001; Dolcet et al., 2001; Muller et al., 2009; Park et al., 2004), suggesting that CNTF may activate multiple pathways to induce axon regeneration. Clear evidence indicating STAT3 as the primary effector of axon regeneration induced by SOCS3 deletion came from a study using double knockout mice lacking SOCS3/STAT3 in adult neurons. While single SOCS3 knockout mice permit significant axon regeneration in the optic nerve, mice bearing double SOCS3/STAT3 deletion fail to regenerate axons (Sun et al., 2011), indicating that STAT3 is required for the axon regeneration in the background of SOCS3 deletion. What downstream targets could mediate STAT3's effects on axon regeneration? Gene profiling studies using purified RGCs demonstrate that many genes implicated in PNS axon regeneration, such as Jun, GAP43, Id2, SOX11, ATF3, and galanin, are significantly altered in axon-regenerating RGCs after SOCS3 deletion (Sun et al., 2011), consistent with the notion that the JAK/STAT pathway is a critical one for PNS axon regeneration.

3.3. STAT3: A facilitator of axon regeneration

The JAK/STAT system provides direct mechanisms to respond to extracellular stimuli. Many ligands including cytokines, hormones, and growth factors, and their receptors activate the JAK/STAT pathway; once activated,

the JAK/STAT regulates various cellular functions, including proliferation, growth, and immune response (Rawlings, Rosler, & Harrison, 2004; Shuai & Liu, 2003). Several studies indicate that the activation of STAT3 and subsequent induction and changes in the neuronal gene expression are key/important/necessary for stimulating axon regeneration in both the PNS and CNS. This statement is supported by high levels of STAT3 activation in neurons with high regenerative capacity, reduction of axon regeneration by pharmacologic and genetic depletion of STAT3 activity, and increase in axon regeneration after genetically enforcing STAT3 activation. In the DRG system, a peripheral axon injury that leads to enhanced axon regeneration is associated with concomitant activation of STAT3 in injured neurons (Schwaiger et al., 2000; Sheu, Kulhanek, & Eckenstein, 2000). In contrast, failure of axon regrowth after a central lesion parallels the inability of STAT3 to be activated (Schwaiger et al., 2000), pointing to distinct responsive mechanisms to axotomy in PNS versus CNS. STAT3 activation as a consequence of the peripheral conditioning lesion is required for the central axon regrowth (Qiu, Cafferty, McMahon, & Thompson, 2005). These results are consistent with the hypothesis that neurons fail to respond to injury in the CNS, while a peripheral lesion would initiate a regenerative response. Suppressing STAT3 activity diminishes regenerative response after PNS injury (Bareyre et al., 2011), while overexpression of STAT3 enhances neurite outgrowth *in vitro* and axon regeneration *in vivo* (Bareyre et al., 2011; Smith et al., 2011). Recent findings further defined the functional role of STAT3 in the initiation but not elongation phase during axon regeneration. Specifically, through real-time fluorescent imaging of STAT3-deficient and competent axons after injury, the authors showed that STAT3 overexpression promotes axon sprouting but not sustained long-distance growth of cultured neurons (Bareyre et al., 2011).

How does STAT3 activation facilitate axon regeneration? Transcription is necessary for neuronal transformation into a regenerative-capable state after injury. In fact, multiple regeneration-associated transcriptional factors have been identified (e.g., KLF, AP1, CREB, NFAT, and ATF3) (Blackmore et al., 2012; Moore & Goldberg, 2011; Tedeschi, 2011). STAT3, as a transcriptional activator, is known to activate more than 100 downstream targets, some of which are known to affect axon growth including the cell cycle inhibitor P21/Cip1/Waf1 (Tanaka et al., 2002), the small proline rich protein 1a (SPRR1A) (Pradervand et al., 2004), and the IFN regulatory factor 1 (IRF1) (Harroch, Revel, & Chebath, 1994;

Smith et al., 2011). Gp130 is also upregulated by STAT3 activation, suggesting a positive feedback loop that potentiates STAT3's effects (O'Brien & Manolagas, 1997; Smith et al., 2011). STAT3 activation is also implicated in epigenetic modulation, raising a possibility that epigenetic mechanisms contribute to STAT3-mediated axon growth (Trakhtenberg & Goldberg, 2012). STAT3 has been shown to turn on transcription of an epigenetic regulator DNA methyltransferase 1 (DNMT1) in cancer cell lines, and in the same context, activated STAT3 forms transcriptionally repressive complexes with DNMT1 and histone deacetylase 1 at the promoter of SHP-1 phosphatase, a tumor suppressor. The repression is mediated in part by promoter silencing through DNA methylation (Zhang et al., 2005, 2006). Moreover, in the epithelial cell line MCF-10, STAT3 activation is able to upregulate expression of miR-21 which has been implicated with a pro-regenerative role in adult DRG neurons after axotomy (Iliopoulos, Jaeger, Hirsch, Bulyk, & Struhl, 2010; Strickland et al., 2011; Trakhtenberg & Goldberg, 2012).

While the STAT3-mediated effect is attributed mainly to its nuclear transcriptional role, evidence suggests that STAT3 could also act through nontranscriptional mechanisms. STAT3 interacts with microtubules to promote cell migration, an effect that is mediated by its competition with the binding of the microtubule-associated protein stathmin (Ng et al., 2006). STAT3 is also found in mitochondria (Wegrzyn et al., 2009). Mitochondrial STAT3 regulates metabolic function in mitochondria to support growth of certain types of cancer cells (Gough et al., 2009). More recently, mitochondrial STAT3 was shown to facilitate neurite outgrowth in response to nerve growth factor (NGF). NGF increases the level of STAT3 serine but not tyrosine phosphorylation in PC12 cells and cortical neurons, and serine phosphorylated STAT3 was localized in mitochondria but not in the nucleus. A serine DN-STAT3 mutant attenuates NGF-stimulated neurite outgrowth, suggesting a role for mitochondria-targeted STAT3 in facilitating axon growth (Zhou & Too, 2011). Recent findings also indicate STAT3 as an injury signal retrogradely conveyed from the site of lesion to the cell body. After peripheral nerve injury, phosphorylated (i.e., active) STAT3 is detected in the injured axons and later in the soma (Lee, Neitzel, Devlin, & MacLennan, 2004). A subset of STAT3 transcripts is axonally targeted at the default state by its 3′UTR. Upon axonal injury, the STAT3 protein is locally synthesized and phosphorylated in axoplasm. This activated form of phosphorylated (p)-STAT3 is then packaged into the dynein-transport pathway by interaction with the Importin system and retrogradely transported.

Detection of nuclear p-STAT3 correlates with upregulated transcription of STAT3-responsive genes. Functionally, axonal STAT3 and its retrograde transport to the cell body prevent sensory neuronal death after axotomy but exert minimal effect on axon growth (Ben-Yaakov et al., 2012). It was also suggested that delay in detection of nuclear p-STAT3 depends on distance between the injury site and cell body (Ben-Yaakov et al., 2012). Overall, these findings indicate that STAT3 could have diverse roles, from conveying injury signals to the cell body, to facilitating gene transcription and mitochondrial function in order to foster axon regeneration. However, the detailed mechanisms underlying STAT3's effects on axon growth remain to be elucidated.

4. SYNERGISTIC EFFECTS FROM SIMULTANEOUSLY TARGETING PTEN AND OTHER GROWTH-PROMOTING FACTORS

The process of axon regeneration is multifaceted that requires activation of the regenerative program in response to injury signals to initiate growth cone formation, followed by sustained axon extension. This process is likely mediated by activation and modification of multiple signaling pathways working in concert, leading to enhanced gene transcription and protein translation. In the visual system, deletion of either PTEN or SOCS3 alone in adult RGCs promotes some degree of axon regeneration (Park et al., 2008; Smith et al., 2009), but the regeneration occurs shortly after injury, subsides substantially, and involves only a small population of total retinal neurons after single treatments. However, combining PTEN deletion with other growth-enhancing factors results in much more robust axon regeneration when compared to targeting PTEN alone. For instance, intraocular inflammation is known to stimulate RGC axon regeneration after lesion (Fischer, Heiduschka, & Thanos, 2001; Leon, Yin, Nguyen, Irwin, & Benowitz, 2000). cAMP elevation has a minimal effect on its own but enhances CNTF (Cui, Yip, Zhao, So, & Harvey, 2003) or inflammation effects on axon growth (Yin et al., 2006, 2009). PTEN deletion in RGCs combined with inflammation and cAMP analogues promotes a much greater extent of axon regeneration in the optic nerve compared to targeting them individually (Kurimoto et al., 2010). More recently, double deletion of PTEN and SOCS3 was shown to result in much stronger CNS axon regeneration compared to deleting either gene alone (Sun et al., 2011).

How does the simultaneous targeting of PTEN with these factors synergistically enhance axon regeneration? Elucidation of molecular mechanisms underlying the synergistic effects may reveal important insights into the process of axon regeneration. Targeting multiple factors concomitantly could either activate complementary pathways or activate key-pathways to a greater extent than when targeting them individually. For instance, either inflammation/cAMP elevation or PTEN deletion results in enhanced activation of MAPK, (i.e., one of the signaling pathways known to facilitate axon regeneration), but combined treatment leads to even greater MAPK activation compared to single treatments (Kurimoto et al., 2010). In a series of knockout mouse studies, it was demonstrated that axon regeneration induced after PTEN deletion is mediated primarily by mTOR activation (Park et al., 2008), whereas that induced after SOCS3 deletion is independent of mTOR, but instead requires STAT3 activation (Smith et al., 2009; Sun et al., 2011). Robust axon regeneration induced after codeletion of PTEN and SOCS3 was concomitant with coactivation of mTOR and STAT3 (Sun et al., 2011). Thus, these studies suggest that mTOR and STAT3 represent two distinctive but complementary arms of the regenerative program. Considering that mTOR regulates protein translation, while STAT3 is a transcription factor involved in altering gene expression, it is conceivable that the synergy induced after coactivation of these pathways reflects an increase in both gene transcription and protein translation. Furthermore, past studies using nonneuronal cells support a positive correlation between mTOR and STAT3 activation. mTOR activation correlates with increased STAT3 expression, phosphorylation, and nuclear localization (Goncharova et al., 2009; Yokogami et al., 2000; Zhou et al., 2007). When activated by receptor tyrosine kinases, STAT3 has a relatively short half-life in the nucleus in the presence of nuclear phosphotyrosyl phosphatase, the nuclear export system, and SOCS family members (Alexander & Hilton, 2004; Bhattacharya & Schindler, 2003; Mustelin, Vang, & Bottini, 2005; Schindler, Levy, & Decker, 2007). Through direct phosphorylation, mTOR may positively regulate transcriptional activity of STAT3 in RGCs. Transcriptional profiling of RGCs after injury reveals distinct gene expression patterns among the PTEN, SOCS3, and PTEN/SOCS3-deleted neurons. PTEN/SOCS3 double deletion results in enhanced upregulation of a subset of regeneration-associated genes that were shown to be moderately changed after any single deletion. Moreover, PTEN/SOCS3 deletion upregulates mTOR's positive

regulators, including Rheb and insulin growth factor 1 (IGF1), which could act as a "feed-forward" mechanism to further potentiate mTOR activation and axon growth. Interestingly, deleting PTEN and/or SOCS3 leads to reduction of KLF4, a transcription factor known to impede axon regeneration (Moore et al., 2009), and an upregulation of KLF6, a member of the same gene family known to facilitate axon regeneration (Moore et al., 2009). Thus, axon regeneration induced after manipulating PTEN and SOCS3 may in part be due to their ability to shift the balance of KLF genes toward those that favor axon growth. Despite these insights, however, the underlying mechanisms of synergistic axon regeneration after modifying multiple genes remain largely unknown and require further investigation.

5. SUMMARY AND PERSPECTIVES

Recent progress in promoting robust regeneration of mammalian CNS axons using genetic manipulation of neurons supports the notion that activating intrinsic growth programs is critical to reverse axon regeneration failure. Depleting PTEN in adult CNS neurons enhances axon regrowth, an effect that could be further potentiated by simultaneously targeting SOCS3 or other growth-enhancing factors (Kurimoto et al., 2010; Park et al., 2008; Sun et al., 2011). The pursuit of robust and sustained regeneration of injured CNS axons raises several important questions. First, what are the main molecular mechanisms underlying the synergistic effects induced after inactivating PTEN and SOCS3 in neurons? Deciphering the mechanisms underlying this form of axon regeneration may further extend our understanding of axon regeneration failure. PTEN and SOCS3 are two signaling suppressors whose perturbation is likely to affect myriad downstream effectors. Accordingly, a wide range of cellular processes could be activated including cytoskeleton dynamics, growth cone formation, axonal transport, and axon extension. These events are key to successful axon regeneration. PTEN and SOCS3 deletion in RGCs results in hyperactivation of mTOR and STAT3, and preventing activation of these two molecules attenuates axon regeneration (Park, Liu, Hu, Kanter, & He, 2010; Park et al., 2008; Smith et al., 2009; Sun et al., 2011). Thus, it is conceivable that while mTOR may determine the competence of axon regeneration, gp130/STAT3 dependent signals likely represent injury signals that could switch on or off the regenerative program (Fig. 7.3). Elucidating the genetic interplay between signaling
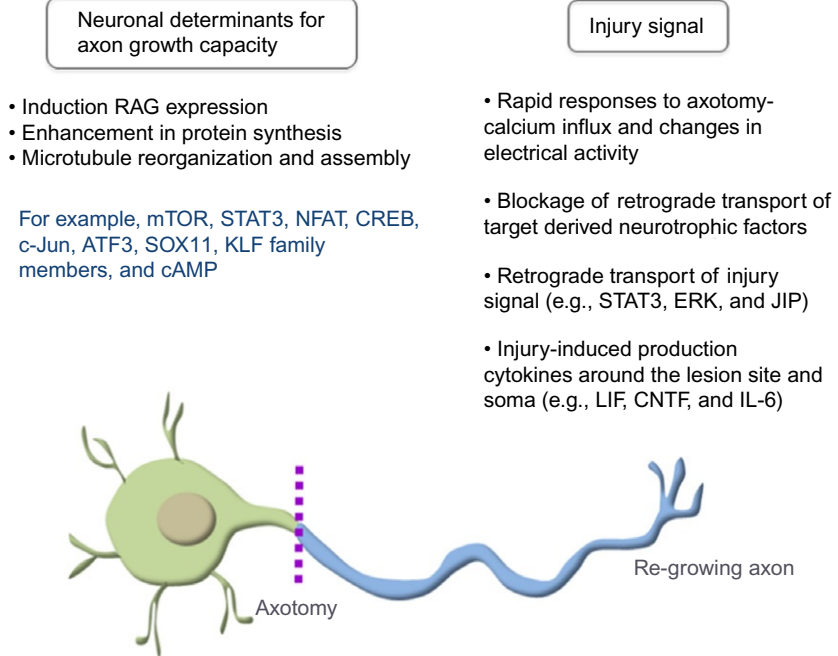
| Neuronal determinants for axon growth capacity | Injury signal |

• Induction RAG expression
• Enhancement in protein synthesis
• Microtubule reorganization and assembly

For example, mTOR, STAT3, NFAT, CREB, c-Jun, ATF3, SOX11, KLF family members, and cAMP

• Rapid responses to axotomy-calcium influx and changes in electrical activity

• Blockage of retrograde transport of target derived neurotrophic factors

• Retrograde transport of injury signal (e.g., STAT3, ERK, and JIP)

• Injury-induced production cytokines around the lesion site and soma (e.g., LIF, CNTF, and IL-6)

Re-growing axon

Axotomy

Figure 7.3 A model for axon regeneration after injury. Upon axonal injury, several immediate changes convey signals to initiate axon regrowth. These early signal include abrupt elevation of intracellular Ca^{2+} and interruption of electrical activity. Anterograde and retrograde trafficking of vesicles and trophic factors are also interrupted. Injury-induced cytokines are upregulated at the injury site and around the neuronal cell body, which likely operate as injury-induced signals for triggering axon growth program. For successful regeneration, injury signals (e.g., Importing, STAT3, and ERK) are conveyed retrogradely to the cell body. Importantly, an injured neuron must be capable of sensing these signals and also have sufficient cellular machineries to facilitate transcription of regeneration-associated genes (RAG), enhanced protein synthesis and cytoskeletal reorganization.

pathways and their downstream effectors during the regenerative response will be a major challenge for future research. Second, what is the functional outcome of new connections resulting from PTEN and SOCS3 manipulation? Sustained and long-distance axon regeneration is likely to be crucial for meaningful functional recovery after many forms of CNS injury including spinal cord injury and optic neuropathy. In addition to axon elongation, however, regenerated axons must find their appropriate targets and make productive functional connections. Given that perturbing PTEN and SOCS3 pathways in neurons alter normal

cellular functions (Luikart et al., 2011; Rodger, Drummond, Hellstrom, Robertson, & Harvey, 2012), it is of paramount importance to determine if the axons in question are able to achieve these important post-regeneration events. Answering these questions will help us in the future to translate recent findings into new therapeutic strategies.

ACKNOWLEDGMENT

REFERENCES

Abe, N., Borson, S. H., Gambello, M. J., Wang, F., & Cavalli, V. (2010). Mammalian target of rapamycin (mTOR) activation increases axonal growth capacity of injured peripheral nerves. *The Journal of Biological Chemistry*, *285*, 28034–28043.

Abe, N., & Cavalli, V. (2008). Nerve injury signaling. *Current Opinion in Neurobiology*, *18*, 276–283.

Adler, R., Landa, K. B., Manthorpe, M., & Varon, S. (1979). Cholinergic neuronotrophic factors: Intraocular distribution of trophic activity for ciliary neurons. *Science*, *204*, 1434–1436.

Aguayo, A. J., Bray, G. M., Carter, D. A., Villegas-Perez, M. P., Vidal-Sanz, M., & Rasminsky, M. (1990). Regrowth and connectivity of injured central nervous system axons in adult rodents. *Acta Neurobiologiae Experimentalis (Wars)*, *50*, 381–389.

Aguayo, A. J., David, S., & Bray, G. M. (1981). Influences of the glial environment on the elongation of axons after injury: Transplantation studies in adult rodents. *The Journal of Experimental Biology*, *95*, 231–240.

Alexander, W. S., & Hilton, D. J. (2004). The role of suppressors of cytokine signaling (SOCS) proteins in regulation of the immune response. *Annual Review of Immunology*, *22*, 503–529.

Alonzi, T., Middleton, G., Wyatt, S., Buchman, V., Betz, U. A., Muller, W., et al. (2001). Role of STAT3 and PI 3-kinase/Akt in mediating the survival actions of cytokines on sensory neurons. *Molecular and Cellular Neuroscience*, *18*, 270–282.

Atwal, J. K., Pinkston-Gosse, J., Syken, J., Stawicki, S., Wu, Y., Shatz, C., et al. (2008). PirB is a functional receptor for myelin inhibitors of axonal regeneration. *Science*, *322*, 967–970.

Baker, B. J., Akhtar, L. N., & Benveniste, E. N. (2009). SOCS1 and SOCS3 in the control of CNS immunity. *Trends in Immunology*, *30*, 392–400.

Barbin, G., Manthorpe, M., & Varon, S. (1984). Purification of the chick eye ciliary neuronotrophic factor. *Journal of Neurochemistry*, *43*, 1468–1478.

Bareyre, F. M., Garzorz, N., Lang, C., Misgeld, T., Buning, H., & Kerschensteiner, M. (2011). In vivo imaging reveals a phase-specific role of STAT3 during central and peripheral nervous system axon regeneration. *Proceedings of the National Academy of Sciences of the United States of America*, *108*, 6282–6287.

Ben-Yaakov, K., Dagan, S. Y., Segal-Ruder, Y., Shalem, O., Vuppalanchi, D., Willis, D. E., et al. (2012). Axonal transcription factors signal retrogradely in lesioned peripheral nerve. *The EMBO Journal*, *31*, 1350–1363.

Bhattacharya, S., & Schindler, C. (2003). Regulation of Stat3 nuclear export. *The Journal of Clinical Investigation*, *111*, 553–559.

Bisby, M. A., & Pollock, B. (1983). Increased regeneration rate in peripheral nerve axons following double lesions: Enhancement of the conditioning lesion phenomenon. *Journal of Neurobiology*, *14*, 467–472.

Blackmore, M. G., Wang, Z., Lerch, J. K., Motti, D., Zhang, Y. P., Shields, C. B., et al. (2012). Kruppel-like Factor 7 engineered for transcriptional activation promotes axon regeneration in the adult corticospinal tract. *Proceedings of the National Academy of Sciences of the United States of America*, *109*, 7517–7522.

Bradke, F., Fawcett, J. W., & Spira, M. E. (2012). Assembly of a new growth cone after axotomy: The precursor to axon regeneration. *Nature Reviews Neuroscience*, *13*, 183–193.

Cafferty, W. B., Gardiner, N. J., Das, P., Qiu, J., McMahon, S. B., & Thompson, S. W. (2004). Conditioning injury-induced spinal axon regeneration fails in interleukin-6 knock-out mice. *The Journal of Neuroscience*, *24*, 4432–4443.

Cafferty, W. B., Gardiner, N. J., Gavazzi, I., Powell, J., McMahon, S. B., Heath, J. K., et al. (2001). Leukemia inhibitory factor determines the growth status of injured adult sensory neurons. *The Journal of Neuroscience*, *21*, 7161–7170.

Cardone, M. H., Roy, N., Stennicke, H. R., Salvesen, G. S., Franke, T. F., Stanbridge, E., et al. (1998). Regulation of cell death protease caspase-9 by phosphorylation. *Science*, *282*, 1318–1321.

Carracedo, A., Alimonti, A., & Pandolfi, P. P. (2011). PTEN level in tumor suppression: How much is too little? *Cancer Research*, *71*, 629–633.

Cen, L. P., Luo, J. M., Zhang, C. W., Fan, Y. M., Song, Y., So, K. F., et al. (2007). Chemotactic effect of ciliary neurotrophic factor on macrophages in retinal ganglion cell survival and axonal regeneration. *Investigative Ophthalmology & Visual Science*, *48*, 4257–4266.

Chadborn, N. H., Ahmed, A. I., Holt, M. R., Prinjha, R., Dunn, G. A., Jones, G. E., et al. (2006). PTEN couples Sema3A signalling to growth cone collapse. *Journal of Cell Science*, *119*, 951–957.

Christie, K. J., Webber, C. A., Martinez, J. A., Singh, B., & Zochodne, D. W. (2010). PTEN inhibition to facilitate intrinsic regenerative outgrowth of adult peripheral axons. *The Journal of Neuroscience*, *30*, 9306–9315.

Cooney, R. N. (2002). Suppressors of cytokine signaling (SOCS): Inhibitors of the JAK/STAT pathway. *Shock*, *17*, 83–90.

Croker, B. A., Kiu, H., & Nicholson, S. E. (2008). SOCS regulation of the JAK/STAT signalling pathway. *Seminars in Cell & Developmental Biology*, *19*, 414–422.

Cui, Q., & Harvey, A. R. (2000). CNTF promotes the regrowth of retinal ganglion cell axons into murine peripheral nerve grafts. *Neuroreport*, *11*, 3999–4002.

Cui, Q., Yip, H. K., Zhao, R. C., So, K. F., & Harvey, A. R. (2003). Intraocular elevation of cyclic AMP potentiates ciliary neurotrophic factor-induced regeneration of adult rat retinal ganglion cell axons. *Molecular and Cellular Neuroscience*, *22*, 49–61.

Curtis, R., Scherer, S. S., Somogyi, R., Adryan, K. M., Ip, N. Y., Zhu, Y., et al. (1994). Retrograde axonal transport of LIF is increased by peripheral nerve injury: Correlation with increased LIF expression in distal nerve. *Neuron*, *12*, 191–204.

Davis, S., Aldrich, T. H., Stahl, N., Pan, L., Taga, T., Kishimoto, T., et al. (1993). LIFR beta and gp130 as heterodimerizing signal transducers of the tripartite CNTF receptor. *Science*, *260*, 1805–1808.

Di Cristofano, A., & Pandolfi, P. P. (2000). The multiple roles of PTEN in tumor suppression. *Cell*, *100*, 387–390.

Dickendesher, T. L., Baldwin, K. T., Mironova, Y. A., Koriyama, Y., Raiker, S. J., Askew, K. L., et al. (2012). NgR1 and NgR3 are receptors for chondroitin sulfate proteoglycans. *Nature Neuroscience*, *15*, 703–712.

Diehl, J. A., Cheng, M., Roussel, M. F., & Sherr, C. J. (1998). Glycogen synthase kinase-3beta regulates cyclin D1 proteolysis and subcellular localization. *Genes & Development*, *12*, 3499–3511.

Dobashi, Y., Watanabe, Y., Miwa, C., Suzuki, S., & Koyama, S. (2011). Mammalian target of rapamycin: A central node of complex signaling cascades. *International Journal of Clinical and Experimental Pathology*, *4*, 476–495.

Dolcet, X., Soler, R. M., Gould, T. W., Egea, J., Oppenheim, R. W., & Comella, J. X. (2001). Cytokines promote motoneuron survival through the Janus kinase-dependent activation of the phosphatidylinositol 3-kinase pathway. *Molecular and Cellular Neurosciences*, *18*, 619–631.

Domeniconi, M., Cao, Z., Spencer, T., Sivasankaran, R., Wang, K., Nikulina, E., et al. (2002). Myelin-associated glycoprotein interacts with the Nogo66 receptor to inhibit neurite outgrowth. *Neuron*, *35*, 283–290.

Fan, J., & Raper, J. A. (1995). Localized collapsing cues can steer growth cones without inducing their full collapse. *Neuron*, *14*, 263–274.

Filbin, M. T. (2003). Myelin-associated inhibitors of axonal regeneration in the adult mammalian CNS. *Nature Reviews Neuroscience*, *4*, 703–713.

Fischer, D., Heiduschka, P., & Thanos, S. (2001). Lens-injury-stimulated axonal regeneration throughout the optic pathway of adult rats. *Experimental Neurology*, *172*, 257–272.

Fischer, D., Petkova, V., Thanos, S., & Benowitz, L. I. (2004). Switching mature retinal ganglion cells to a robust growth state in vivo: Gene expression and synergy with RhoA inactivation. *The Journal of Neuroscience*, *24*, 8726–8740.

Fitch, M. T., & Silver, J. (2008). CNS injury, glial scars, and inflammation: Inhibitory extracellular matrices and regeneration failure. *Experimental Neurology*, *209*, 294–301.

Fukata, Y., Itoh, T. J., Kimura, T., Menager, C., Nishimura, T., Shiromizu, T., et al. (2002). CRMP-2 binds to tubulin heterodimers to promote microtubule assembly. *Nature Cell Biology*, *4*, 583–591.

Galiano, M., Liu, Z. Q., Kalla, R., Bohatschek, M., Koppius, A., Gschwendtner, A., et al. (2001). Interleukin-6 (IL6) and cellular response to facial nerve injury: Effects on lymphocyte recruitment, early microglial activation and axonal outgrowth in IL6-deficient mice. *The European Journal of Neuroscience*, *14*, 327–341.

Goncharova, E. A., Goncharov, D. A., Damera, G., Tliba, O., Amrani, Y., Panettieri, R. A., Jr., et al. (2009). Signal transducer and activator of transcription 3 is required for abnormal proliferation and survival of TSC2-deficient cells: Relevance to pulmonary lymphangioleiomyomatosis. *Molecular Pharmacology*, *76*, 766–777.

Gough, D. J., Corlett, A., Schlessinger, K., Wegrzyn, J., Larner, A. C., & Levy, D. E. (2009). Mitochondrial STAT3 supports Ras-dependent oncogenic transformation. *Science*, *324*, 1713–1716.

Hall, A., & Lalli, G. (2010). Rho and Ras GTPases in axon growth, guidance, and branching. *Cold Spring Harbor Perspectives in Biology*, *2*, a001818.

Hans, V. H., Kossmann, T., Lenzlinger, P. M., Probstmeier, R., Imhof, H. G., Trentz, O., et al. (1999). Experimental axonal injury triggers interleukin–6 mRNA, protein synthesis and release into cerebrospinal fluid. *Journal of Cerebral Blood Flow and Metabolism*, *19*, 184–194.

Harroch, S., Revel, M., & Chebath, J. (1994). Induction by interleukin-6 of interferon regulatory factor 1 (IRF-1) gene expression through the palindromic interferon response element pIRE and cell type-dependent control of IRF-1 binding to DNA. *The EMBO Journal*, *13*, 1942–1949.

Hay, N., & Sonenberg, N. (2004). Upstream and downstream of mTOR. *Genes & Development*, *18*, 1926–1945.

Heinrich, P. C., Behrmann, I., Haan, S., Hermanns, H. M., Muller-Newen, G., & Schaper, F. (2003). Principles of interleukin (IL)-6-type cytokine signalling and its regulation. *The Biochemical Journal*, *374*, 1–20.

Hellstrom, M., Muhling, J., Ehlert, E. M., Verhaagen, J., Pollett, M. A., Hu, Y., et al. (2011). Negative impact of rAAV2 mediated expression of SOCS3 on the regeneration of adult retinal ganglion cell axons. *Molecular and Cellular Neuroscience*, *46*, 507–515.

Hers, I., Vincent, E. E., & Tavare, J. M. (2011). Akt signalling in health and disease. *Cellular Signalling*, *23*, 1515–1527.

Hoffman, P. N. (2010). A conditioning lesion induces changes in gene expression and axonal transport that enhance regeneration by increasing the intrinsic growth state of axons. *Experimental Neurology*, *223*, 11–18.

Huang, J., & Manning, B. D. (2009). A complex interplay between Akt, TSC2 and the two mTOR complexes. *Biochemical Society Transactions*, *37*, 217–222.

Hur Saijilafu, E. M., Lee, B. D., Kim, S. J., Xu, W. L., & Zhou, F. Q. (2011). GSK3 controls axon growth via CLASP-mediated regulation of growth cone microtubules. *Genes & Development*, *25*, 1968–1981.

Hur, E. M., & Zhou, F. Q. (2010). GSK3 signalling in neural development. *Nature Reviews Neuroscience*, *11*, 539–551.

Hyatt Sachs, H., Rohrer, H., & Zigmond, R. E. (2010). The conditioning lesion effect on sympathetic neurite outgrowth is dependent on gp130 cytokines. *Experimental Neurology*, *223*, 516–522.

Iliopoulos, D., Jaeger, S. A., Hirsch, H. A., Bulyk, M. L., & Struhl, K. (2010). STAT3 activation of miR–21 and miR–181b–1 via PTEN and CYLD are part of the epigenetic switch linking inflammation to cancer. *Molecular Cell*, *39*, 493–506.

Jackson, R. E., & Eickholt, B. J. (2009). Semaphorin signalling. *Current Biology*, *19*, R504–R507.

Jo, S. A., Wang, E., & Benowitz, L. I. (1999). Ciliary neurotrophic factor is an axogenesis factor for retinal ganglion cells. *Neuroscience*, *89*, 579–591.

Kim, J. E., & Chen, J. (2004). Regulation of peroxisome proliferator–activated receptor–gamma activity by mammalian target of rapamycin and amino acids in adipogenesis. *Diabetes*, *53*, 2748–2756.

Kim, S. R., Chen, X., Oo, T. F., Kareva, T., Yarygina, O., Wang, C., et al. (2011). Dopaminergic pathway reconstruction by Akt/Rheb-induced axon regeneration. *Annals of Neurology*, *70*, 110–120.

Kim, Y. T., Hur, E. M., Snider, W. D., & Zhou, F. Q. (2011). Role of GSK3 signaling in neuronal morphogenesis. *Frontiers in Molecular Neuroscience*, *4*, 48.

Kim, D. H., & Sabatini, D. M. (2004). Raptor and mTOR: Subunits of a nutrient-sensitive complex. *Current Topics in Microbiology and Immunology*, *279*, 259–270.

Kim, D. H., Sarbassov, D. D., Ali, S. M., King, J. E., Latek, R. R., Erdjument-Bromage, H., et al. (2002). mTOR interacts with raptor to form a nutrient-sensitive complex that signals to the cell growth machinery. *Cell*, *110*, 163–175.

Kirby, J., Ning, K., Ferraiuolo, L., Heath, P. R., Ismail, A., Kuo, S. W., et al. (2011). Phosphatase and tensin homologue/protein kinase B pathway linked to motor neuron survival in human superoxide dismutase 1-related amyotrophic lateral sclerosis. *Brain*, *134*, 506–517.

Kirsch, M., Schneider, T., Lee, M. Y., & Hofmann, H. D. (1998). Lesion-induced changes in the expression of ciliary neurotrophic factor and its receptor in rat optic nerve. *Glia*, *23*, 239–248.

Kirsch, M., Terheggen, U., & Hofmann, H. D. (2003). Ciliary neurotrophic factor is an early lesion-induced retrograde signal for axotomized facial motoneurons. *Molecular and Cellular Neuroscience*, *24*, 130–138.

Kristof, A. S., Marks-Konczalik, J., Billings, E., & Moss, J. (2003). Stimulation of signal transducer and activator of transcription-1 (STAT1)-dependent gene transcription by lipopolysaccharide and interferon-gamma is regulated by mammalian target of rapamycin. *The Journal of Biological Chemistry*, *278*, 33637–33644.

Kurimoto, T., Yin, Y., Omura, K., Gilbert, H. Y., Kim, D., Cen, L. P., et al. (2010). Long-distance axon regeneration in the mature optic nerve: Contributions of oncomodulin, cAMP, and pten gene deletion. *The Journal of Neuroscience*, *30*, 15654–15663.

Kwon, C. H., Zhu, X., Zhang, J., & Baker, S. J. (2003). mTor is required for hypertrophy of Pten-deficient neuronal soma in vivo. *Proceedings of the National Academy of Sciences of the United States of America*, *100*, 12923–12928.

Kwon, C. H., Zhu, X., Zhang, J., Knoop, L. L., Tharp, R., Smeyne, R. J., et al. (2001). Pten regulates neuronal soma size: A mouse model of Lhermitte-Duclos disease. *Nature Genetics*, *29*, 404–411.

Laplante, M., & Sabatini, D. M. (2012). mTOR signaling in growth control and disease. *Cell*, *149*, 274–293.

Leaver, S. G., Cui, Q., Plant, G. W., Arulpragasam, A., Hisheh, S., Verhaagen, J., et al. (2006). AAV-mediated expression of CNTF promotes long-term survival and regeneration of adult rat retinal ganglion cells. *Gene Therapy*, *13*, 1328–1341.

Lee, J. K., Geoffroy, C. G., Chan, A. F., Tolentino, K. E., Crawford, M. J., Leal, M. A., et al. (2010). Assessing spinal axon regeneration and sprouting in Nogo-, MAG-, and OMgp-deficient mice. *Neuron*, *66*, 663–670.

Lee, N., Neitzel, K. L., Devlin, B. K., & MacLennan, A. J. (2004). STAT3 phosphorylation in injured axons before sensory and motor neuron nuclei: Potential role for STAT3 as a retrograde signaling transcription factor. *The Journal of Comparative Neurology*, *474*, 535–545.

Lehmann, U., Schmitz, J., Weissenbach, M., Sobota, R. M., Hortner, M., Friederichs, K., et al. (2003). SHP2 and SOCS3 contribute to Tyr-759-dependent attenuation of interleukin-6 signaling through gp130. *The Journal of Biological Chemistry*, *278*, 661–671.

Leibinger, M., Andreadaki, A., & Fischer, D. (2012). Role of mTOR in neuroprotection and axon regeneration after inflammatory stimulation. *Neurobiology of Disease*, *46*, 314–324.

Leibinger, M., Muller, A., Andreadaki, A., Hauk, T. G., Kirsch, M., & Fischer, D. (2009). Neuroprotective and axon growth-promoting effects following inflammatory stimulation on mature retinal ganglion cells in mice depend on ciliary neurotrophic factor and leukemia inhibitory factor. *The Journal of Neuroscience*, *29*, 14334–14341.

Leon, S., Yin, Y., Nguyen, J., Irwin, N., & Benowitz, L. I. (2000). Lens injury stimulates axon regeneration in the mature rat optic nerve. *The Journal of Neuroscience*, *20*, 4615–4626.

Leslie, N. R., & Downes, C. P. (2004). PTEN function: How normal cells control it and tumour cells lose it. *The Biochemical Journal*, *382*, 1–11.

Li, Y., de Haar, C., Peppelenbosch, M. P., & van der Woude, C. J. (2012). SOCS3 in immune regulation of inflammatory bowel disease and inflammatory bowel disease-related cancer. *Cytokine & Growth Factor Reviews*, *23*, 127–138.

Li, D., Qu, Y., Mao, M., Zhang, X., Li, J., Ferriero, D., et al. (2009). Involvement of the PTEN-AKT-FOXO3a pathway in neuronal apoptosis in developing rat brain after hypoxia-ischemia. *Journal of Cerebral Blood Flow and Metabolism*, *29*, 1903–1913.

Lin, L. F., Mismer, D., Lile, J. D., Armes, L. G., Butler, E. T., 3rd, Vannice, J. L., et al. (1989). Purification, cloning, and expression of ciliary neurotrophic factor (CNTF). *Science*, *246*, 1023–1025.

Lingor, P., Tonges, L., Pieper, N., Bermel, C., Barski, E., Planchamp, V., et al. (2008). ROCK inhibition and CNTF interact on intrinsic signalling pathways and differentially regulate survival and regeneration in retinal ganglion cells. *Brain*, *131*, 250–263.

Liu, B. P., Fournier, A., GrandPre, T., & Strittmatter, S. M. (2002). Myelin-associated glycoprotein as a functional ligand for the Nogo-66 receptor. *Science*, *297*, 1190–1193.

Liu, C. M., Hur, E. M., & Zhou, F. Q. (2012). Coordinating gene expression and axon assembly to control axon growth: Potential role of GSK3 signaling. *Frontiers in Molecular Neuroscience*, *5*, 3.

Liu, K., Lu, Y., Lee, J. K., Samara, R., Willenberg, R., Sears-Kraxberger, I., et al. (2010). PTEN deletion enhances the regenerative ability of adult corticospinal neurons. *Nature Neuroscience*, *13*, 1075–1081.

Liu, W., Zhou, Y., Reske, S. N., & Shen, C. (2008). PTEN mutation: Many birds with one stone in tumorigenesis. *Anticancer Research*, *28*, 3613–3619.

Luikart, B. W., Schnell, E., Washburn, E. K., Bensen, A. L., Tovar, K. R., & Westbrook, G. L. (2011). Pten knockdown in vivo increases excitatory drive onto dentate granule cells. *The Journal of Neuroscience*, *31*, 4345–4354.

Ma, X. M., & Blenis, J. (2009). Molecular mechanisms of mTOR–mediated translational control. *Nature Reviews Molecular Cell Biology*, *10*, 307–318.

McQuarrie, I. G., Grafstein, B., & Gershon, M. D. (1977). Axonal regeneration in the rat sciatic nerve: Effect of a conditioning lesion and of dbcAMP. *Brain Research*, *132*, 443–453.

Mey, J., & Thanos, S. (1993). Intravitreal injections of neurotrophic factors support the survival of axotomized retinal ganglion cells in adult rats in vivo. *Brain Research*, *602*, 304–317.

Miao, T., Wu, D., Zhang, Y., Bo, X., Subang, M. C., Wang, P., et al. (2006). Suppressor of cytokine signaling-3 suppresses the ability of activated signal transducer and activator of transcription-3 to stimulate neurite growth in rat primary sensory neurons. *The Journal of Neuroscience*, *26*, 9512–9519.

Monnier, P. P., Sierra, A., Schwab, J. M., Henke-Fahle, S., & Mueller, B. K. (2003). The Rho/ROCK pathway mediates neurite growth-inhibitory activity associated with the chondroitin sulfate proteoglycans of the CNS glial scar. *Molecular and Cellular Neuroscience*, *22*, 319–330.

Moore, D. L., Blackmore, M. G., Hu, Y., Kaestner, K. H., Bixby, J. L., Lemmon, V. P., et al. (2009). KLF family members regulate intrinsic axon regeneration ability. *Science*, *326*, 298–301.

Moore, D. L., & Goldberg, J. L. (2011). Multiple transcription factor families regulate axon growth and regeneration. *Developmental Neurobiology*, *71*, 1186–1211.

Muller, A., Hauk, T. G., Leibinger, M., Marienfeld, R., & Fischer, D. (2009). Exogenous CNTF stimulates axon regeneration of retinal ganglion cells partially via endogenous CNTF. *Molecular and Cellular Neurosciences*, *41*, 233–246.

Murphy, P. G., Grondin, J., Altares, M., & Richardson, P. M. (1995). Induction of interleukin-6 in axotomized sensory neurons. *The Journal of Neuroscience*, *15*, 5130–5138.

Mustelin, T., Vang, T., & Bottini, N. (2005). Protein tyrosine phosphatases and the immune response. *Nature Reviews Immunology*, *5*, 43–57.

Neumann, S., & Woolf, C. J. (1999). Regeneration of dorsal column fibers into and beyond the lesion site following adult spinal cord injury. *Neuron*, *23*, 83–91.

Ng, D. C., Lin, B. H., Lim, C. P., Huang, G., Zhang, T., Poli, V., et al. (2006). Stat3 regulates microtubules by antagonizing the depolymerization activity of stathmin. *The Journal of Cell Biology*, *172*, 245–257.

Niederost, B., Oertle, T., Fritsche, J., McKinney, R. A., & Bandtlow, C. E. (2002). Nogo-A and myelin-associated glycoprotein mediate neurite growth inhibition by antagonistic regulation of RhoA and Rac1. *The Journal of Neuroscience*, *22*, 10368–10376.

Ning, K., Drepper, C., Valori, C. F., Ahsan, M., Wyles, M., Higginbottom, A., et al. (2010). PTEN depletion rescues axonal growth defect and improves survival in SMN-deficient motor neurons. *Human Molecular Genetics*, *19*, 3159–3168.

O'Brien, C. A., & Manolagas, S. C. (1997). Isolation and characterization of the human gp130 promoter. Regulation by STATS. *The Journal of Biological Chemistry*, *272*, 15003–15010.

Oh, W. J., & Jacinto, E. (2011). mTOR complex 2 signaling and functions. *Cell Cycle*, *10*, 2305–2316.

Okumura, E., Fukuhara, T., Yoshida, H., Hanada Si, S., Kozutsumi, R., Mori, M., et al. (2002). Akt inhibits Myt1 in the signalling pathway that leads to meiotic G2/M-phase transition. *Nature Cell Biology*, *4*, 111–116.

Park, K. K., Hu, Y., Muhling, J., Pollett, M. A., Dallimore, E. J., Turnley, A. M., et al. (2009). Cytokine-induced SOCS expression is inhibited by cAMP analogue: Impact on regeneration in injured retina. *Molecular and Cellular Neuroscience*, *41*, 313–324.

Park, K. K., Liu, K., Hu, Y., Kanter, J. L., & He, Z. (2010). PTEN/mTOR and axon regeneration. *Experimental Neurology*, *223*, 45–50.

Park, K. K., Liu, K., Hu, Y., Smith, P. D., Wang, C., Cai, B., et al. (2008). Promoting axon regeneration in the adult CNS by modulation of the PTEN/mTOR pathway. *Science*, *322*, 963–966.

Park, K., Luo, J. M., Hisheh, S., Harvey, A. R., & Cui, Q. (2004). Cellular mechanisms associated with spontaneous and ciliary neurotrophic factor-cAMP-induced survival and axonal regeneration of adult retinal ganglion cells. *The Journal of Neuroscience*, *24*, 10806–10815.

Perdigoto, A. L., Chaudhry, N., Barnes, G. N., Filbin, M. T., & Carter, B. D. (2011). A novel role for PTEN in the inhibition of neurite outgrowth by myelin-associated glycoprotein in cortical neurons. *Molecular and Cellular Neuroscience*, *46*, 235–244.

Pradervand, S., Yasukawa, H., Muller, O. G., Kjekshus, H., Nakamura, T., St Amand, T. R., et al. (2004). Small proline-rich protein 1A is a gp130 pathway- and stress-inducible cardioprotective protein. *The EMBO Journal*, *23*, 4517–4525.

Proud, C. G. (2007). Signalling to translation: How signal transduction pathways control the protein synthetic machinery. *The Biochemical Journal*, *403*, 217–234.

Proud, C. G. (2009). mTORC1 signalling and mRNA translation. *Biochemical Society Transactions*, *37*, 227–231.

Qiu, J., Cafferty, W. B., McMahon, S. B., & Thompson, S. W. (2005). Conditioning injury-induced spinal axon regeneration requires signal transducer and activator of transcription 3 activation. *The Journal of Neuroscience*, *25*, 1645–1653.

Rawlings, J. S., Rosler, K. M., & Harrison, D. A. (2004). The JAK/STAT signaling pathway. *Journal of Cell Science*, *117*, 1281–1283.

Richardson, P. M., & Issa, V. M. (1984). Peripheral injury enhances central regeneration of primary sensory neurones. *Nature*, *309*, 791–793.

Richardson, P. M., McGuinness, U. M., & Aguayo, A. J. (1980). Axons from CNS neurons regenerate into PNS grafts. *Nature*, *284*, 264–265.

Rodger, J., Drummond, E. S., Hellstrom, M., Robertson, D., & Harvey, A. R. (2012). Long-term gene therapy causes transgene-specific changes in the morphology of regenerating retinal ganglion cells. *PLoS One*, 7, e31061.

Sahenk, Z., Seharaseyon, J., & Mendell, J. R. (1994). CNTF potentiates peripheral nerve regeneration. *Brain Research*, *655*, 246–250.

Sarbassov, D. D., Guertin, D. A., Ali, S. M., & Sabatini, D. M. (2005). Phosphorylation and regulation of Akt/PKB by the rictor-mTOR complex. *Science*, *307*, 1098–1101.

Schindler, C., Levy, D. E., & Decker, T. (2007). JAK-STAT signaling: From interferons to cytokines. *The Journal of Biological Chemistry*, *282*, 20059–20063.

Schwaiger, F. W., Hager, G., Schmitt, A. B., Horvat, A., Hager, G., Streif, R., et al. (2000). Peripheral but not central axotomy induces changes in Janus kinases (JAK) and signal transducers and activators of transcription (STAT). *The European Journal of Neuroscience*, *12*, 1165–1176.

Schwartz, M., Sivron, T., Eitan, S., Hirschberg, D. L., Lotan, M., & Elman-Faber, A. (1994). Cytokines and cytokine-related substances regulating glial cell response to injury of the central nervous system. *Progress in Brain Research*, *103*, 331–341.

Selles-Navarro, I., Ellezam, B., Fajardo, R., Latour, M., & McKerracher, L. (2001). Retinal ganglion cell and nonneuronal cell responses to a microcrush lesion of adult rat optic nerve. *Experimental Neurology*, *167*, 282–289.

Shen, Y., Tenney, A. P., Busch, S. A., Horn, K. P., Cuascut, F. X., Liu, K., et al. (2009). PTPsigma is a receptor for chondroitin sulfate proteoglycan, an inhibitor of neural regeneration. *Science*, *326*, 592–596.

Sheu, J. Y., Kulhanek, D. J., & Eckenstein, F. P. (2000). Differential patterns of ERK and STAT3 phosphorylation after sciatic nerve transection in the rat. *Experimental Neurology*, *166*, 392–402.

Shi, G. D., OuYang, Y. P., Shi, J. G., Liu, Y., Yuan, W., & Jia, L. S. (2011). PTEN deletion prevents ischemic brain injury by activating the mTOR signaling pathway. *Biochemical and Biophysical Research Communications*, *404*, 941–945.

Shuai, K., & Liu, B. (2003). Regulation of JAK-STAT signalling in the immune system. *Nature Reviews Immunology*, *3*, 900–911.

Smith, R. P., Lerch-Haner, J. K., Pardinas, J. R., Buchser, W. J., Bixby, J. L., & Lemmon, V. P. (2011). Transcriptional profiling of intrinsic PNS factors in the postnatal mouse. *Molecular and Cellular Neurosciences*, *46*, 32–44.

Smith, P. D., Sun, F., Park, K. K., Cai, B., Wang, C., Kuwako, K., et al. (2009). SOCS3 deletion promotes optic nerve regeneration in vivo. *Neuron*, *64*, 617–623.

Song, G., Ouyang, G., & Bao, S. (2005). The activation of Akt/PKB signaling pathway and cell survival. *Journal of Cellular and Molecular Medicine*, *9*, 59–71.

Stahl, N., & Yancopoulos, G. D. (1994). The tripartite CNTF receptor complex: Activation and signaling involves components shared with other cytokines. *Journal of Neurobiology*, *25*, 1454–1466.

Strebovsky, J., Walker, P., & Dalpke, A. H. (2012). Suppressor of cytokine signaling proteins as regulators of innate immune signaling. *Frontiers in Bioscience*, *17*, 1627–1639.

Strickland, I. T., Richards, L., Holmes, F. E., Wynick, D., Uney, J. B., & Wong, L. F. (2011). Axotomy-induced miR-21 promotes axon growth in adult dorsal root ganglion neurons. *PLoS One*, *6*, e23423.

Subang, M. C., & Richardson, P. M. (2001). Synthesis of leukemia inhibitory factor in injured peripheral nerves and their cells. *Brain Research*, *900*, 329–331.

Sun, F., Park, K. K., Belin, S., Wang, D., Lu, T., Chen, G., et al. (2011). Sustained axon regeneration induced by co-deletion of PTEN and SOCS3. *Nature*, *480*, 372–375.

Taga, T., Hibi, M., Hirata, Y., Yamasaki, K., Yasukawa, K., Matsuda, T., et al. (1989). Interleukin-6 triggers the association of its receptor with a possible signal transducer, gp130. *Cell*, *58*, 573–581.

Taga, T., & Kishimoto, T. (1997). Gp130 and the interleukin-6 family of cytokines. *Annual Review of Immunology*, *15*, 797–819.

Tamguney, T., & Stokoe, D. (2007). New insights into PTEN. *Journal of Cell Science*, *120*, 4071–4079.

Tamiya, T., Kashiwagi, I., Takahashi, R., Yasukawa, H., & Yoshimura, A. (2011). Suppressors of cytokine signaling (SOCS) proteins and JAK/STAT pathways: Regulation of T-cell inflammation by SOCS1 and SOCS3. *Arteriosclerosis, Thrombosis, and Vascular Biology*, *31*, 980–985.

Tanaka, H., Yamashita, T., Asada, M., Mizutani, S., Yoshikawa, H., & Tohyama, M. (2002). Cytoplasmic p21(Cip1/WAF1) regulates neurite remodeling by inhibiting Rho-kinase activity. *The Journal of Cell Biology*, *158*, 321–329.

Tedeschi, A. (2011). Tuning the orchestra: Transcriptional pathways controlling axon regeneration. *Frontiers in Molecular Neuroscience*, *4*, 60.

Thompson, S. W., Vernallis, A. B., Heath, J. K., & Priestley, J. V. (1997). Leukaemia inhibitory factor is retrogradely transported by a distinct population of adult rat sensory neurons: Co-localization with trkA and other neurochemical markers. *The European Journal of Neuroscience*, *9*, 1244–1251.

Trakhtenberg, E. F., & Goldberg, J. L. (2012). Epigenetic regulation of axon and dendrite growth. *Frontiers in Molecular Neuroscience*, *5*, 24.

van Adel, B. A., Arnold, J. M., Phipps, J., Doering, L. C., & Ball, A. K. (2005). Ciliary neurotrophic factor protects retinal ganglion cells from axotomy-induced apoptosis via modulation of retinal glia in vivo. *Journal of Neurobiology*, *63*, 215–234.

Veldman, M. B., Bemben, M. A., Thompson, R. C., & Goldman, D. (2007). Gene expression analysis of zebrafish retinal ganglion cells during optic nerve regeneration identifies

KLF6a and KLF7a as important regulators of axon regeneration. *Developmental Biology*, *312*, 596–612.

Venkatesh, K., Chivatakarn, O., Lee, H., Joshi, P. S., Kantor, D. B., Newman, B. A., et al. (2005). The Nogo-66 receptor homolog NgR2 is a sialic acid-dependent receptor selective for myelin-associated glycoprotein. *The Journal of Neuroscience*, *25*, 808–822.

Verma, P., Chierzi, S., Codd, A. M., Campbell, D. S., Meyer, R. L., Holt, C. E., et al. (2005). Axonal protein synthesis and degradation are necessary for efficient growth cone regeneration. *The Journal of Neuroscience*, *25*, 331–342.

Vinson, M., Strijbos, P. J., Rowles, A., Facci, L., Moore, S. E., Simmons, D. L., et al. (2001). Myelin-associated glycoprotein interacts with ganglioside GT1b. A mechanism for neurite outgrowth inhibition. *The Journal of Biological Chemistry*, *276*, 20280–20285.

Vogt, P. K., Gymnopoulos, M., & Hart, J. R. (2009). PI 3-kinase and cancer: Changing accents. *Current Opinion in Genetics & Development*, *19*, 12–17.

Vyas, A. A., Patel, H. V., Fromholt, S. E., Heffer-Lauc, M., Vyas, K. A., Dang, J., et al. (2002). Gangliosides are functional nerve cell ligands for myelin-associated glycoprotein (MAG), an inhibitor of nerve regeneration. *Proceedings of the National Academy of Sciences of the United States of America*, *99*, 8412–8417.

Wang, H., Zhang, Q., Wen, Q., Zheng, Y., Philip, L., Jiang, H., et al. (2012). Proline-rich Akt substrate of 40kDa (PRAS40): A novel downstream target of PI3k/Akt signaling pathway. *Cellular Signalling*, *24*, 17–24.

Wegrzyn, J., Potla, R., Chwae, Y. J., Sepuri, N. B., Zhang, Q., Koeck, T., et al. (2009). Function of mitochondrial Stat3 in cellular respiration. *Science*, *323*, 793–797.

Yang, L. J., Zeller, C. B., Shaper, N. L., Kiso, M., Hasegawa, A., Shapiro, R. E., et al. (1996). Gangliosides are neuronal ligands for myelin-associated glycoprotein. *Proceedings of the National Academy of Sciences of the United States of America*, *93*, 814–818.

Yin, Y., Cui, Q., Gilbert, H. Y., Yang, Y., Yang, Z., Berlinicke, C., et al. (2009). Oncomodulin links inflammation to optic nerve regeneration. *Proceedings of the National Academy of Sciences of the United States of America*, *106*, 19587–19592.

Yin, Y., Cui, Q., Li, Y., Irwin, N., Fischer, D., Harvey, A. R., et al. (2003). Macrophage-derived factors stimulate optic nerve regeneration. *The Journal of Neuroscience: The Official Journal of the Society for Neuroscience*, *23*, 2284–2293.

Yin, Y., Henzl, M. T., Lorber, B., Nakazawa, T., Thomas, T. T., Jiang, F., et al. (2006). Oncomodulin is a macrophage-derived signal for axon regeneration in retinal ganglion cells. *Nature Neuroscience*, *9*, 843–852.

Yiu, G., & He, Z. (2006). Glial inhibition of CNS axon regeneration. *Nature Reviews Neuroscience*, *7*, 617–627.

Yokogami, K., Wakisaka, S., Avruch, J., & Reeves, S. A. (2000). Serine phosphorylation and maximal activation of STAT3 during CNTF signaling is mediated by the rapamycin target mTOR. *Current Biology*, *10*, 47–50.

Yoshimura, T., Kawano, Y., Arimura, N., Kawabata, S., Kikuchi, A., & Kaibuchi, K. (2005). GSK-3beta regulates phosphorylation of CRMP-2 and neuronal polarity. *Cell*, *120*, 137–149.

Zhang, Q., Wang, H. Y., Marzec, M., Raghunath, P. N., Nagasawa, T., & Wasik, M. A. (2005). STAT3- and DNA methyltransferase 1-mediated epigenetic silencing of SHP-1 tyrosine phosphatase tumor suppressor gene in malignant T lymphocytes. *Proceedings of the National Academy of Sciences of the United States of America*, *102*, 6948–6953.

Zhang, Q., Wang, H. Y., Woetmann, A., Raghunath, P. N., Odum, N., & Wasik, M. A. (2006). STAT3 induces transcription of the DNA methyltransferase 1 gene (DNMT1) in malignant T lymphocytes. *Blood*, *108*, 1058–1064.

Zheng, B., Atwal, J., Ho, C., Case, L., He, X. L., Garcia, K. C., et al. (2005). Genetic deletion of the Nogo receptor does not reduce neurite inhibition in vitro or promote

corticospinal tract regeneration in vivo. *Proceedings of the National Academy of Sciences of the United States of America*, *102*, 1205–1210.

Zhou, L., & Too, H. P. (2011). Mitochondrial localized STAT3 is involved in NGF induced neurite outgrowth. *PLoS One*, *6*, e21680.

Zhou, J., Wulfkuhle, J., Zhang, H., Gu, P., Yang, Y., Deng, J., et al. (2007). Activation of the PTEN/mTOR/STAT3 pathway in breast cancer stem-like cells is required for viability and maintenance. *Proceedings of the National Academy of Sciences of the United States of America*, *104*, 16158–16163.

Zigmond, R. E., & Sun, Y. (1997). Regulation of neuropeptide expression in sympathetic neurons. Paracrine and retrograde influences. *Annals of the New York Academy of Sciences*, *814*, 181–197.

Retrograde Signaling in the Optic Nerve Is Necessary for Electrical Responsiveness of Retinal Ganglion Cells

Tsung-Han Chou,[1] Kevin K. Park,[2] Xueting Luo,[2] and Vittorio Porciatti[1]

Purpose. We investigated the role of retrograde signaling in the optic nerve on retinal ganglion cell (RGC) electrical responsiveness in the mouse model.

Methods. Electrical response of RGC was measured by pattern electroretinogram (PERG) in 43 C57BL/6J mice 4 to 6 months old under ketamine/xylazine anesthesia. PERGs were recorded before and at different times after blockade of axon transport with lidocaine at either the retrobulbar level (2 μL, 40 μg/μL) or at level of the superior colliculus (SC, 1 μL, 40 μg/μL). PERGs also were recorded before and at different times after optic nerve crush 1.5 mm behind the eye, followed by TUJ1-positive RGC counts of excised retinas. As controls, PERGs also were recorded after either saline injections or sham optic nerve surgery. The photopic flash electroretinogram (FERG) and visual evoked potential (FVEP) also were recorded before lidocaine and at relevant times afterwards.

Results. Lidocaine injection caused rapid (retrobulbar ~10 minutes, SC 1 hour), reversible reduction of PERG amplitude (≥50%). Optic nerve crush caused rapid (10–20 minutes), irreversible reduction of PERG amplitude (70–75%), increase of PERG latency (>25%), as well as RGC loss (88%) 1 month after crush. FVEP was unaltered by lidocaine. For all procedures, the FERG was unaltered.

Conclusions. As experimental interventions were made at postretinal level(s), PERG changes were likely associated with altered supply of retrogradely-delivered material from the SC. This implies that retrograde transport of target-derived molecules is necessary for normal RGC electrical responsiveness. The time course of early PERG changes is consistent with the speed of fast retrograde axon transport. (*Invest Ophthalmol Vis Sci.* 2013;54:1236–1243) DOI:10.1167/iovs.12-11188

Optic nerve diseases, such as glaucoma, optic neuritis, and Leber's hereditary optic neuropathy (LHON), are a family of disorders whose final common pathway is retinal ganglion cell (RGC) degeneration resulting in blindness. Increasing evidence in animal models of glaucoma and optic nerve diseases shows that RGC death is preceded by a stage of optic neuropathy that includes impairment of axon transport.[1–8] In experimental models of glaucoma and optic nerve disease, RGC death also has been shown to be preceded by loss of RGC electrical responsiveness that can be measured either at single cell level[9] or noninvasively over time with the pattern electroretinogram (PERG).[10–14] Importantly, PERG abnormalities in human and mouse glaucoma models may be improved after IOP reduction,[15–20] suggesting that loss of PERG signal preceding death is reversible.

Thus, there is interest in investigating the factors that alter RGC electrical responsiveness to design therapeutic strategies to restore impaired function and prolong cell survival. Here, we investigated the role of retrograde signaling on RGC responsiveness in the mouse. We showed that lidocaine injected into the eye orbit or within the superior colliculus (SC) causes reversible reduction of PERG signal. Retrobulbar optic nerve crush causes rapid, irreversible loss of PERG signal that precedes RGC death. Altogether, results suggested that intact retrograde signaling is necessary for normal RGC responsiveness. Preliminary results of our study have been reported previously in abstract form (Chou TH, et al. *IOVS* 2012;53:ARVO E-Abstract 1956).

MATERIALS AND METHODS

Animals and Husbandry

Our study was approved by the Animal Care and Use Committee at University of Miami. All experiments were conducted according to the ARVO Statement for the Use of Animals in Ophthalmic and Vision Research. C57BL/6J mice (B6) purchased from the Jackson Laboratory (Bar Harbor, ME) were kept in our AAALAC-certified vivarium, using standard 12:12-hour light-dark cycle and fed with Grain Based Diet (Lab Diet: 500, Opti-diet; PMI Nutrition International, Inc., Brentwood, MO). For the present study, 43 C7BL/6J mice of 3 to 4 months of age were used.

Interventional Procedures

Mice were weighed and anesthetized with intraperitoneal (IP) injections (0.5–0.7 mL/kg) of a mixture of ketamine 42.8 mg/mL and xylazine 8.6 mg/ml. Lidocaine was injected either retrobulbarly or at the level of the SC. Retrobulbar injections of lidocaine (2 μL, 40 μg/μL) were performed with a 23-gauge needle using a supraorbital approach. Care was taken that the procedure did not cause orbital hemorrhage. For intracollicular lidocaine injections, the head fur was shaved and the surgical site prepared with 10% povidone-iodine. An incision of the scalp was performed to expose the skull. A small hole was drilled 2.9 mm behind the bregma and 0.5 mm lateral to the midline of the right hemisphere by using a high-speed dental drill. Lidocaine (1 μL, 40 μg/μL) was injected slowly at a depth of 1.6 mm below the dura using a Hamilton syringe.

Optic nerve crush was performed as described previously.[21,22] The left optic nerve was exposed intraorbitally after incision of the

temporal conjunctiva followed by blunt dissection, and crushed with jeweler's forceps (Dumont #5; Roboz Surgical Instrument Co., Inc., Gaithersburg, MD) for 5 seconds approximately 1 to 1.5 mm behind the optic disc. To preserve the retinal blood supply, care was taken not to damage the underlying ophthalmic artery. After the surgical procedure, mice received a subcutaneous injection of buprenorphine (0.05 mg/kg; Bedford Laboratories, Bedford, OH) as postoperative analgesic. Eye ointment containing atropine sulfate was applied preoperatively to protect the cornea during surgery.

PERG Recording

A detailed description of the PERG technique has been reported previously.[19,23,24] In brief, mice were weighed and anesthetized with intraperitoneal injections (0.5–0.7 mL/kg) of a mixture of ketamine 42.8 mg/mL and xylazine 8.6 mg/ml. Mice then were restrained gently in a custom-made holder that allowed unobstructed vision. The body of the animal was kept at a constant body temperature of 37.0°C using a feedback-controlled heating pad (TCAT-2LV; Physitemp Instruments, Inc., Clifton, NJ). The eyes of anesthetized mice typically were wide open and in a stable position, with optical axes pointing laterally and upwardly.[25,26]

A PERG electrode (0.25 mm diameter silver wire configured to a semicircular loop of 2 mm radius) was placed on the extrapupillary corneal surface by means of a micromanipulator. A small drop of balanced saline was applied topically every 30 minutes to prevent corneal dryness. Reference and ground electrodes were stainless steel needles inserted under the skin of the posterior scalp along the midline and of the tail, respectively.

Visual stimuli consisted of contrast-reversing (2 reversals/s) horizontal bars (0.05 cycles/deg, 100% contrast, mean luminance 50 cd/m^2) generated by a programmable graphic card (VSG; Cambridge Research Systems, Rochester, UK) on a CRT display (Sony Multiscan 500; Sony, New York, NY) whose center was aligned with the projection of the pupil. The pupils were not dilated, and eyes were not refracted for the viewing distance, since the mouse eye has a large depth of focus.[27–29] At the viewing distance of 15 cm, the stimulus field covered an area of 69.4 × 63.4 degrees. Three consecutive PERG responses to 600 contrast reversals each were recorded. The responses were superimposed to check for consistency and then averaged (1800 sweeps). The PERG waveform consisted of a major positive peak at around 80 ms to 120 ms (defined as P100) followed by a slower negative wave with a broad trough at around 200 ms to 300 ms (defined as N250).[23] The PERG amplitude was the sum of the P100 and N250 amplitudes. The PERG latency was the time to the P100 peak. Representative examples are shown in Figure 1.

Protocol

After recording a baseline PERG, lidocaine was injected either behind the globe (retrobulbar) or within the SC (intracollicular), and PERG recorded at the first available postinterventional opportunity (approximately 10 minutes for retrobulbar lidocaine and within 1 hour for intracollicular lidocaine), and at different times during the same day and in subsequent days. After recording a baseline PERG, the optic nerve of one side was crushed and the PERG then was recorded at the first available postinterventional opportunity (10–20 minutes after surgery), and at different times during the same day and in subsequent days. One month after optic nerve crush, mice were euthanized, and retinas and optic nerves harvested for RGC immunohistochemistry.

Immunohistochemistry for RGC Counts

Whole mount retinal staining and RGC counting were performed as described previously.[21] Antibodies were diluted in blocking solution consisting of 5% normal goat serum (NGS) and 0.3% Triton X-100 in PBS. Retinas were blocked for 1 hour at room temperature, and incubated with primary antibody, mouse neuronal class β-III tubulin

(clone TUJ1, 1:400 dilution; Covance, Princeton, NJ) overnight at 4°C, and washed three times for 10 minutes each with PBS. Secondary antibody then was applied (1:200; Jackson Laboratory) and incubated for 1 hour at room temperature. Retinas were washed again three times for 10 minutes each with PBS before a cover slip was attached with Fluoromount-G (Southern Biotech, Birmingham, AL). For RGC counting, 9 to 12 fields of the whole mount retinas immunostained with TUJ1 antibody were sampled randomly at approximately 0.5, 1, and 1.5 mm from the center of the optic nerve in each retinal quadrant under a fluorescence microscope. Quantification of TUJ1-positive RGCs is represented as percentage of TUJ1-positive RGCs compared to the uninjured contralateral retinas. In previous studies of our group (e.g., Park et al.[21]) as well as of others,[30,31] it has been shown that TUJ1-positive cells overlap completely with retrogradely transported FluoroGold-positive cells, but did not overlap with ChAT-positive amacrine cells. Thus, TUJ1 immunoreactivity could be used to estimate the total number of surviving RGCs.

Controls

As a control of nonspecific effects of lidocaine injections, the PERG was recorded before and after injections of PBS either retrobulbar or intracollicular, using identical volume and procedures. As a control for nonspecific effects of optic nerve crush, the optic nerve was exposed as described above, but not crushed. As a control for generalized effect of lidocaine/optic nerve crush to outer retinal neurons, a photopic ERG (FERG) was recorded in response to diffuse bright flashes on a rod-saturating background as described previously.[23] The FERG was recorded before and after lidocaine/optic nerve crush, at post-treatment times when the PERG had the lowest amplitude compared to baseline. The FERG waveform consisted of a major positive b-wave peaking at approximately 50 ms followed by a slower negative wave also known as photopic negative response (PhNR).[23,32] The FERG amplitude was measured from the peak of the b-wave to the trough of the PhNR (see examples in Fig. 4). As a control for postsynaptic effects of retrobulbar lidocaine, flash-evoked VEPs (FVEPs) were recorded in response to diffuse light flashes similarly to the FERG. FVEPs were recorded from stainless steel screws (shaft length 2.4 mm, shaft diameter 1.57 mm; PlasticsOne, Roanoke, VA) inserted chronically into the skull contralateral to the stimulated eye 2 mm lateral to the lambda suture, which corresponds to the monocular visual cortex[33,34] (see examples in Fig. 4).

Statistics

In all experiments, posttreatment PERG changes were expressed as percentage variation compared to the mean baseline value, and analyzed with ANOVA followed by post hoc Dunnett tests. A P value of <0.05 was considered significant.

RESULTS

Retrobulbar Lidocaine

The effect of retrobulbar lidocaine injection on the PERG is summarized in Figure 1. The PERG amplitude tended to decrease (Fig. 1A), while the PERG latency tended to increase (Fig. 1C), already 10 minutes after injection and reached a minimum at around 30 minutes to 1 hour. The PERG amplitude recovered to baseline values within the next 5 days after injection. The effect of retrobulbar lidocaine on PERG amplitude was significant (ANOVA $P < 0.001$, post hoc comparisons versus baseline group [Dunnett] revealed significant [$P < 0.05$] changes at 20 and 30 minutes, and 1 hour). PERG latency tended to increase after retrobulbar lidocaine, but the effect was not significant (ANOVA $P = 0.14$). As shown in Figures 1B and 1D, retrobulbar injection of saline had no effect on PERG amplitude and latency.
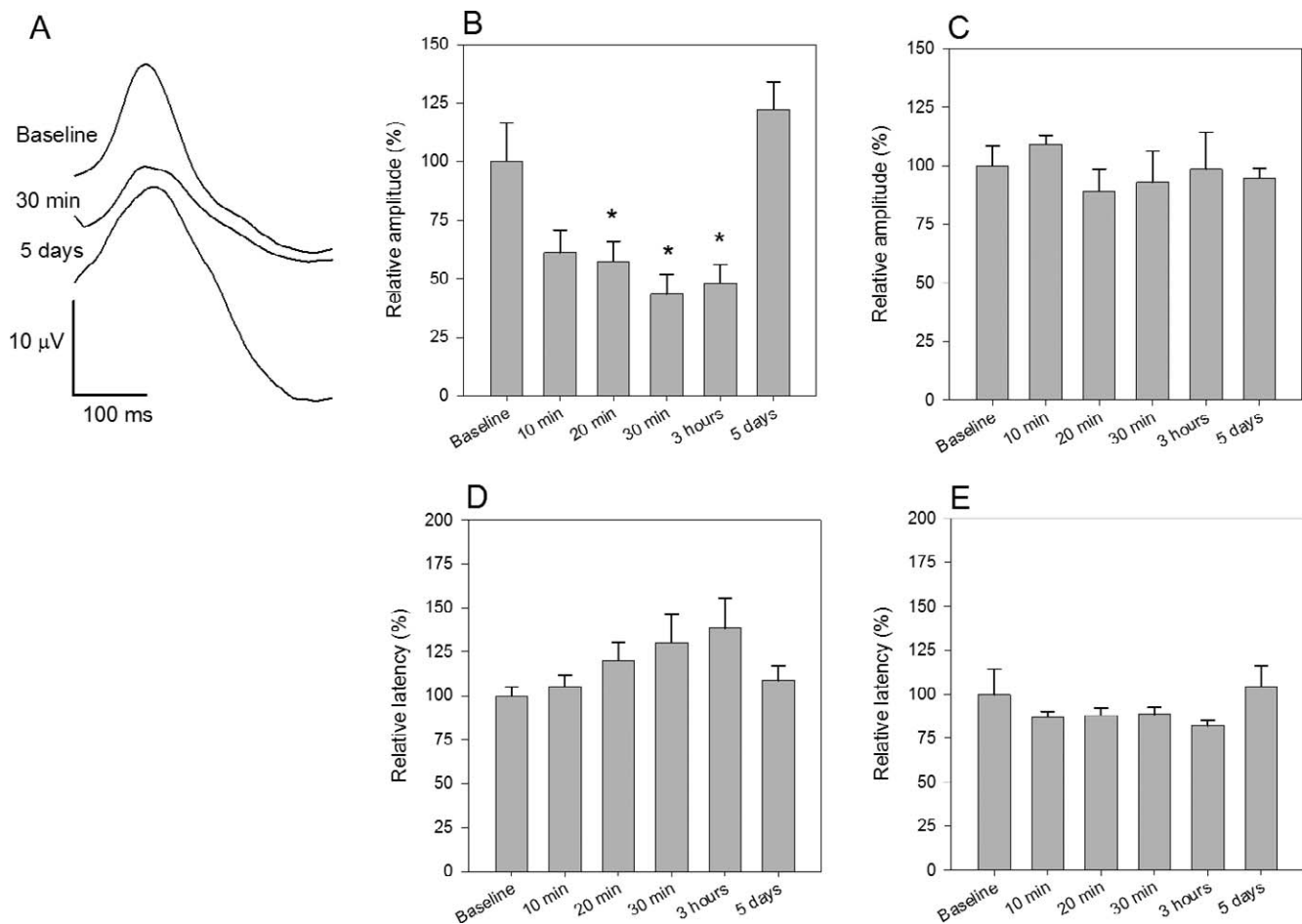
FIGURE 1. Effect of retrobulbar lidocaine injection on PERG. (**A**) Representative examples of PERG waveforms recorded before, and 30 minutes and 5 days after injection. (**B**) Mean PERG amplitude (**B**) and latency (**D**) before and at different times after injection. (**C**, **E**) Mean PERG amplitude (**C**) and latency (**E**) before and after retrobulbar saline injection. All data were normalized to mean baseline values ([**B**] 28.4 μV, SEM 2.7; [**D**] 94.0 ms, SEM 4.6, $n = 9$; [**C**] 26.3 μV, SEM 2.1; [**E**] 92.5 ms, SEM 10.5, $n = 5$). *Errors bars* represent the SEM. Significance ($P < 0.05$) of the effect compared to baseline is represented by *asterisks* above *bars*.

Intracollicular Lidocaine

The effect of intracollicular lidocaine injection on the PERG is summarized in Figure 2. The PERG amplitude decreased (Fig. 2A) 1 hour after injection and then progressively tended to a recovery, which was complete within the next 5 days. The effect of intracollicular lidocaine on PERG amplitude was significant (ANOVA $P < 0.001$, post hoc comparisons versus baseline [Dunnett] revealed significant [$P < 0.05$] changes at 20 and 30 minutes, and 1 hour). PERG latency tended to increase, but the effect was not significant (ANOVA $P = 0.053$, Fig. 2C). Intracollicular injection of saline (Fig. 2B) had a smaller effect on PERG amplitude (ANOVA $P = 0.009$), which was significant ($P < 0.05$) at 20 minutes only.

Optic Nerve Crush

Intraorbital optic nerve crush resulted in much reduced PERG amplitude already 10 to 20 minutes after surgery, which remained approximately at the same reduced level over 1 month observation (Fig. 3A). The effect was significant (ANOVA $P < 0.001$, post hoc t-tests $P < 0.001$ for all postsurgical points compared to baseline). One month after optic nerve crush, retinas were harvested, and TUJ1-positive RGCs counted (Fig. 3E) and compared to RGC counts in noninjured retinas (Fig. 3F). TUJ1-positive RGC survival in mice that received optic

nerve crush was on average 12% (SEM 1.4). Optic nerve crush also resulted in a progressive increase of PERG latency (Fig. 3C, ANOVA $P = 0.033$). Post hoc test showed significant ($P < 0.05$) increase compared to baseline at 5 days and 1 month after surgery. Sham surgery did not result in significant changes of PERG amplitude (Fig. 3B) and latency (Fig. 3D).

Control FERG and Photopic Visual Evoked Potential (FVEP)

The FERG was recorded before retrobulbar lidocaine/optic nerve crush and at post treatment times at which the PERG had the lowest amplitude compared to baseline. Individual FERG waveforms were averaged and displayed in Figure 4 as grand-average ± SEM. For retrobulbar lidocaine and optic nerve crush, pre- and post treatment FERGs had virtually identical grand-average waveform. Figure 4 also shows that the FVEP had very similar waveform recorded before and after retrobulbar lidocaine injection.

DISCUSSION

Axon transport defects are a common theme in neurodegenerative diseases,[35] including glaucoma,[3,5,36,37] and may have a role in the pathogenesis of RGC death.[8,38] Little is known on
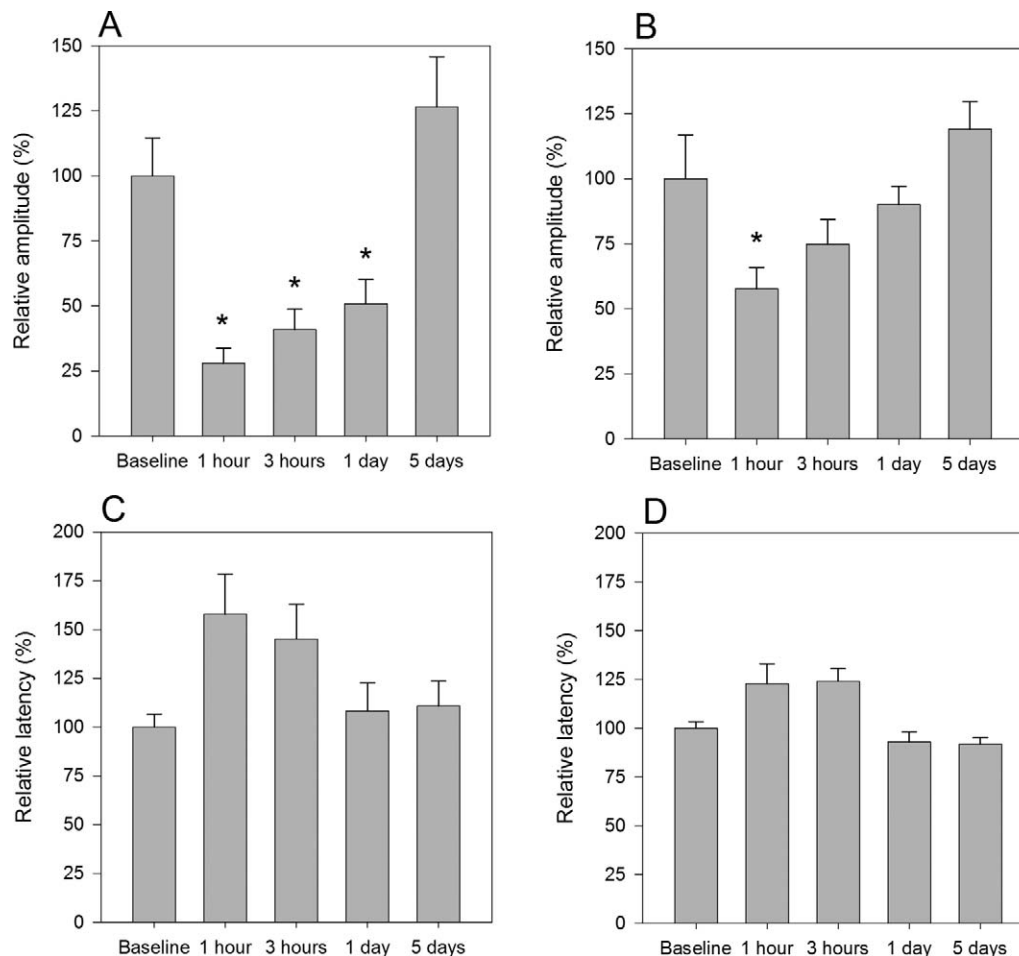
FIGURE 2. Effect of intracollicular lidocaine injection on PERG. (**A**) Mean PERG amplitude recorded before and at different times after intracollicular lidocaine injection. (**C**) Mean PERG latency before and after lidocaine injection. (**B, D**) Control experiments with intracollicular saline injection. All data were normalized to mean baseline values ([**A**] 26.1 μV, SEM 3.8; [**C**] 83.0 ms, SEM 5.4, $n = 5$; [**B**] 25.3 μV, SEM 4.1; [**D**] 92.5 ms, SEM 2.9). *Errors bars* represent the SEM. Significance ($P < 0.05$) of the effect compared to baseline is represented by *asterisks* above *bars*.

the relationship between reduced axon transport and RGC function.[39] Here, we addressed this problem by recording the PERG—a signal that depends on the physiologic integrity of RGC—before and after manipulations at postretinal level that impair retrograde signaling in the retinocollicular pathway. Lidocaine is a well established method to block axon transport[40-42] without damaging optic nerve structures,[43] and acts at very low concentrations.[44] At sufficient concentrations, lidocaine also is known to alter signal conduction by blocking voltage-gated sodium channels in the neuronal cell membrane,[45] thereby suppressing postsynaptic activity. As FVEPs were not altered significantly after retrobulbar lidocaine, our results indicated that the action of lidocaine on sodium channels was insufficient to impair signal conduction along the optic nerve. Insufficient blockage of sodium channels also suggests that a direct action of lidocaine on action potentials of RGCs is unlikely. It also is unlikely that lidocaine entered the retina via the cardiovascular system and impaired directly RGC spiking activity, as in this case the concentration of lidocaine at the retina would have been minimal. Finally, it is unlikely that optic nerve crush caused ischemic damage to the retina, as shown in previous studies.[21,22] For lidocaine injection and optic nerve crush, the FERG—a signal originating in the outer retina—was unaltered. This suggested that the effects of all manipulations did not cause generalized retinal dysfunction.

Altogether, as the effects of all postretinal manipulations on PERG were qualitatively similar and major unspecific effects on RGC could be ruled out, the results strongly suggested that PERG changes were linked to altered supply of retrogradely-delivered material via axon transport. Reversible blockade of axon transport was not expected to cause damage to RGC,[43,46] whereas for optic nerve crush RGC loss was expected to start approximately 5 days after surgery.[21,47] However, the effects of the optic nerve crush could include an acute physiologic effect on RGC signaling[48] that added to the effect mediated by impairment of retrograde signaling.

The main result of our study is that lidocaine injections caused rapid, reversible reduction of PERG signal to at least 50% of its baseline value. PERG effects after intracollicular lidocaine injection could be measured within 1 hour after treatment, and recovered progressively over 4 days. After retrobulbar lidocaine injection, PERG effects could be measured as early as 10 to 20 minutes posttreatment, reached a maximum at 30 minutes, and recovered within 5 days. The effects of retrobulbar optic nerve crush on PERG also could be measured as early 10 to 20 minutes after surgery, and remained stable at reduced level over 1-month follow-up, after which histology demonstrated a drastic (88%) decrease of TUJ1-positive RGC counts in the retina. That the earliest effects on PERG of retrobulbar lidocaine were rather similar in magnitude and time course to those obtained with retrobulbar optic nerve
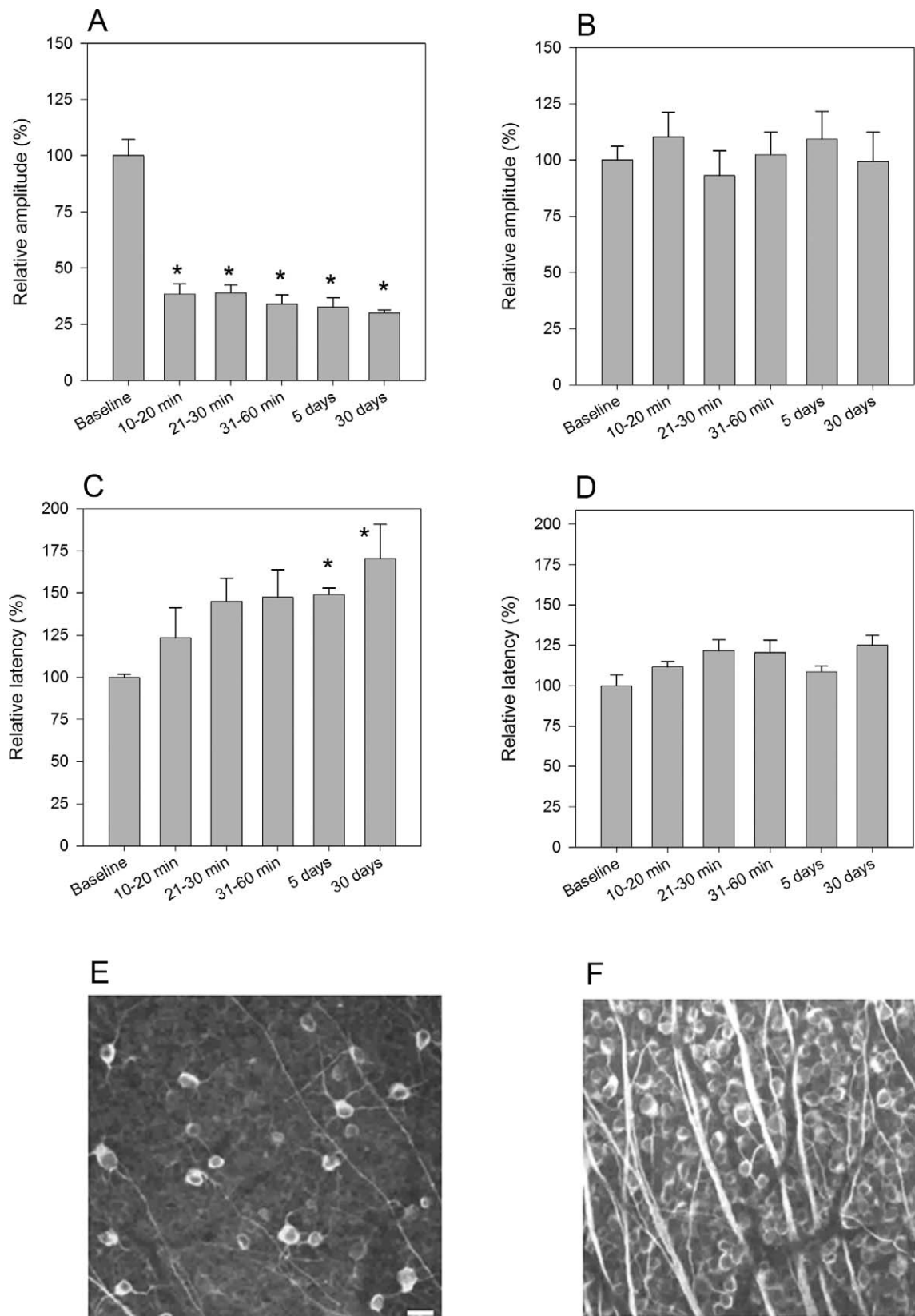
FIGURE 3. Effect of optic nerve crush on PERG and RGC death. (**A**, **C**) Mean PERG amplitude (**A**) and latency (**C**) before and at different times after optic nerve crush 1.5 mm behind the globe. (**B**, **D**) Mean PERG amplitude (**B**) and latency (**D**) in control mice that received sham surgery. All data were normalized to mean baseline values ([**A**] 21.7 µV, SEM 2.4; [**C**] 83.6 ms, SEM 1.1; [**B**] 18.3 µV, SEM 1.8; [**D**] 81.3, SEM 2.4). *Errors bars* represent the SEM (*n* = 5). Significance (*P* < 0.05) of the effect compared to baseline is represented by *asterisks* above *bars*. (**E**, **F**) Representative examples of TUJ1-positive RGC in mice that received optic nerve crush 1 month before (**E**) and in control, sham injured mice (**F**). RGC survival in mice that received optic nerve crush was 12% (SEM 1.4). *Scale bar*: 10 µm.
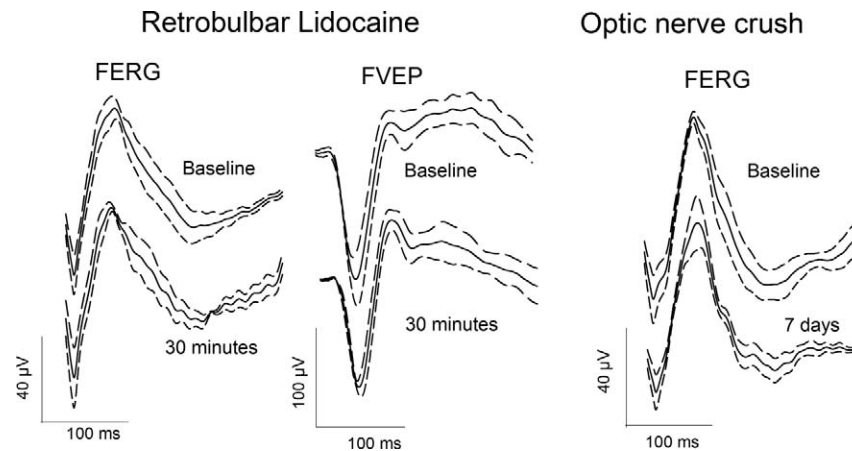
FIGURE 4. Lack of effect of retrobulbar lidocaine and optic nerve crush on FERG and FVEP. *Left*: Grand average FERG and FVEP waveforms (*continuous lines*) and superimposed ± SEMs (*dashed lines*) recorded before and 30 minutes after retrobulbar injection of 2 μL of lidocaine 40 mg/mL. FERGs were recorded from the eye ipsilateral to the injected side. FVEPs were recorded from the monocular visual cortex contralateral to the stimulated eye. *Right*: Grand average FERG waveforms (*continuous lines*) and superimposed ± SEMs (*dashed lines*) recorded before and 7 days after crush of the ipsilateral optic nerve performed 1.5 mm behind the eye.

crush suggested that the latter also were mediated largely by impairment of retrograde axon transport rather that direct injury to RGC.[48] Dramatic losses of PERG signal after either optic nerve section[49] or crush[32] in the mouse have been reported before, but these studies were not designed to monitor early postsurgical events.

Our study provided only a reasonable approximation of the time course of the PERG effects, as there were constraints due the time needed for the experimental procedures. For retrobulbar injection and optic nerve crush, the earliest opportunity to record a postprocedural PERG was approximately 10 minutes. For intracollicular injections, the earliest opportunity was 1 hour later. Thus, we cannot exclude that the PERG effects could have manifested somewhat earlier compared to the values we were able to measure. If we assume 10 to 15 minutes postprocedural delay for proximal interventions (retrobulbar lidocaine, optic nerve crush) and 60 minutes delay for distal intervention (intracollicular lidocaine); if we also assume that the delay was due to the speed of retrograde axon transport, and the retinocollicular distance would be approximately 11 mm,[50] then the corresponding velocities of axon transport would be approximately 0.12 mm/min (1.5 mm distance/12.5 min) and 0.18 mm/min (11 mm distance/60 min). These calculated velocities are well in the range of those reported for fast retrograde transport in a number of studies.[1,51] It should be taken into account that the mouse optic nerve has an unmyelinated portion of 0.6 to 0.8 mm immediately adjacent to the sclera.[52] This might have represented a vulnerable location that drove the earliest effect of retrobulbar lidocaine.

What is the retrograde signal(s) whose reduced supply caused reduced electric responsiveness of RGC? Our study does not provide direct answers to this important question, which will be addressed in a subsequent study. A reasonable hypothesis is that target-derived brain derived neurotrophic factor (BDNF) may represent a likely molecular candidate. Available evidence shows that intraocular pressure elevation in an experimental glaucoma model causes obstructed axon transport of BDNF and its receptor, TrkB, eventually leading to RGC death.[38] BDNF has been shown to depolarize neurons just as rapidly as the neurotransmitter glutamate, even at very low concentrations.[53–55] Rapid actions of neurotrophins include changes in neuronal excitability, synaptic transmission, and neural plasticity. Of interest, intracollicular injection of saline

also temporarily reduced the PERG signal, although to a smaller/shorter extent compared to intracollicular lidocaine injection. It is possible that intracollicular injection of 1 μL saline mechanically caused temporary impairment of the target-derived supply of retrogradely-transported material that sustains RGC responsiveness. RGC responsiveness also may be sustained in part by other postsynaptic targets, such as the dorsal geniculate nucleus and the suprachiasmatic nucleus.

In conclusion, our results showed that impairment of retrograde signaling causes rapid, substantial decrease of PERG amplitude and increase in PERG latency that may be reversible. Results implied that intact retrograde signaling is necessary for the normal electrical responsiveness of retinal ganglion cells. Numerous reports of early PERG impairment in glaucoma,[56,57] optic nerve diseases,[58] and diabetes[59,60] at least in part may be due to altered axon transport. Also, recovery of PERG amplitude losses after either IOP lowering[15,17,18,61,62] or removal of pituitary tumors[63] may be related to restoration of axon transport. Thus, the PERG may represent a promising marker of early, reversible axonal dysfunction preceding RGC death in glaucoma and optic nerve diseases.[64]

References

1. Morgan JE. Circulation and axonal transport in the optic nerve. *Eye (Lond)*. 2004;18:1089–1095.

2. Whitmore AV, Libby RT, John SW. Glaucoma: thinking in new ways-a role for autonomous axonal self-destruction and other compartmentalised processes? *Prog Retin Eye Res*. 2005;24:639–662.

3. Buckingham BP, Inman DM, Lambert W, et al. Progressive ganglion cell degeneration precedes neuronal loss in a mouse model of glaucoma. *J Neurosci*. 2008;28:2735–2744.

4. Soto I, Oglesby E, Buckingham BP, et al. Retinal ganglion cells downregulate gene expression and lose their axons within the optic nerve head in a mouse glaucoma model. *J Neurosci*. 2008;28:548–561.

5. Crish SD, Sappington RM, Inman DM, Horner PJ, Calkins DJ. Distal axonopathy with structural persistence in glaucomatous neurodegeneration. *Proc Natl Acad Sci*. 2010;107:5196–5201.

6. Carelli V, Ross-Cisneros FN, Sadun AA. Optic nerve degeneration and mitochondrial dysfunction: genetic and acquired optic neuropathies. *Neurochem Int*. 2002;40:573–584.

7. Chidlow G, Ebneter A, Wood JP, Casson RJ. The optic nerve head is the site of axonal transport disruption, axonal cytoskeleton damage and putative axonal regeneration failure in a rat model of glaucoma. *Acta Neuropathol*. 2011;121:737–751.

8. Vidal-Sanz M, Salinas-Navarro M, Nadal-Nicolas FM, et al. Understanding glaucomatous damage: anatomical and functional data from ocular hypertensive rodent retinas. *Prog Retin Eye Res*. 2012;31:1–27.

9. Weber AJ, Harman CD. Structure-function relations of parasol cells in the normal and glaucomatous primate retina. *Invest Ophthalmol Vis Sci*. 2005;46:3197–3207.

10. Saleh M, Nagaraju M, Porciatti V. Longitudinal evaluation of retinal ganglion cell function and IOP in the DBA/2J mouse model of glaucoma. *Invest Ophthalmol Vis Sci*. 2007;48:4564–4572.

11. Howell GR, Libby RT, Marchant JK, et al. Absence of glaucoma in DBA/2J mice homozygous for wild-type versions of Gpnmb and Tyrp1. *BMC Genet*. 2007;8:45.

12. Enriquez-Algeciras M, Ding D, Chou TH, et al. Evaluation of a transgenic mice model of multiple sclerosis with non invasive methods. *Invest Ophthalmol Vis Sci*. 2011;52:2405–2411.

13. Howell GR, Soto I, Zhu X, et al. Radiation treatment inhibits monocyte entry into the optic nerve head and prevents neuronal damage in a mouse model of glaucoma. *J Clin Invest*. 2012;122:1246–1261.

14. Yu H, Koilkonda RD, Chou TH, et al. Gene delivery to mitochondria by targeting modified adenoassociated virus suppresses Leber's hereditary optic neuropathy in a mouse model. *Proc Natl Acad Sci U S A*. 2012;109:E1238–E1247.

15. Ventura LM, Porciatti V. Restoration of retinal ganglion cell function in early glaucoma after intraocular pressure reduction: a pilot study. *Ophthalmology*. 2005;112:20–27.

16. Ventura LM, Golubev I, Feuer WJ, Porciatti V. Pattern electroretinogram progression in glaucoma suspects [published online ahead of print November 7, 2011]. *J Glaucoma*.

17. Sehi M, Grewal DS, Goodkin ML, Greenfield DS. Reversal of retinal ganglion cell dysfunction after surgical reduction of intraocular pressure. *Ophthalmology*. 2010;117:2329–2336.

18. Nagaraju M, Saleh M, Porciatti V. IOP-dependent retinal ganglion cell dysfunction in glaucomatous DBA/2J mice. *Invest Ophthalmol Vis Sci*. 2007;48:4573–4579.

19. Porciatti V, Nagaraju M. Head-up tilt lowers IOP and improves RGC dysfunction in glaucomatous DBA/2J mice. *Exp Eye Res*. 2010;90:452–460.

20. Ventura LM, Feuer WJ, Porciatti V. Progressive loss of retinal ganglion cell function is hindered with IOP-lowering treatment in early glaucoma. *Invest Ophthalmol Vis Sci*. 2012;53:659–663.

21. Park KK, Liu K, Hu Y, et al. Promoting axon regeneration in the adult CNS by modulation of the PTEN/mTOR pathway. *Science*. 2008;322:963–966.

22. Templeton JP, Geisert EE. A practical approach to optic nerve crush in the mouse. *Mol Vis*. 2012;18:2147–2152.

23. Porciatti V, Saleh M, Nagaraju M. The pattern electroretinogram as a tool to monitor progressive retinal ganglion cell dysfunction in the DBA/2J mouse model of glaucoma. *Invest Ophthalmol Vis Sci*. 2007;48:745–751.

24. Porciatti V. The mouse pattern electroretinogram. *Doc Ophthalmol*. 2007;115:145–153.

25. Drager UC, Hubel DH. Physiology of visual cells in mouse superior colliculus and correlation with somatosensory and auditory input. *Nature*. 1975;253:203–204.

26. Oommen BS, Stahl JS. Eye orientation during static tilts and its relationship to spontaneous head pitch in the laboratory mouse. *Brain Res*. 2008;1193:57–66.

27. Remtulla S, Hallett PE. A schematic eye for the mouse, and comparisons with the rat. *Vision Res*. 1985;25:21–31.

28. Schmucker C, Schaeffel F. A paraxial schematic eye model for the growing C57BL/6 mouse. *Vision Res*. 2004;44:1857–1867.

29. Artal P, Herreros de Tejada P, Munoz Tedo C, Green DG. Retinal image quality in the rodent eye. *Vis Neurosci*. 1998;15:597–605.

30. Robinson GA, Madison RD. Axotomized mouse retinal ganglion cells containing melanopsin show enhanced survival, but not enhanced axon regrowth into a peripheral nerve graft. *Vision Res*. 2004;44:2667–2674.

31. Brown NL, Patel S, Brzezinski J, Glaser T. Math5 is required for retinal ganglion cell and optic nerve formation. *Development*. 2001;128:2497–2508.

32. Miura G, Wang MH, Ivers KM, Frishman LJ. Retinal pathway origins of the pattern ERG of the mouse. *Exp Eye Res*. 2009;89:49–62.

33. Porciatti V, Pizzorusso T, Maffei L. The visual physiology of the wild type mouse determined with pattern VEPs. *Vision Res*. 1999;39:3071–3081.

34. Rossi FM, Pizzorusso T, Porciatti V, Marubio LM, Maffei L, Changeux JP. Requirement of the nicotinic acetylcholine receptor beta 2 subunit for the anatomical and functional development of the visual system. *Proc Natl Acad Sci U S A*. 2001;98:6453–6458.

35. Roy S, Zhang B, Lee VM, Trojanowski JQ. Axonal transport defects: a common theme in neurodegenerative diseases. *Acta Neuropathol*. 2005;109:5–13.

36. Almasieh M, Wilson AM, Morquette B, Cueva Vargas JL, Di Polo A. The molecular basis of retinal ganglion cell death in glaucoma. *Prog Retin Eye Res*. 2012;31:152–181.

37. Salinas-Navarro M, Mayor-Torroglosa S, Jimenez-Lopez M, et al. A computerized analysis of the entire retinal ganglion cell population and its spatial distribution in adult rats. *Vision Res*. 2009;49:115–126.

38. Pease ME, McKinnon SJ, Quigley HA, Kerrigan-Baumrind LA, Zack DJ. Obstructed axonal transport of BDNF and its receptor TrkB in experimental glaucoma. *Invest Ophthalmol Vis Sci*. 2000;41:764–774.

39. Weber AJ, Harman CD, Viswanathan S. Effects of optic nerve injury, glaucoma, and neuroprotection on the survival, structure, and function of ganglion cells in the mammalian retina. *J Physiol*. 2008;586:4393–4400.

40. Byers MR, Fink BR, Kennedy RD, Middaugh ME, Hendrickson AE. Effects of lidocaine on axonal morphology, microtubules, and rapid transport in rabbit vagus nerve in vitro. *J Neurobiol*. 1973;4:125–143.

41. Bisby MA. Inhibition of axonal transport in nerves chronically treated with local anesthetics. *Exp Neurol*. 1975;47:481–489.

42. Fink BR, Kish SJ. Reversible inhibition of rapid axonal transport in vivo by lidocaine hydrochloride. *Anesthesiology*. 1976;44:139–146.

43. Fagiolini M, Caleo M, Strettoi E, Maffei L. Axonal transport blockade in the neonatal rat optic nerve induces limited retinal ganglion cell death. *J Neurosci*. 1997;17:7045–7052.

44. Kanai A, Hiruma H, Katakura T, Sase S, Kawakami T, Hoka S. Low-concentration lidocaine rapidly inhibits axonal transport in cultured mouse dorsal root ganglion neurons. *Anesthesiology*. 2001;95:675–680.

45. Catterall WA. Molecular mechanisms of gating and drug block of sodium channels. *Novartis Found Symp*. 2002;241:206–218, discussion 218-232.

46. Wang X, Baldridge WH, Chauhan BC. Acute endothelin-1 application induces reversible fast axonal transport blockade in adult rat optic nerve. *Invest Opht Vis Sci*. 2008;49:961–967.

47. Bien A, Seidenbecher CI, Bockers TM, Sabel BA, Kreutz MR. Apoptotic versus necrotic characteristics of retinal ganglion

cell death after partial optic nerve injury. *J Neurotrauma*. 1999;16:153–163.

48. Mandolesi G, Madeddu F, Bozzi Y, Maffei L, Ratto GM. Acute physiological response of mammalian central neurons to axotomy: ionic regulation and electrical activity. *FASEB J*. 2004;18:1934–1936.

49. Porciatti V, Pizzorusso T, Cenni MC, Maffei L. The visual response of retinal ganglion cells is not altered by optic nerve transection in transgenic mice overexpressing Bcl-2. *Proc Natl Acad Sci U S A*. 1996;93:14955–14959.

50. Chan KC, Li J, Kau P, et al. In vivo retinotopic mapping of superior colliculus using manganese-enhanced magnetic resonance imaging. *Neuroimage*. 2011;54:389–395.

51. Caleo M. Different rates of horseradish peroxidase transport in the optic nerve of neonatal and adult rats. *Neuroscience*. 1996; 72:725–730.

52. May CA, Lutjen-Drecoll E. Morphology of the murine optic nerve. *Invest Ophthalmol Vis Sci*. 2002;43:2206–2212.

53. Kafitz KW, Rose CR, Konnerth A. Neurotrophin-evoked rapid excitation of central neurons. *Prog Brain Res*. 2000;128:243–249.

54. Kafitz KW, Rose CR, Thoenen H, Konnerth A. Neurotrophin-evoked rapid excitation through TrkB receptors. *Nature*. 1999;401:918–921.

55. Blum R, Kafitz KW, Konnerth A. Neurotrophin-evoked depolarization requires the sodium channel Na(V)1.9. *Nature*. 2002;419:687–693.

56. Ventura LM, Porciatti V, Ishida K, Feuer WJ, Parrish RK 2nd. Pattern electroretinogram abnormality and glaucoma. *Ophthalmology*. 2005;112:10–19.

57. Bach M, Hoffmann MB. Update on the pattern electroretinogram in glaucoma. *Optom Vis Sci*. 2008;85:386–395.

58. Holder GE. Pattern electroretinography (PERG) and an integrated approach to visual pathway diagnosis. *Prog Retin Eye Res*. 2001;20:531–561.

59. Di Leo MA, Falsini B, Caputo S, Ghirlanda G, Porciatti V, Greco AV. Spatial frequency-selective losses with pattern electroretinogram in type 1 (insulin-dependent) diabetic patients without retinopathy. *Diabetologia*. 1990;33:726–730.

60. Ventura LM, Golubev I, Feuer WJ, Porciatti V. The PERG in diabetic glaucoma suspects with no evidence of retinopathy. *J Glaucoma*. 2009;19:243–247.

61. Nesher R, Trick GL, Kass MA, Gordon MO. Steady-state pattern electroretinogram following long term unilateral administration of timolol to ocular hypertensive subjects. *Doc Ophthalmol*. 1990;75:101–109.

62. Colotto A, Salgarello T, Giudiceandrea A, et al. Pattern electroretinogram in treated ocular hypertension: a cross-sectional study after timolol maleate therapy. *Ophthalmic Res*. 1995;27:168–177.

63. Ventura LM, Venzara FX III, Porciatti V. Reversible dysfunction of retinal ganglion cells in non-secreting pituitary tumors. *Doc Ophthalmol*. 2009;118:155–162.

64. Porciatti V, Ventura LM. Retinal ganglion cell functional plasticity and optic neuropathy: a comprehensive model. *J Neuroophthalmol*. 2012;32:354–358.